Graduate School ETD Form 9
(Revised 12/07)

PURDUE UNIVERSITY
GRADUATE SCHOOL
Thesis/Dissertation Acceptance

This is to certify that the thesis/dissertation prepared

By Samantha L. Deitz

Entitled
MOLECULAR BASIS AND MODIFICATION OF A NEURAL CREST DEFICIT IN A DOWN SYNDROME MOUSE MODEL

For the degree of Master of Science

Is approved by the final examining committee:

Randall J. Roper
Chair

Ellen A.G. Chernoff

Hua-Chen Chang

To the best of my knowledge and as understood by the student in the *Research Integrity and Copyright Disclaimer (Graduate School Form 20)*, this thesis/dissertation adheres to the provisions of Purdue University's "Policy on Integrity in Research" and the use of copyrighted material.

Approved by Major Professor(s): Randall J. Roper

Approved by: Simon Atkinson 05/03/2012
Head of the Graduate Program Date

Graduate School Form 20
(Revised 9/10)

PURDUE UNIVERSITY
GRADUATE SCHOOL

Research Integrity and Copyright Disclaimer

Title of Thesis/Dissertation:

MOLECULAR BASIS AND MODIFICATION OF A NEURAL CREST DEFICIT IN A DOWN SYNDROME MOUSE MODEL

For the degree of Master of Science

I certify that in the preparation of this thesis, I have observed the provisions of *Purdue University Executive Memorandum No. C-22,* September 6, 1991, *Policy on Integrity in Research.**

Further, I certify that this work is free of plagiarism and all materials appearing in this thesis/dissertation have been properly quoted and attributed.

I certify that all copyrighted material incorporated into this thesis/dissertation is in compliance with the United States' copyright law and that I have received written permission from the copyright owners for my use of their work, which is beyond the scope of the law. I agree to indemnify and save harmless Purdue University from any and all claims that may be asserted or that may arise from any copyright violation.

Samantha L. Deitz

Printed Name and Signature of Candidate

05/03/2012

Date (month/day/year)

*Located at http://www.purdue.edu/policies/pages/teach_res_outreach/c_22.html

MOLECULAR BASIS AND MODIFICATION OF A NEURAL CREST DEFICIT IN A DOWN SYNDROME MOUSE MODEL

A Thesis

Submitted to the Faculty

of

Purdue University

by

Samantha L. Deitz

In Partial Fulfillment of the

Requirements for the Degree

of

Master of Science

August 2012

Purdue University

Indianapolis, Indiana

For my friends and family for their support, encouragement, and challenges to my way of thinking. Your advice and questions have been priceless.

ACKNOWLEDGEMENTS

I would like to thank my mentor, Dr. Randall Roper, for his perseverance with me through troubleshooting protocols, his undying persistence, and the many lab and life skills he has instilled in me through my six years in his laboratory. He has not only molded me into an inquisitive scientist with a healthy level of skepticism, but also into an individual who does not accept no for an answer. I would like to thank my committee members, Dr. Ellen Chernoff and Dr. Hua-Chen Chang, for their valuable feedback and guidance through the thesis writing process. Lastly, I would like to thank the many Roper Lab members I have had the privilege of getting to know over my time in the laboratory for their support, encouragement, and friendship.

TABLE OF CONTENTS

Page

LIST OF TABLES

LIST OF FIGURES

Figure Page

ABSTRACT

Deitz, Samantha L. M.S., Purdue University, August 2012. Molecular Basis and Modification of a Neural Crest Deficit in a Down Syndrome Mouse Model. Major Professor: Randall J. Roper.

Down syndrome (DS) is the result of trisomy of human chromosome 21 (Hsa 21) and occurs in approximately 1/700 live births. Mouse models of DS have been crucial in understanding the gene-phenotype relationships that underlie many DS anomalies. The Ts65Dn mouse model, trisomic for half of the Hsa 21 orthologs, replicates many DS phenotypes including craniofacial alterations such as a small, dysmorphic mandible, midface, and maxilla. Other mouse models, such as the Ts1Rhr which contains a triplication of 33 Hsa 21 orthologs, have been used to better understand the genes responsible for craniofacial alterations. Our laboratory has demonstrated that the postnatal mandibular phenotype found in Ts65Dn mice can be traced back to an original neural crest cell (NCC) deficit in the developing first pharyngeal arch (PA1) at embryonic day 9.5 (E9.5). Furthermore, evidence suggested that both a proliferation deficit in the PA1 and a migration deficit of NCC from the neural tube (NT) could be the mechanism behind this deficit. However, the molecular mechanisms behind these deficits remain to be elucidated. Due to the involvement of the Hsa 21 genes *DYRK1A* and *RCAN1* in

regulation of signaling pathways including NFATc (NFAT2), a transcription factor known to influence cellular proliferation and, later, bone development, we hypothesized that dysregulation of these genes could underlie to cellular deficit in the PA1. Furthermore, we hypothesized targeting *Dyrk1a* by decreasing activity or available protein could ameliorate the established deficits.

Through the use of RNA isolation techniques and cell culture systems of cells from the PA1 and NT of E9.5 Ts65Dn, Ts1Rhr, and control embryos, we established that trisomic genes *Dyrk1a* and *Rcan1* are dysregulated in both structures and that these two genes may interact. Furthermore, we established that a proliferation deficit in the Ts65Dn PA1 and a migration deficit in the Ts65Dn PA1 and NT exists at E9.5 and can be rescued to euploid levels *in vitro* with the addition of the Dyrk1a inhibitor, EGCG, a green tea polyphenol. We also confirmed that harmine, a more highly studied and specific Dyrk1a inhibitor, is capable of similar effects on proliferation of PA1 cells from E9.5 Ts65Dn embryos. Furthermore, when Ts65Dn pregnant mothers were treated with EGCG *in vivo*, the cellular deficit found in the developing E9.5 embryonic PA1 was rescued to near euploid volume and NCC number. Treatment with EGCG did not adversely impact litter size or embryonic development. Interestingly, euploid embryonic volume increased with EGCG treatment. Expression analysis of the E9.5 PA1 of EGCG treated Ts65Dn and control embryos revealed dysregulation of several genes involved in craniofacial and developmental pathways including *Dyrk1a*, *Rcan1*, *Ets2* and members of the sonic hedgehog pathway. Our novel results provide a foundation for better

understanding the molecular mechanisms of craniofacial development and may provide evidence-based therapeutic options to improve the quality of life for individuals with DS.

CHAPTER 1. INTRODUCTION

1.1 Down Syndrome

Down syndrome (DS) occurs in 1/700 live births and is the result of trisomy of human chromosome (Hsa) 21 (PARKER *et al.* 2010). This disorder is the most common genetic form of intellectual disability (ID) and has been well studied and characterized independently by genotype and phenotype (KORBEL *et al.* 2009; LYLE *et al.* 2009). DS was first coarsely described in 1846 by Édouard Onésimus Séguin, the first President of the current American Association for Mental Deficiency, as a form of cretinism, including 'shortcomings of the integuments…truncated fingers and nose' which are reminiscent of DS, but does not irrevocably describe the syndrome itself (BERG and KOROSSY 2001; NERI and OPITZ 2009). The disorder was described ethnically by physician John Langdon Down, after whom the disorder was named, in 1866. In his observations, he stated that those he studied with what is now known as Down syndrome were 'merely varieties of the human race having a common origin' but that these individuals were derived from 'the Mongolian great family' based on his idea that these individuals resembled those from Mongolia who were once thought to have impeded development (DOWN 1866; MEGARBANE *et al.* 2009). The genetic cause of this disorder was not identified until 1959 by Jerome Lejeune. With the advent of karyotyping techniques and a general need for

more fundamental explanation of the disorder's origin, Lejeune set out to understand what genetic insult was responsible for these phenotypes. In 1959 he published that DS resulted from an extra chromosome 21, leading to the clinical condition of Trisomy 21 (LEJEUNE *et al.* 1959a; LEJEUNE *et al.* 1959b). These results were later confirmed by numerous groups, followed by the observation that Trisomy 21 could also results from the additional presence of only a portion of Hsa 21 with regard to the normal genetic complement (MEGARBANE *et al.* 2009). Since the discovery of the initial genetic insult of the disorder, much research has taken place to better understand the mechanisms by which the third copy of Hsa 21 causes the phenotypes observed in individuals with DS.

Though the genotype-phenotype relationships are not well understood in DS, the mechanism of transmission has been well-studied. The transmission of trisomy generally occurs through meiotic nondisjunction (95% of all cases) in meiosis I and II, of which 88% originates maternally, 8% paternally, and 4% mitotically (ANTONARAKIS 1991; MULLER *et al.* 2000). Less commonly, DS has also been shown to occur as an unbalanced Robertsonian translocation (under 5%) in which the long arm of Hsa 21 translocates with the long arm of Hsa 14, leading to the possibility of inheritance of Trisomy 21. This may occur more frequently in telocentric chromosomes such as 21 compared to acrocentric chromosomes, due to relative instability of the physical nature of the chromosome (CLARKE *et al.* 1989). In addition, mosaicism, which occurs in less than 1% of individuals with DS, results in some somatic cells which display the genetic abnormality while others maintain a diploid state. The origins of the mosaicism may stem from

either a normal zygote or trisomic zygote having undergone errors in mitosis at any of multiple cleavages early in development (Figure 1.1) (RICHARDS 1969).

Several risk factors play a role in the development of Trisomy 21 which have been well described and continue to be investigated. A significant risk factor for maternal nondisjunction is the characteristic advanced maternal age (ALLEN *et al.* 2009). However, it should be noted that a majority of individuals with DS are born to younger women (under the age of 35 at delivery), due to a higher percentage of children born to younger mothers (Table 1.1) (AGOPIAN *et al.* 2012; HUETHER *et al.* 1998). Though only hypotheses, the reasoning for this risk has been attributed to the accumulation of environmental assaults in the oocyte, which have remained arrested in development or degradation of cell cycling machinery needed to complete meiosis I or II (SHERMAN *et al.* 2005). Changes in the maternal genome, such as mutations in the gene encoding methylenetetrahydrofolate reductase, may subject mothers to an increased risk of having a child with DS (JAMES *et al.* 1999). This may be true of several aneuploidies due to the association of abnormal folate and methyl metabolism with DNA hypomethylation and abnormalities in chromosome segregation (CHRISTMAN *et al.* 1993; POGRIBNY *et al.* 1997). Paternal nondisjunction, though much less common than maternal nondisjunction, also may lead to 6-10% of cases of Trisomy 21 through errors in spermatogenesis, with equal occurrences of meiosis I and II cases (as opposed to maternal nondisjunction, occurring at a 3:1 ratio) (PETERSEN *et al.* 1993; SAVAGE *et al.* 1998). Other hypothesized risk factors that have been identified include a father who is

between 20 and 24 years, compared to 25 to 29 years old, and Hispanic, as well as women with less than a high school education (AGOPIAN *et al.* 2012).

Regardless, this genetic anomaly is easily identified in the first trimester through diagnostic tools such as amniocentesis, which samples the amnion containing fetal tissue, for analysis between 15 and 20 weeks gestation; chorionic villus sampling, which utilizes tissue from the placenta (fetal derived) for analysis at approximately 10-12 weeks gestation; and several newly-developed non-invasive methods including multiplexed maternal plasma DNA sequencing, for use in high risk pregnancies (CHIU *et al.* 2011). In essence, multiplexed maternal plasma DNA sequencing works off the following principle: during pregnancy, DNA from the fetus is present in maternal blood in a cell-free form. In order to test for the presence of Trisomy 21, one would aim to detect a higher level of Hsa 21 sequence comparatively to other chromosomes from the fetus, only after distinguishing the fetal genome from the reference genome of the mother (CHIU *et al.* 2010). This technique also has broad impacts due to its ability to detect other genetic anomalies. Recently, the MateriT21 PLUS test, validated by Sequenom CMM, was developed to sensitively test circulating fetal cell-free DNA in maternal blood, detecting 210 of 212 cases of Trisomy 21 at 99.1% sensitivity with uses also being developed to detect Trisomy 13 and Trisomy 18 using similar methods (EHRICH *et al.* 2011; PALOMAKI *et al.* 2011). In addition, ultrasound screenings can provide a non-invasive diagnostic tool for the assessment of anatomical markers, such as nuchal thickening, increased nuchal lucency, and shortened long bones (KUBAS 1999).

Individuals with DS present with myriad phenotypes which occur in differing penetrance and severity between individuals and in multiple organ systems at different stages of development. All individuals display ID and craniofacial abnormalities, while approximately 45-50% of individuals display cardiac defects, most commonly including septal defects (EPSTEIN 2001; VAN CLEVE *et al.* 2006; VAN CLEVE and COHEN 2006). Furthermore, while some individuals with ID are only moderately impaired and may be able to function independently, other individuals have severe cognitive impairment and very few reach a near normal levels of cognitive and intellectual development in adulthood (DE *et al.* 2000; ROUBERTOUX and CARLIER 2010). Individuals with DS also present with higher instances of leukemia and Hirschprung disease than the general population (HASLE 2001) and display early-onset of Alzheimer disease(AD)-like pathology with all individuals with DS developing AD-like pathology over age 40 (WISNIEWSKI *et al.* 1985).

Interestingly, not all individuals present with a full copy of Hsa 21 or presence of all three copies of Hsa21 in every cell, even though they are described as having DS. Individuals who display partial Trisomy 21 or mosaicism, respectively, typically display a milder phenotype than those individuals with full Trisomy 21 (DE *et al.* 2000; KOTZOT and SCHINZEL 2000; WILLIAMS *et al.* 1990) and contribute valuable information essential for understanding the genotype-phenotype correlations which underlie the basis of Down syndrome pathophysiology. For example, a man with low Trisomy 21 mosaicism currently functions with some clinical signs of DS with normal ID; however, he was diagnosed at birth due to his clinical features of the face and appendages, as well as hypotonia and impaired motor skills. Interestingly, he performed well throughout

regular schooling and in sports, and despite not finishing college, lives a relatively normal lifestyle despite his mosaicism (DE *et al.* 2000). In addition, an individual with a de novo, unbalanced translocation leading to a triplication involving the segment 21q11 to 21q22.1, displayed mild phenotypes but not those typical of individuals with DS. Findings provided from this study indicated that duplication of the area from the centromere to 21q22.1 may be important in the development of some DS phenotypes (WILLIAMS *et al.* 1990), aiding in the understanding of genotype-phenotype relationships.

Despite the phenotypes which appear to have a largely negative influence on health, individuals with DS display some physiological advantages over the normosomic population. While individuals with DS display a higher incidence of several types of cancer, including acute myeloid, lymphoblastic, and megakaryoblastic leukemias (HITZLER 2007), retinoblastoma, and germ cell tumors (HASLE 2001), as a whole, individuals with DS display a lower incidence of solid tumors (HASLE 2001; SATGE and VEKEMANS 2011).

1.2 Human Genotype-Phenotype Relationships

The understanding of how specific genes work either alone, in concert with genes on Hsa 21, or even with other genes throughout the rest of the genome is vital to proposing therapeutics for individual phenotypes for those with DS. Two major studies were key in establishing an understanding of these relationships in the early 1990s. Delabar and colleagues phenotypically and molecularly analyzed 10 individuals with partial Trisomy 21, identifying six regions for 24 features of DS, including short stature, joint hyperlaxity, hypotonia, ID, and craniofacial anomalies (DELABAR *et al.* 1993). The

resultant regions of interest spanned a 0.4-3Mb area on 21q22.2 to proximal 21q22.3 and an approximate 6Mb region on 21q22.2 and part of 21q22.3 (DELABAR *et al.* 1993). It was originally purported that this one or more of the genes in this region was responsible for the major phenotypes associated with DS, including cognitive impairment, craniofacial dysmorphology (DELABAR *et al.* 1993). In addition, Korenberg and colleagues performed a similar study in which cell lines from 16 individuals with partial Trisomy 21 were molecularly analyzed and combined with clinical evaluations of these individuals to create a 'phenotypic map' which included 25 features of DS mapped to 2-20 Mb regions in which genes likely responsible for these phenotypes were found (KORENBERG *et al.* 1994). However, investigators have hypothesized that a single DS chromosomal region is likely not responsible for the typical features associated with DS (KORBEL *et al.* 2009; KORENBERG *et al.* 1994; LYLE *et al.* 2009). These studies laid the groundwork for understanding the involvement of one or multiple genes in the development of a specific phenotype and were instrumental in defining a region of the fewest number of genes purported to be responsible for the major phenotypes of DS, named the Down Syndrome Critical Region (DSCR). This region has since been triplicated in a DS mouse model to better understand its involvement in DS phenotypes.

Several studies have recently aimed to increase the understanding of these relationships by use of mapping partial Trisomy 21 cases from humans, creating mouse models of partial trisomies which are orthologous to Hsa 21 genes, and analyzing tissue from individuals with DS and/or tissues from DS mouse models. High-resolution analysis of human segmental trisomies, comprised of an analysis of 30 individuals with rare

segmental trisomies and well characterized phenotypes, was performed by Korbel and colleagues to understand the contribution of small genetic segments to DS phenotypes. Through the compilation of karyotypes, fluorescence *in situ* hybridization (FISH) analysis to determine breakpoints and orientation, high resolution mapping via quantitative Southern blotting, and sequencing, a highly detailed description of each individual's genetic signature was compared using the phenotypic map. Investigators identified regions of 1.8-16.3 Mb likely implicated in eight DS phenotypes, including Hirschsprung disease, severe ID, DS-related Alzheimer disease (AD), and DS-specific congenital heart disease (KORBEL *et al.* 2009). A similar study by Lyle and colleagues introduced the idea of susceptibility regions of the genome for DS phenotypes using similar methodologies (LYLE *et al.* 2009). Investigators found a region between positions 37.94 and 38.64 on Hsa21 containing the genes *KCNJ6, DSCR4,* and *KCNJ15* as a susceptibility for ID, between 37.4 and 38.4 and 46.5 to qter for hypotonia, and 31.5 Mb to qter for congenital heart disease (Figure 1.2) (LYLE *et al.* 2009). These studies provided a vast amount of information, specifically in understanding which gene(s)/genetic regions may be responsible for a specific DS phenotype (KORBEL *et al.* 2009).

An interesting example of single gene-phenotype relationships includes the Hsa 21 gene synaptojanin-1 (*SYNJ1*) which illustrates the importance of single genes in phenotypes and their contribution as a member of a group of genes to a particular phenotype. Synaptojanin-1 is an inositol phosphatase involved in synaptic vesicle recycling and endocytosis via clathrin-coated vesicles (CREMONA *et al.* 1999). Brains from individuals with DS display an increase in the number and size of astrocytes and a high

level of synaptojanin-1 expression (ARAI *et al.* 2002). Few studies have been performed in humans in order to understand these relationships, however, due to the inability to obtain appropriate tissue samples for these studies, but mouse models are available to understand these relationships more conclusively.

1.3 Mouse Models of Down Syndrome

Mouse models have been used for over a decade to better understand the genotype-phenotype correlations in DS. Mice display a high level of homology to humans in organ systems and general development, including craniofacial bones (Figure 1.3). Mice are easily maintained with a high level of tissue access at embryonic stages which is not available from individuals with DS. The completion of sequencing for Hsa 21 (HATTORI *et al.* 2000) and the mouse genome (WATERSTON *et al.* 2002) have now provided the opportunity to compare sequences of entire chromosomes to determine functional relationships of genes (ANTONARAKIS *et al.* 2004; MURAL *et al.* 2002)

Genes found on Hsa 21 are dispersed among three mouse chromosomes, Mmu 10, 16, and 17, presenting a challenge in engineering a mouse model fully representative of the genetic condition of DS, despite the homology between mouse and human genomes (Figure 1.4). However, many genes map to these mouse chromosomes which are not orthologous to Hsa 21 genes, adding another layer of complexity. For example, Hsa 21 genes including *Sod1*, *App*, *Ets2*, and *Ifnra/Ifnrb* are located on distal Mmu 16, but Mmu 16 genes such as the λ light change immunoglobulin genes (*IGL*) and protamine genes (*PRM1* and *PRM2*) are not found on Hsa 21, though

they have not been shown to have any involvement in DS pathogenesis (THREADGILL *et al.* 1991). The most commonly used mouse model, Ts(17^{16})65Dn or Ts65Dn, represents a triplication of approximately half of the gene orthologs found on Hsa 21 (Figure 1.5). The extrachromosomal segment found in this mouse model is comprised of the telomeric end of Mmu 16, attached to the centromere and approximately 10 Mb of Mmu 17, including the genes corresponding to the 21q21-22.3 region on Hsa 21 (DAVISSON *et al.* 1993; REINHOLDT *et al.* 2011). However, the centromeric portion and other gene content of Mmu 17 to which the extrachromsomal segment is attached does not map to Hsa 21. The dosage of these genes is currently unknown, introducing an extra variable in understanding the role of these Hsa 21 orthologs in Ts65Dn mice (DAVISSON *et al.* 1993; REINHOLDT *et al.* 2011). The Ts65Dn mouse also contains a triplication of the DSCR, once thought to contribute to the primary phenotypes of DS, and is the most commonly studied DS mouse model (REEVES *et al.* 1995).

This mouse model appears to closely mirror phenotypes of DS, including small stature, craniofacial dysmorphology, ID, behavioral abnormalities, impaired integration of visual and spatial learning and decreased susceptibility to solid tumor development (REEVES *et al.* 1995; RICHTSMEIER *et al.* 2000; SUSSAN *et al.* 2008). Ts65Dn mice are smaller than euploid littermates to the point that they appear visually different in body size by genotype shortly after birth (CONTESTABILE *et al.* 2009b; ROPER *et al.* 2006b). Of particular interest, Ts65Dn mice replicate many of the craniofacial features associated with DS, including a small, dysmorphic mandible, brachycephaly, and a small midface. A study by Richtsmeier and colleagues utilized EDMA, Euclidean Distance Matrix Analysis, to

measure three-dimensional coordinate locations of cranial and mandibular landmarks in Ts65Dn and euploid mice. The comprehensive results showed that Ts65Dn mice display reduced width across the posterior maxilla, shortened to varying degrees in rostro-caudal dimensions, reduced overall maxillae, and reduced distance along the rostro-caudal axis of the maxillae, revealing a smaller overall flattened face compared to euploid counterparts. In addition, the Ts65Dn neurocranium is reduced in size with similar or larger distances along the medio-lateral axis, resulting in a broad, brachycephalic phenotype compared to euploid mice. Furthermore, 97% of the linear distances analyzed using mandibular landmarks were smaller in Ts65Dn mice than euploid mice (RICHTSMEIER *et al.* 2000). These phenotypes are highly representative of DS craniofacial alterations and are even representative of the high level of variability in craniofacial phenotypes that individuals with DS often display (RICHTSMEIER *et al.* 2000).

Ts65Dn mice display alterations in bone mineral density and strength (BLAZEK *et al.* 2011), in line with the low bone mineral content found in adults, adolescents, and children with DS (BAPTISTA *et al.* 2005; GONZALEZ-AGUERO *et al.* 2011). Ts65Dn neonates display cardiac anomalies which lead to subsequent mortality (MOORE 2006), including anomalies of the aortic arches in neonates which appear similar to those of neonates with DS (CHAOUI *et al.* 2005; MCELHINNEY *et al.* 2002). The incidence of gross cardiac vascular abnormalities is only 17% in Ts65Dn neonates, however, compared to 50% of individuals with DS having congenital heart defects and differences are present in the anomalies themselves (FREEMAN *et al.* 1998; WESSELS *et al.* 2003; WILLIAMS *et al.* 2008). Interestingly, Ts65Dn neonates do not display the severe phenotype of complete

atrioventricular canal abnormality as in individuals with DS and many differences exist in other less common abnormalities between Ts65Dn and DS neonates (WILLIAMS *et al.* 2008). Phenotypically, the structure and function of the Ts65Dn brain has been extensively studied. Ts65Dn mice display reduced long term potentiation (LTP), deficits in novel object recognition, learning, and memory, and a smaller overall brain volume (ALDRIDGE *et al.* 2007; BELICHENKO *et al.* 2009; ESCORIHUELA *et al.* 1998). Interestingly, Ts65Dn mice have also been successfully used to predict phenotypes in individuals with DS which have not previously been identified. In a study by Baxter and colleagues, Ts65Dn mice were found to have a reduction in granule cell density in the cerebellum—a phenotype later investigated and confirmed in the DS cerebellum (BAXTER *et al.* 2000).

Many other mouse models of DS have been developed that represent different partial trisomies for mouse orthologs of Hsa 21 (Figure 1.5). The Ts1Rhr mouse model containing a triplication of the 33 orthologs including those between *Cbr3* and *Mx2* which (comprising the DSCR) was developed to better understand the contribution of this region to major DS phenotypes (OLSON *et al.* 2007). Interestingly, when the Ts1Rhr mouse model was created and craniofacial morphology assessed, the mandible was found to be larger in Ts1Rhr mice compared to euploid littermates and thus the DSCR was found to be insufficient in producing DS-like facial phenotypes (OLSON *et al.* 2004a). Furthermore, Ts65Dn mice containing monosomy for the DSCR showed measurements of the mandible similar to those in Ts65Dn, indicating that the DSCR is largely unnecessary for this phenotype (OLSON *et al.* 2004a). Additional studies, though altered slightly in methodology, have been inconclusive as to the contribution of this region to

brain phenotypes in Ts1Rhr mice (BELICHENKO *et al.* 2009; OLSON *et al.* 2007). While the Ts1Rhr mouse model does represent a number of genes thought to be involved in a number of DS phenotypes and can be used extensively to understand the role of a specific subset of genes in DS phenotypes, it does not definitively model all phenotypic aspects of the disorder. Furthermore, allelic differences identified when studying mice and embryos from the Ts1Rhr line on two genetically different backgrounds revealed alterations in embryonic phenotypes (embryonic and mandibular precursor size) and postnatal weight, litter size, and transmission of the trisomy (DEITZ and ROPER 2011). These allelic differences are important to keep in mind when comparing studies using the same mouse model as well as studies across mouse models.

Several other segmentally trisomic mice have been developed to better understand candidate genes and regions, as well as the contributions of genetic material from one chromosome versus another (Figure 1.5). For example, the Tc1 mouse is transchromosomic—it contains not only its normal complement of genes, but also an engineered chromosome containing multiple Hsa 21 regions (approximately 92% of all known Hsa 21 genes), reflecting more closely the dosage difference present between trisomic and normosomic individuals (O'DOHERTY *et al.* 2005). Tc1 mice display reduced LTP, a mild learning impairment, tendency toward hyperactivity, and failure of fusion between the ventricular septum and proximal outflow tract cushions of the heart compared to euploid littermates and in line with DS phenotypes (O'DOHERTY *et al.* 2005). Interestingly, Tc1 mice show no alterations in craniofacial development (O'DOHERTY *et al.*

2005). It is important to note, however, that these mice are mosaic for the Trisomy and this mosaicism varies among mice and tissues (DAS and REEVES 2011).

In addition, the Ts1Cje, a segmentally trisomic mouse for *Hunk* to *Zfp295* or approximately 81 Hsa 21 orthologs, displays some, but not all DS phenotypes, though they show many parallels to Ts65Dn phenotypes (SAGO *et al.* 1998). For example, Ts1Cje mice display learning and memory impairment, behavioral abnormalities indicative of hippocampal dysfunction, and reduced LTP, though several of these phenotypes appear to be less severe than in Ts65Dn mice (BELICHENKO *et al.* 2009; OLSON *et al.* 2007; SAGO *et al.* 1998; SIAREY *et al.* 2005). Furthermore, Ts1Cje display craniofacial alterations similar to those in Ts65Dn mice and individuals with DS, with the exception of brachycephaly (RICHTSMEIER *et al.* 2002). Interestingly, though Ts1Cje mice display significantly reduced cerebellar volume (similar to Ts65Dn), showed little change in granule cell and Purkinje cell density, indicating a significant alteration in phenotype compared to Ts65Dn and a role for triplicated genes dissimilar between the two models (OLSON *et al.* 2004b).

Ts1Yey, Ts2Yey, and Ts3Yey are three other mouse models which have been developed to test the effects of triplication of Hsa 21 orthologs in three copies in the mouse. Ts1Yey, Ts2Yey, and Ts3Yey mice are trisomic for Has 21 gene orthologs found on Mmu 16, Mmu 10, and Mmu17, respectively (YU *et al.* 2010a). Ts1Yey and Ts3Yey mice display some learning impairment (YU *et al.* 2010b). Ts2Yey mice, however, do not display alterations in learning or memory (YU *et al.* 2010a). A combination of these three models called the 'triple trisomy' model (Ts1Yey;Ts2Yey;Ts3Yey) mimics most behavioral

phenotypes also observed in Ts65Dn mice (YU *et al.* 2010a). Further research is necessary to better classify these models and their genotype-phenotype relationships.

The Ts1Yah mouse model contains a triplication of 12 genes from *Abcg1-U2af1* found in the Hsa 21 sub-telomeric region and was developed to understand what, if any, contribution these genes make to DS phenotypes. Ts1Yah mice display defects in novel object recognition, open field, and Y-maze tests. However, these mice show improved hippocampal-dependent spatial memory and enhanced LTP in the hippocampus, with several genes including *Ndufv3*, *Wdr4*, *Pknox1*, and *Cbs*, all candidates for the gain in cognitive function when overexpressed (PEREIRA *et al.* 2009). As described, segmentally trisomic mouse models have added significant information to the field which helps describe how the genes found in these segments contribute to various phenotypes.

1.4 Mouse Genotype-Phenotype Relationships

Mice have been readily used for over a decade in DS to better understand how trisomic genes impact the development of phenotypes, allowing for accessibility to numerous tissues and all stages of development. In particular, using models trisomic or monosomic for a single gene, or using knock-in and knockout approaches have made DS mouse models even more valuable to the research community. Genes such as that encoding amyloid precursor protein (*APP)* have been heavily studied for their contribution to DS phenotypes including the development of Alzheimer disease (AD)-like pathology in all individuals trisomic for this gene. Ts65Dn mice display cognitive deficits in the Morris water maze, cholinergic neuronal degeneration, and decreased nerve

growth factor (NGF) transport, all related to changes in the hippocampus—a major target of AD pathological insults (SALEHI *et al.* 2006; SEO and ISACSON 2005). Using mice generated from a cross of Ts65Dn mice females (three copies of *App*) with males with just one copy of *App* (a single copy deletion), investigators found that offspring were viable with no detectable nervous system abnormalities (CATALDO *et al.* 2003). Furthermore, while Ts65Dn mice with three copies of *App* have decreased NGF transport, knock down of one copy of *App* dramatically increased NGF transport, cultivating a direct relationship between copy number of *App* and NGF retrograde transport in Ts65Dn mice (SALEHI *et al.* 2007).

Brains from Ts65Dn mice display an increase in the number and size of astrocytes and a high level of synaptojanin-1 expression (ANTONARAKIS *et al.* 2004). Interestingly, Ts65Dn mice disomic for S*ynj1* (*Synj1* knockout mice) display smaller brains than euploid littermates, postnatally, at a time when gliogenesis is prominent, thus indicating a potential astroglial population may cause this decreased brain size (HERRERA *et al.* 2009). Recently, Herrera and colleagues explored this interaction *in vivo* and found that in *Synj1* knockout mouse brains, glial markers were down regulated compared to euploids, but no changes in neuronal markers, indicating that *Synj1* is involved in astrogliogenesis but not neurogenesis (HERRERA *et al.* 2009). Interestingly, synaptic morphology and endocytosis, appear to be regulated by multiple genes, including *Synj1* as well as *Itsn1* and *Rcan1*. A recent study investigated the effects of these three genes on the altered synapses and endocytosis seen as a DS neuronal phenotype. Investigators found that overexpression of each gene individually in the

context of a normal genetic complement did lead to abnormal synapses, but overexpression of all three genes in the context of a normal genetic complement were necessary in order to cause the full phenotype of impaired vesicular recycling with regulation of genes by other genes within this group of three (CHANG and MIN 2009).

1.5 *Dyrk1a*: a Candidate Gene for Craniofacial Development Regulation

Dual-specificity tyrosine-(Y)-phosphorylation regulated kinase 1A, *DYRK1A* , a gene mapped to 21q22.13 and triplicated in the Ts65Dn and Ts1Rhr mouse models, is a serine-threonine kinase and a homolog of the *Drosophila minibrain (Mnb)* gene, known to be involved in neuronal proliferation and postembryonic neurogenesis (TEJEDOR *et al.* 1995). Dyrk1a is known to phosphorylate several transcription factors including Nfat (nuclear factor of activated T cells) in mouse cortical neurons and RNAi studies in *Drosophila,* and the forkhead transcription factor FKHR in HEK-293 cells (ARRON *et al.* 2006; GWACK *et al.* 2006; WOODS *et al.* 2001), giving it the potential to impact various cellular events (Figure 1.6A) and is also capable of self-phosphorylation at its kinase domain (KENTRUP *et al.* 1996). In addition, *DYRK1A* is hypothesized to act in concert with another Hsa 21 gene, *RCAN1*, a calcineurin inhibitor (Figure 1.6B), in the localization of the transcription factor NFAT (ARRON *et al.* 2006; EPSTEIN 2006). This transcription factor plays a role in lymphoid development, morphogenesis of the vertebrate heart valves, vascular organization, brain development and skeletal development and homeostasis (GRAEF *et al.* 2001; SITARA and ALIPRANTIS 2010; WINSLOW *et al.* 2006).

Mutations in this gene have been reported to lead to reduced optic lobes and central brain hemispheres in adult *Drosophila* (SMITH *et al.* 1997), and its overexpression has been linked to DS pathophysiology of Alzheimer disease (KIMURA *et al.* 2007; RYOO *et al.* 2007). *In vitro*, Dyrk1a is known to induce phosphorylation of p53 and inhibits proliferation of embryonic neural cells (PARK *et al.* 2010), while overexpression of *Dyrk1a* inhibits proliferation and induces premature neural differentiation of neural progenitor cells (YABUT *et al.* 2010), lending to the suggesting of *Dyrk1a* as a strong candidate for neurological abnormalities in DS. In addition, knockout mice for *Dyrk1a* are embryonic lethal and *Dyrk1a* heterozygotes exhibit developmental delay and decreased viability, indicating an effect of gene dosage (FOTAKI *et al.* 2002). Expression patterns have been sparingly defined throughout the adult and developing brain in mice (HAMMERLE *et al.* 2002; SMITH *et al.* 1997) and heart in rats (OKUI *et al.* 1999), but the actual role of *Dyrk1a* in many of these cases remains to be elucidated.

Mice carrying deletions of components of the NFAT pathway share similar skull and facial phenotypes to those of DS (ARRON *et al.* 2006). Regulation of this pathway is modulated by several components: calcium is responsible for stimulating calcineurin, a phosphatase, which binds directly to NFATc (also known as NFAT2) proteins leading to dephosphorylation and nuclear translocation of NFATc (BEALS *et al.* 1997); *DSCR1/RCAN1* endogenously inhibits the binding of calcineurin to NFAT, preventing its calcineurin from dephosphorylating NFAT and allowing its nuclear translocation (FUENTES *et al.* 2000); and DYRK1A primes substrates for phosphorylation by GSK3, which then phosphorylates NFATc proteins in the nucleus, leading to translocation to the cytoplasm (BEALS *et al.*

1997; GRAEF *et al.* 2001). Thus, it has been hypothesized that, in the cases of DS compared to individuals with a normal genetic complement, three copies rather than two of *DYRK1A* and *RCAN1* would lead to a synergistic effect on NFAT by causing high levels of cytoplasmic localization of NFAT when compared to its homeostatic state (ARRON *et al.* 2006) (Figure 1.7).

Of particular interest in this pathway is how *DYRK1A* and *RCAN1* are regulated both independently and in the presence of one another. Recently, Dyrk1a was found to directly interact and phosphorylate *Rcan1*, which in turn leads to the priming of Gsk3β and further *Rcan1* phosphorylation. This phosphorylation was also shown to inhibit the phosphatase activity of calcineurin, leading to reduced Nfat nuclear localization and thus transcriptional activity (JUNG *et al.* 2011). Both of these genes are triplicated in DS and the Ts65Dn and Ts1Rhr mouse models of DS and are found in the DSCR. From this information, it can thus be hypothesized that these genes would maintain a relative 1.5 fold expression to euploid tissue if no other factors are involved. Therefore, due to the inhibitory actions of both *Dyrk1a* and *Rcan1*, a feedback loop in which both *Dyrk1a* and *Rcan1* are expressed approximately 1.5 fold in a tissue would occur, leading to cytoplasmic Nfat. Furthermore, a study in bone homeostasis showed that forced expression of NFATc1 induced *DYRK1A* expression, suggesting a negative feedback loop which regulates NFAT activity (LEE *et al.* 2009). If this paradigm holds true temperospatially, then cycling of *Dyrk1a* levels, as *Dyrk1a* is a downstream target of Nfat activation, would hypothetically lead to increased activation of *Rcan1* in the presence of excess *Dyrk1a* and thus increased cytoplasmic localization of Nfat.

1.6 Craniofacial Development

All individuals with DS are known to display a form of craniofacial phenotypes through which they are often first classified at birth. Though not typically used as a fetal marker of DS, it has been hypothesized that a shortened mandible may be representative of the craniofacial anomalies associated with DS as a prenatal marker, especially considering the secondary phenotypes which arise, characterizing the syndrome. The craniofacial skeleton is affected extensively, leading to the adverse phenotypes which impact quality of life and independence for these individuals.

Craniofacial alterations most commonly associated with DS include both skeletal anomalies and alterations in soft tissue. The characteristic facial bone alterations span the architecture of the skull and include a shortened midface, small, dysmorphic mandible, small oral cavity, relative macroglossia, and brachycephaly (a decrease in the distance from the anterior to the posterior of the skull) (GUIHARD-COSTA *et al.* 2006; GUIMARAES *et al.* 2008). In conjunction with skeletal abnormalities, soft tissue alterations including upslanting palpebral fissures, inner epicanthic folds, and a generalized hypotonia compound problems which arise from these primary features (EPSTEIN 2001). Due to these alterations, secondary phenotypes are often noted clinically and include both structural and functional complications. Many individuals with DS present with impaired mastication and speech, narrow airways, airway and esophageal obstructions, dental anomalies and sleep apnea that appear to be comorbid with Down syndrome (SHOTT 2006; VENAIL *et al.* 2004). Of consequence is the interaction between tissues in the region of the developing skull and face and thus, alterations in this process due to

changes set in place from Trisomy 21 may cause a gross effect on multiple features of the DS skull and face (HELMS and SCHNEIDER 2003; KNIGHT and SCHILLING 2006).

The development of the craniofacial skeleton is a complex process mediated by the interactions of several tissues. The embryonic precursor to the mandible, the first pharyngeal arch, or PA1, develops from cells migrating primarily from rhombomere 2 (mandibular component) and rhombomere 1 and the caudal mesencephalon (maxillary component) (LUMSDEN *et al.* 1991). Cells populating the PA1 consist of cranial neural crest cells (NCC), a migratory population of cells which undergoes epithelial-to-mesenchymal transition (EMT) in order to delaminate from the closing dorsal neural folds in mammals (ACLOQUE *et al.* 2009). These cells are known to sculpt the development of the facial prominences and the pharyngeal arches through their contributions to the connective tissues of the face and the development of the facial skeleton (CORDERO *et al.* 2010) and in essence lay the scaffold upon which the head and face become constructed, thus implicating them in the morphology of the face (TRAINOR 2010). Cranial NCC contribute not only to the development of bone and cartilage of the head, but also to connective tissue and peripheral nervous tissue (SANTAGATI and RIJLI 2003). Furthermore, other populations of NCC play vital roles in the development of specific cell types in the peripheral nervous system, including glial cells and neurons, melanocytes, dental pulp and dentin, cardiac tissue, and smooth muscle lining (DUPIN and SOMMER 2012). This particular subset of cell, however, when it interacts with surface ectoderm, mesoderm, and pharyngeal endoderm, contributes to the proper development of the PA1 derivatives, including the mandible (COULY *et al.* 2002).

Due to the contributions of these cells to the structures of the head and neck, alterations in the characteristics of these cells including their migratory patterns and proliferative capacities provide a potential basis for anomalies occurring in these areas, and thus it has been hypothesized that a common mechanism affecting these cells is caused by overexpression of Hsa 21 genes (KIRBY 1991). Similar pathologies also seen in Treacher Collins syndrome of cranial NCC origin in which individuals develop hypoplasia of facial bones including the maxilla and mandible, and alterations of the external and inner ears, leading to secondary phenotypes of malocclusion and conductive hearing loss (PHELPS *et al.* 1981; POSWILLO 1975). Interestingly, these individuals also display alterations in brain development reminiscent of those seen in DS (TEBER *et al.* 2004).

It is important to note that NCC have been associated with a number of congenital anomalies which are not limited to the craniofacial region, but often occur comorbidly with craniofacial alterations. For example, individuals with Di George Syndrome display craniofacial alterations, but also thyroid, parathyroid, thymus, and heart/vessel anomalies which have some relation to NCC origin (KIRBY and STEWART 1984). In addition, individuals with Noonan's Syndrome also display craniofacial alterations which are in conjunction with heart/vessel anomalies (NOONAN 1968).

Several hallmarks of cranial NCC location and activity mark the timeline of PA1 development. At stage 10 on the Carnegie Scale of Development (approximately 3 weeks in humans and 8.25 days in mice), the neural folds from which the cranial NCC delaminate begin to fuse. By stage 11 (approximately 3.5 weeks in humans and 9-9.25 days in mice) the PA1 has begun to form and cranial NCC continue to migrate through

the body to various structures which will contribute to the head and neck. By stage 13 (4 weeks in humans and 9.5 days in mice), nearly all migration of cranial NCC from the NT and neural folds to the PA1 has completed and those cells within the PA1 continue to undergo mitosis (O'RAHILLY and MULLER 2007; YAMAGISHI *et al.* 2006). The PA1, once fully developed, continues to delineate into a number of structures which will become more evident with maturation. For example, tissue from the PA1 will contribute not only to the mandible, but also to tissues of the skull wall, the teeth, the middle ear, part of the tongue, and many other soft tissues of the orofacial region (YAMAGISHI *et al.* 2006). Due to the phenotypes observed in individuals with DS including craniofacial development, the cranial NCC population has been studied to understand the mechanisms behind DS craniofacial phenotypes, especially through the use of DS mouse models.

1.7 Cellular Phenotypes of Down Syndrome

Of particular interest in understanding how DS phenotypes arise during development are the cellular phenotypes of individuals with DS. As previously described, a cranial NCC deficit is present in the developing mandible of Ts65Dn embryos which appear to be caused by the observed proliferation and/or migration deficits from *in vitro* studies (ROPER *et al.* 2009). This deficit has been classified between E9.25 during which no significant alterations in PA1, NCC number, or migration appear to be present, and E9.5 where these alterations become evident quantitatively (ROPER *et al.* 2009). In essence, this creates a window of 6 hours during which the deficit develops and precisely defines a period of time crucial for further study. Furthermore, it is important

to note that this cellular phenotype has been classified *in vitro* using neural tube explants and cresyl-violet stained embryo sections, which showed a decreased propensity of cells delaminating from the neural tube to migrate and proliferate, respectively, in Ts65Dn embryos compared to euploid embryos (ROPER *et al.* 2009).

Other studies have described cellular proliferation deficits *in vitro* using cells derived from individuals with DS including the fetal cerebellum, hippocampus, and skin fibroblasts (CONTESTABILE *et al.* 2007; GUIDI *et al.* 2011; KIMURA *et al.* 2005). Using cells from the hippocampal dentate gyrus from fetuses with DS and Ts65Dn mice, investigators showed that a reduction in the number of proliferating cells occurred compared to euploid controls, marked by a reduction of cells cycling in S phase, but an increase in proliferating cells in G2 (CONTESTABILE *et al.* 2007). This study not only better classified the hypothesized proliferation impairment, but also suggested a role for alterations in the cell cycle as a determinate of cell proliferation propensity (CONTESTABILE *et al.* 2007). Ts65Dn mice also display other cellular deficits, but these have been primarily limited to neurogenesis and a proliferation deficit in neural and granule precursor cells shown through *in vitro* studies (CONTESTABILE *et al.* 2009a; TRAZZI *et al.* 2011). Additionally, neuronal precursors of the cerebellum and hippocampus have been shown to exhibit reduced proliferation rather than apoptosis as previously hypothesized (CHAKRABARTI *et al.* 2007; CONTESTABILE *et al.* 2007; LORENZI and REEVES 2006; ROPER and REEVES 2006). In order to understand overall proliferation of cells in DS, Contestabile and colleagues also evaluated proliferation in peripheral tissues of Ts65Dn neonates *in vivo* and *in vitro* and found a proliferation impairment in cultured fibroblasts, characterized

by fewer actively proliferating cells but no observed change in the cell cycle (CONTESTABILE *et al.* 2009b). This study emphasized that potential for an overall defective proliferation mechanism as a phenotype of DS as inferred from results using Ts65Dn-derived tissue (CONTESTABILE *et al.* 2009b). Interestingly, Tc1 fibroblasts also showed DS-like aberrant proliferation and adhesion, as well as a decreased cell migration propensity *in vitro* (DELOM *et al.* 2009), further solidifying the hypothesis of a generalized proliferation deficit in DS tissues.

1.8 Treatments in Down Syndrome

The focus on therapeutic interventions in DS has primarily been dedicated toward rescuing cognitive deficits in individuals with DS with much emphasis being place on specific gene targets with a phenotype of interest in mind. Several pharmacological therapeutics have since been proposed to overcome, for example, cellular proliferative deficits, in hopes of rescuing cognitive deficits in DS mouse models. However, little has been done to understand the mechanism of this deficit and ameliorate other cellular deficiencies, such as that of the mandibular precursor during developing. Several studies have pioneered these treatments in DS mouse models, including the use of several drugs which effect synaptic plasticity, brain biochemistry, and brain morphology. LTP is reduced in the hippocampus of Ts65Dn mice and occurs in part due to an imbalance between excitatory and inhibitory activity which can be overcome by drugs that inhibit γ-aminobutyric acid A ($GABA_A$) receptors (BELICHENKO *et al.* 2007; KLESCHEVNIKOV *et al.* 2004; SIAREY *et al.* 1997). Picrotoxin (PTX) and pentyletonetetrazol (PTZ) bind non-

competitively to $GABA_A$ receptors acting as antagonists. Studies in Ts65Dn mice treated with PTX or PTZ have revealed complete rescue of novel object recognition test deficits and rescue of learning and memory deficits even after cessation of treatment (FERNANDEZ and GARNER 2007; RUEDA *et al.* 2008) compared to untreated Ts65Dn mice. Clinical trials are currently underway to understand the impacts of PTX and PTZ in humans.

Memantine, an NMDA receptor antagonist, is currently approved as a treatment for moderate to severe AD as it has been routinely shown to lessen cognitive deterioration through a neuroprotective function, with benefits discernible in cognition, function, and global scale measurements over long-term treatment (AREOSA and SHERRIFF 2003). Several groups have thus moved this treatment into the Ts65Dn mouse model of DS in short and long term studies and assessed its effects on memory and degeneration, two phenotypes well-classified in Ts65Dn mice (COSTA *et al.* 2008; LOCKROW *et al.* 2011; RUEDA *et al.* 2010; SCOTT-MCKEAN and COSTA 2011). Memantine treatment was sufficient to improve both spatial and recognition memory performance in Ts65Dn mice, but no morphological changes were observed in the treated mice. Interestingly, treated mice showed elevated levels of brain-derived neurotrophic factor expression in the hippocampus and frontal cortex, indicating that behavioral modification may be a result of memantine treatment (LOCKROW *et al.* 2011; RUEDA *et al.* 2010). Clinical trials are also underway for mematine treatment to understand its efficacy in humans.

Decreased NGF transport has been observed in Ts65Dn hippocampi and models AD pathology. An increase of amyloid-β peptide, a hallmark of AD, also occurs after traumatic brain injury (TBI), leading to an increased risk for AD later in life. NGF has

recently been shown to display trophic properties which produce an anti-amyloidogenic activity (CALISSANO *et al.* 2010) and thus may have a role in the treatment of AD pathology. Mice with induced TBI showed significantly increased APP and Aβ expression, but those treated with NGF intranasally showed attenuated Aβ deposition and improved functional outcomes (TIAN *et al.* 2012). Thus, NGF appears to be an excellent candidate in treatment of AD pathology after initial disease development and would be ideal for study in the Ts65Dn mice. Similarly, L-DOPS corrects deficiencies in norepinephrine found previously in Ts65Dn mice and, in combination with carbidopa, restores learning and memory deficits according to contextual fear conditioning tests (SALEHI *et al.* 2009).

The small, cellular deficit in the cerebellum of individuals with DS is of concern due to the importance of this structure in motor control and various cognitive tasks. A study to understand the origin of this deficit in the Ts65Dn mouse revealed a paucity of granule cell precursors early in postnatal development. Interestingly, these cells showed a marked reduction in sonic hedgehog (Shh) protein signaling mitogenic response. Treatment of newborn trisomic mice with a Shh agonist led to a restoration of granule cell precursors and mitotic cells in the cerebellum to euploid levels. Results from this study not only indicate that this cellular deficit results from defective response to Shh, but also shows that an agonist for Shh can jumpstart pathways necessary to rescue the cellular deficit, linking Shh spatiotemporally to mitosis of these cells (ROPER *et al.* 2006a).

1.9 Inhibitors of Dyrk1a as Treatment in Down Syndrome

There has been a heavy focus on therapies utilizing the inhibition of DYRK1A, due to its complex involvement in DS phenotypes in recent years. Epigallocatechin-3-gallate (EGCG) is the most common polyphenol in green tea, constituting 9-13% of the total dry weight (DUFRESNE and FARNWORTH 2001) and recognized worldwide for its antioxidant properties and other health benefits including positive effects on metabolic syndrome, cognitive function, neuroprotection, cancers, bone health, cardiovascular risk reduction, and many others (Figure 1.8A) (HODGSON and CROFT 2010; NAGLE *et al.* 2006; WILLIAMSON *et al.* 2011). EGCG and many similar components have been well researched and categorized for their use as therapeutics in human cancer prevention in treatment through their ability to decrease angiogenesis and their anti-proliferation effects as well as their ability to prevent oxidative damage in healthy cells (CHEN *et al.* 2011). Green tea polyphenols also maintain several categories of effectors, most notably including receptor tyrosine kinases (RTKs) and gene targets, including *Dyrk1a* (BAIN *et al.* 2007; LARSEN *et al.* 2010), and these compounds appear to affect a wide array of signal transduction pathways downstream including JAK/STAT, MAPK, PI3K/AKT, Wnt, and Notch (SINGH *et al.* 2011). The inhibition of RTKs is especially relevant, since RTKS play a crucial role in the homeostasis of cellular processes, including cell proliferation and apoptosis (LARSEN *et al.* 2010). Furthermore, since EGCG is able to cross the blood-brain and placental barriers (CHU *et al.* 2007) and is already currently available for oral administration at a reasonable cost (SARTIPPOUR *et al.* 2002), the use of this compound during embryonic development, when many of the known deficits in DS are

hypothesized to arise neurologically and otherwise (such as the mandibular precursor), is feasible. Similarly, since *Dyrk1a* is found in three copies in DS and in multiple mouse models of DS at specified times points and tissues (such as the E9.5 PA1 or the DS brain), its use for both *in vitro,* for the determination of efficacy, viability, and a general understanding of adverse effects, and *in vivo* studies to determine the effects of *Dyrk1a* on these phenotypes by reducing only *Dyrk1a* copy number in an otherwise segmentally trisomic system, could potentially be therapeutic.

Several *in vitro* studies using cells from cell lines and mice and *in vivo* studies in mice have been performed to date outlining the wide array of roles EGCG can play in the disease pathophysiology. Nude mice treated with EGCG through oral gavage in the presence of a adjuvant led to inhibition of tumor growth and delayed tumor progression through increased apoptosis, decreased proliferation, and reduced phosphorylation of AKT (ZHANG *et al.* 2008). Mice transgenic for *Dyrk1a* and four other genes fed a diet of green tea polyphenols showed a rescue of brain weight alterations and cognitive deficits observed before treatment, indicating not only the importance of *Dyrk1a* in these phenotypes, but also the translational impact of EGCG *in vivo* (GUEDJ *et al.* 2009).

Little evidence currently exists in the literature regarding these properties in humans, but several recent studies have described some positive effects with no significant adverse side effects noted in all studies. A study conducted by Ellinger and colleagues reveled increased plasma antioxidant capacity, reduction of oxidative stress markers, and reduced lipid peroxidation in individuals on various EGCG and green tea polyphenol regimens (ELLINGER *et al.* 2011). In addition, Polyphenon E, a standardized

green tea polyphenol pharmaceutical, is currently being used in clinical trials for prostate and bladder cancer, as well as leukemia, (HARA 2011; SHANAFELT *et al.* 2009) and has been approved by the FDA for other uses, such as a treatment for warts (TATTI *et al.* 2010), and developments continue to be made in the hope of producing more specific compounds for clinical trials (HARA 2011).

Harmine, a β-carboline alkaloid derived from plants, is another natural Dyrk1a inhibitor which targets the kinase activity of this receptor tyrosine kinase (Figure 1.8B) (BAIN *et al.* 2007; GOCKLER *et al.* 2009). *In vitro* studies using harmine as a Dyrk1a inhibitor have shown its ability to inhibit tau phosphorylation at Alzheimer disease-relevant sites and regulate NFAT expression in osteoclast progenitor cells (EGUSA *et al.* 2011; FROST *et al.* 2011). However, harmine inhibits monoamine oxidase A and could lead to a build up on neurotransmitters in the brain (BOEIRA *et al.* 2001).

INDY, a benzothiazole derivative which has Dyrk1a ATP-competitive binding affinity, is capable of reversing aberrant tau phosphorylation (an Alzheimer disease phenotype) in culture and is sufficient to rescue levels of repressed NFAT signaling induced by *Dyrk1a* overexpression (Figure 1.8C) (OGAWA *et al.* 2010). Further studies using the pro form of this drug will be necessary to understand its efficacy *in vivo*.

A study performed by Wang and colleagues showed the importance of screening compounds for their confirmation and interaction with the ATP binding pocket of DYRK1A, shown to be the target of other potent DYRK1A inhibitors and an optimal site for inhibition (ADAYEV *et al.* 2006; ADAYEV *et al.* 2011). The screening revealed six novel compounds, of which two were selected (compounds 3 and 5) for studies to elucidate

their mechanism (Figures 1.8 and 1.8E). Compounds 3 and 5 displayed similar confirmations to INDY and harmine, respectively, likely accounting for their potency, with compound 3 providing stronger inhibition than EGCG *in vitro* (WANG *et al.* 2012).

1.10 Hypotheses

We hypothesize that the NCC deficit found in Ts65Dn embryos *in vitro* and *in vivo* can be reproduced and refined in our cell culture system and modified using natural Dyrk1a inhibitors to rescue proliferation and migration deficits to euploid levels. We also hypothesize that harmine and EGCG work by independent mechanisms , though both involve inhibition of Dyrk1a, due to their known impacts in similar and dissimilar biochemical pathways and activities. Furthermore, we hypothesize that *in vivo* treatment of Ts65Dn pregnant mother with EGCG will lead to a rescue of the trisomic embryonic mandibular precursor to euploid volume and cell number.

CHAPTER 2. MATERIALS AND METHODS

2.1 Mouse Husbandry

Female B6EiC3 Sn a/A-TS(1716)65Dn (Ts65Dn) and male B6C3F1 mice obtained from The Jackson Laboratory (Bar Harbor, Me) were mated in breeding colonies at Indiana University-Purdue University Indianapolis to produce female offspring for colony maintenance and for breeding to complete embryonic studies described below. Female Ts65Dn mice were bred with Wnt1-lac Z males (B6CBA-Tg(Wnt1-lacZ)206Amc/J (The Jackson Laboratory, Bar Harbor, ME) for embryonic studies. Females were checked for estrus and placed in the cage containing the Wnt1-lacZ male for overnight mating. Females were checked for vaginal plugs the next morning to ascertain timed mating. Noon on the day of the plug was established as embryonic day 0.5 (E0.5) for developing embryos. Pregnant females were isolated from breeding partners until they were killed when embryos were at developmental stage E9.5. Pregnant mothers were euthanized between 10am and 12pm nine days after the plug was found with isoflurane (Vedco, Inc., St. Joseph, MO), followed by cervical dislocation. Embryos were dissected from pregnant females and were assessed for developmental stage by somite number. Somites are collections of mesoderm which have the ability to differentiate into numerous tissue types throughout the body, including cartilage, bone, muscle, and

dermis (CHRIST and ORDAHL 1995) and have recently been shown to act as a staging measurement of intrinsic development (VENTERS *et al.* 2008), though they have been utilized for developmental staging extensively (PALMEIRIM *et al.* 2008). Dissected embryos were then fixed for histological analysis as described below or first pharyngeal arch (PA1) and neural tube (NT) tissues were isolated for further manipulation. Quantification of somites was undertaken for each embryo in order to determine their relative developmental stage. E9.25 embryos from pregnant females killed at approximately 6am nine days after the plug were utilized for RNA from the PA1 and NT if between somite stages 15 and 18, and E9.5 embryos were utilized for RNA, cell culture, or whole mount embryo embedding if between somites stages 21 and 24.

Dp(16Cbr1-ORF9)1Rhr (Ts1Rhr) mice were obtained from Dr. Roger Reeves at The Johns Hopkins University School of Medicine (Baltimore, MD). These mice had been backcrossed toC57BL/6J (B6) mice for 12 generations (N12) to establish the B6.Ts1Rhr line. Females were bred with Wnt1-lacZ mice and checked for pregnancy as described above. Embryos taken from mothers killed nine days after the plug was found on E9.5 were utilized for cell culture as described in section.

2.2 Mouse and Embryo Genotyping

Embryos utilized for this study were genotyped by PCR or fluorescence in situ hybridization (FISH). Molecular probes created from BAC clones 401C2 and 433G17 were utilized in this study (MOORE *et al.* 1999) as they bind to the distal portion on Mmu16 triplicated in the Ts65Dn mouse model. Yolk sacs dropped onto slides were

incubated in pre-warmed saline-sodium citrate buffer (SSC, 175.3 g NaCl and 88.2 g sodium citrate in 800 ml of H_2O, pH 7.0) at 37˚ C for 30 minutes. After incubation, slides were passed through an ethanol wash for the purpose of dehydration. Slides were washed in cold 70%, 85%, and 100% ethanol for two minutes each, respectively. Concomitantly, Denhyb (Insitus Biotechnologies, Albuquerque, NM) was removed from -20˚ C and allowed to warm to room temperature. Upon reaching room temperature, Denhyb was mixed with BAC probes at a 10:1 dilution ratio and heated to 37˚C in a dark water bath. Upon removal from the final ethanol wash, slides were warmed on a 37˚C dry bath for 3 minutes in a dark room. After warming, 7 µl of the Denhyb:probe 10:1 mixture was added to the center of each slide. Each slide was then cover slipped with an 18 x 18 mm glass cover slip and each slip was sealed to the slide using rubber cement. Upon sealing, slides were transferred to a pre-warmed 85˚ C dry bath for 5 minutes and covered to ensure no light penetration. After incubation, slides were quickly transferred to a pre-warmed (37˚ C) humidified chamber to incubate overnight.

One day later, rubber cement was removed from each slide in a darkened room and slides were incubated in 68˚ C pre-warmed 2X SSC for 5 minutes. Slides were then transferred to room temperature 2X SSC for 7 minutes to equilibrate. Simultaneously, DAPI (Chemicon International, Temecula, CA) was warmed to room temperature. After the equilibrating incubation, 8 µl of Antifade/DAPI was added to the center of each slide and each slide was covered with a 22 x 22 mm glass cover slip. Slides were viewed immediately on a Nikon Eclipse 80i microscope using fluorescent green and red filters. Scoring was determined by green and red signals emitted per each nucleus. Each slide

required ten nuclei in signal number agreement in multiple locations on each slide for ploidy determination. Two signals per nuclei were labeled euploid while three signals per nuclei were indicative of the Ts65Dn marker chromosome (Figure 2.1).

After the development of a PCR technique for the extrachromosomal segment breakpoint found in Ts65Dn mice, PCR was used as described in Reinholdt *et al.*, 2011 to genotype all mice in the colony as well as embryos through yolk sac isolation. Yolk sacs taken from embryos during dissection were placed in yolk sac lysis buffer with Proteinase K (12.5 µl of Proteinase K per 1 ml of yolk sac lysis buffer, 50 µL per yolk sac) (Bioline, Taunton, MA) overnight at 55° C, then isolated the next day. To each tube, 0.25 volume of 5M NaCl was added, then tubes were vortexed and spun for 5 minutes at 13,000 rpm at 4° C. Supernatant from each tube was transferred to a new tube with 0.8 volume of isoproponol, vortexed, and left at room temperature for 5 minutes. Tubes were spun for 15 minutes at 13,000 rpm at 4° C, and then the supernatant was discarded. Pellets were then washed with 50 µl cold 70% ethanol, vortexed, and spun for 1 minute at 13,000 rpm at 4° C. Supernatant was discarded and tubes were inverted for no more than 5 minutes in order to dry the pellet. Pellets were resuspended in 20 µl of sterile distilled millipore water and were kept at 4° C.

Ts65Dn mice and embryos were genotyped using FISH until the development of primers for the breakpoint of the Ts65Dn extrachromosomal segment allowed for genotyping of mice and embryos using PCR. This method places primers on either side of the breakpoint between Mmu 16 genes and the Mmu 17 centromere of the translocation chromosome (REINHOLDT *et al.* 2011). Primer sequences for the breakpoint

were Chr17fwd_5'-GTGGCAAGAGACTCAAATTCAAC-3' and Chr16rev_5'-TGGCTTATTATTATCAGGGCATTT-3' and amplified an approximate 275-bp region. Positive control primers utilized were IMR1781_5'-TGTCTGAAGGGCAATGACTG-3' and IMR1782_5'-GCTGATCCGTGGCATCTATT-3' to amplify a 544-bp product (REINHOLDT *et al.* 2011). In at 25 µl reaction mixture, all primers were utilized at a 0.4 µM concentration each with 1 µl of DNA from mice and 2 µl of DNA from embryo yolk sacs. PCR cycling conditions were 94° C for 2 min, 34 cycles of 94° C for 45 sec, 55° C for 45 sec, and 72° C for 1 min, 72° C for 7 min, and a 4° C hold (REINHOLDT *et al.* 2011). PCR product was visualized on a 1.5% agarose gel made with 5 µl of SYBR Safe DNA gel stain (Invitrogen, Carlsbad, CA). Ts1Rhr mice and embryos were genotyped as previously established (DEITZ and ROPER 2011) using the same isolation techniques as Ts65Dn samples.

2.3 RNA Isolation

The PA1 and NT of embryos determined to be at the E9.5 developmental stage were dissected from the embryos in an RNase free environment using 30 gauge needles. Structures dissected were specified by a cut matching the line of the body for the PA1 and above the otic vesicle but below the midbrain for the NT (Figure 1.7). Tissues were placed in RNase free tubes and RNA was extracted using the PureLink RNA Micro Kit (Invitrogen, Carlsbad, CA). A final volume of 15 ml of RNA was obtained for each sample and quantification of purity and concentration was performed using the Nanodrop ND-1000 (Thermo Scientific, Waltham, MA) for nucleic acid.

2.4 Cell Culture

For the quantification of cell proliferation and migration, the PA1 and NT were removed as described in section 2.3 and placed into 0.025% trypsin/ 0.1% collagenase/DPBS (0.01 g collagenase, 100 µl 2.5% trypsin and DPBS to make a 10 ml solution) for 4 minutes at 37° C. Cells were triturated approximately ten times per sample after incubation and then spun down at 10,000 rpm for 6 minutes. The supernatant was extracted from each tube and cells were resuspended in 50 µl of MCDM, made of 50 µM 2-mercaptoethanol (1:100 in H_2O, Sigma, St. Louis, MO), 35 ng/ml retinoic acid (1:1000 in DMSO, Sigma, St. Louis, MO), 10% chick embryo extract (CEE, Seralab, West Sussex, UK), 20 ng/ml bFGF (Sigma, St. Louis, MO), 1% N2 Supplement (Invitrogen, Carlsbad, CA), 2% B27 (Invitrogen, Carlsbad, CA), 25 µl penicillin/streptomycin (P/S, Invitrogen, Carlsbad, CA) and 8.7 ml of low glucose DMEM (Invitrogen, Carlsbad, CA) per 10 ml batch of media, then filtered through a 22 µm filter with a 20 ml syringe (ZHAO *et al.* 2006). Resuspended cells were plated on fibronectin-coated 96-well plates (Becton, Dickinson and Company, Franklin Lakes, NJ) (proliferation assays) or fibronectin-coated coverslips (migration assays). Fibronectin-coated coverslips were made on the day of cell seeding. A barrier was created around the perimeter of the 22 x 22 mm glass coverslips using a Pap Pen (hydrophobic slide marker, Research Products International, Mount Prospect, IL) and allowed to dry for 15 min in at 60 x 15 mm petri dish. Poly-*D*-lysine (Sigma, St. Louis, MO) was diluted to 100 µg/ml in 1 M HEPES Solution (Cellgro, Manassas, VA) and 200 µl of this solution was pipetted onto each coverslip. Coverslips were incubated for 30 minutes at 5% CO_2 and 37° C. Poly-D-

lysine was removed from the coverslips and discarded and coverslips were washed twice with sterile filtered HEPES. Fibronectin (diluted 1:10 in HEPES, Becton, Dickinson and Company, Franklin Lakes, NJ) was added to each coverslip to cover the area inside the hydrophobic barrier and coverslips were incubated for 30 minutes at 5% CO_2 and 37° C in the NAPCO Series 8000 DH CO_2 Incubator (Thermo Scientific, Waltham, MA). Fibronectin was then removed and discarded and coverslips were again rinsed with HEPES. Each coverslip was washed with MCDM before cell seeding. Cells were incubated at 5% CO_2 and 37° C in MCDM until confluence (approximately 12-24 hours, depending on genotype and tissue). During migration assays, media changes occurred daily until assays were completed.

2.4.1 Proliferation Assay

Cells derived from PA1 and NT tissues were dissected from the embryo as shown in Figure 3.1A and were treated with trypsin/collagenase/DPBS to ensure breakdown of the tissues into individual cells. Cells were grown on the 48 well plate for 24 hours, then were quantified for cell titer using a hemacytometer. For proliferation assays, cells were grown to confluency on 96 well plates, transferred to 48 well plates, quantified, and replated on new wells at a density of approximately 1×10^4. From each sample consisting of suspended cells and 200 µl MCDM, 10 µl was removed for quantification. For each cell titer, three counts were taken on a hemocytometer and average to obtain a cell titer per 4×10^{-3} mm^2, representative of 1/25 of the original sample. To obtain the number of cells per cubic millimeter (or one microliter), this value was multiplied by 25.

Lastly, to obtain the titer for the remaining sample in the well, the value was multiplied by the remaining volume or 190 µl. Therefore, cell titer was established by 4750 x the average number of cells counted (FREI 2011). Cell titer was adjusted to $1x10^4$ for all wells to account for alterations in PA1 size and growth parameters before treatment.

Cells were allowed to grow on the plate for eight hours, media was replaced and the AQueous One Cell Titer Solution (Promega, Madison, WI) was added to each well for four hours, including one control well containing no cells. Cells were treated with dimethyl sulfoxide (DMSO, Fair Lawn, NJ), (-) Epigallocatechin gallate (EGCG) from green tea (Sigma, St. Louis, MO) in DMSO or harmine (Sigma, St. Louis, MO) in DMSO. EGCG treatments included doses of 10 µM, 25 µM and 100 µM in DMSO and harmine treatments included doses of 1 µM and 10 µM in DMSO for four hours, then the media was replaced and cells were incubated with MCDM only for four hours. Cell Titer 96 AQueous One Solution Reagent was added to each well and one control well with media and incubated for four hours. This solution contains an MTS tetrazolium compound which is bioreduced by proliferating cells through dehydrogenase enzymes into a colored formazan product which is soluble in MCDM. For quantification, 100 µl of supernatant was collected from each cell sample. Proliferation was assessed using a spectrophotometer at 490 nm and plotted on a standard curve to determine the number of cells in each well. Proliferation of trisomic and euploid tissues was compared within the cell assay to determine fold changes of proliferation for each trisomic sample relative to euploid samples.

2.4.2 Migration Assay

Cells were placed on fibronectin-coated coverslips to allow for ease of access to the cell and growth substrate. Plated cells were incubated at 5% CO_2 and 37° C for 24 hours in MCDM or until confluent, and then the scratch assay was performed as described (LIANG *et al.* 2007) by creating a diagonal scratch across the cell layer on the coverslip (Figure 2.2). Media was changed to remove and debris from the scratch and cells were treated for four hours with DMSO, EGCG in DMSO or harmine in DMSO at concentrations described in section 2.4.1. Pictures were taken at 0, 24, 48, and 72 hours after the scratch was made for quantification of migration. MCDM was changed daily with care taken to avoid disturbing the cells. Using Image J, the number of cells in the scratch were quantified and recorded as follows: each scratch was outlined to ensure conformity among scratch width before proceeding to quantification. Any images with inconsistent scratch widths were not utilized in this analysis. Using the counting tool, the number of cells within each scratch not touching the borders outlining the scratch was quantified for three images per culture. An average of these three numbers was then used as a migration count for that sample. Migration rates were established as the number of cells fully migrated into the scratch divided by the length of time since the scratch test was initiated in hours. Trisomic migration rates were then compared to euploid migration rates of the same tissue and culture group.

2.5 Quantitative (q)PCR

RNA was thawed from storage at -80˚ C for conversion to cDNA. Using the TaqMan Reverse Transcription Reagents (Applied Biosystems, Carlsbad, CA) a master mix was created for conversion to cDNA. For each reaction, 29.5 µl master mix, 19.25 µl of RNA (samples were diluted using sterile millipore water), and 1.25 µl reverse transcriptase were used to convert one sample of RNA to cDNA. Using this cDNA, master mixes were created for the reference gene (*actin*, *Ev1*) and 3 target genes. Each master mix consisted of 4 µl PCR grade water, 1 µl of probe, and 10 µl of TaqMan Gene Expression Master Mix (Applied Biosystems, Carlsbad, CA) for a total of 15 µl of master mix per well. For this analysis, 12 wells were utilized per probe and genotype, with trisomic and euploid genotypes requiring a total of 24 wells per probe. Therefore, the reaction described was multiplied by 24 to fill a plate appropriately with probe master mix. To the corresponding wells, as shown in Figure 2.3, 5 µl of cDNA was added with care taken not to contaminate cDNA samples or probe master mix already in the plate. Samples were then analyzed in duplicates using the AB 7300 Real Time PCR System (Applied Biosystems, Carlsbad, CA). Each plate was run with reference gene and 3 target genes (12 cDNA samples or 6 Eu and 6 Ts samples per plate) (Figure 2.3). Crossing point (Cp) values from each duplicate trisomic sample were then averaged and divided by the average Cp value of the two euploid samples as performed by the 7300 System Software (Applied Biosystems, Carlsbad, CA). Relative quantification was performed on Ts65Dn and euploid littermate PA1 from both treated and untreated embryos. Expression was

quantified for *Ev1* (*actin*, housekeeping gene), *Dyrk1a, Rcan1, Shh, Gli1, Ptch1,* and *Ets2* probes. Expected euploid levels of expression are equal to 1 for comparisons.

2.6 *In vivo* Assessment of the Effects of EGCG

2.6.1 Treatment Technique

In order to study the effects of EGCG *in vivo*, Ts65Dn females bred with Wnt1-lacZ males were utilized. Pregnancy was established by the presence of a vaginal plug on the morning after breeding. Pregnant females were weighed on the day of plug and daily on E7-E9. Females which gained approximately two grams by E7 since the day of establishment of the plug were orally gavaged using a 22 gauge needle with PBS or EGCG in diluted in PBS. Mice were treated with 200 mg/kg body weight using 20 mg/ml or 150 mg/kg body weight using 15 mg/ml (5 Eu mothers, 5 Ts mothers) solution or PBS (1 Eu mother, 2 Ts mothers) of equivalent volume twice daily on E7 and E8 with approximately 8 hours between doses. Mice were strictly monitored for general health assessed by daily weight changes, locomotor activity in the cage, and response to handling over the two day period of treatment before euthanizing.

2.6.2 Embryo Processing

Females were euthanized at E9.5 and whole embryos were dissected. Yolk sacs were obtained for genotyping by PCR and embryos were fixed 0.2% gluteraldehyde with 5 mM EGTA and 2 mM $MgCl_2$ in 0.1 phosphate buffer for 15 min at room temperature,

washed three times for 5 min each in was buffer (2 mM $MgCl_2$, 0.02% Nonidet P-40 in 0.1 M phosphate buffer) and stained with 0.025% 5-bromo-4-chloro-3-indoyl-β-*D*-galactopyranoside in 5 mM potassium ferricyanide, 5 mM potassium ferrocyanide for 1 h at 37° C. Embryos were then washed in wash buffer and postfixed in 4% paraformaldehyde overnight at 4° C. The following day, embryos were processed through dehydration in 1 ml increasing concentrations of ethanol (10 min each in 50%, 70%, 70%, 95%, 95%, 100%, and 100% ethanol), clearing with xylenes (10 min in 1:1 100% ethanol:Xylenes, 10 min Xylenes, and 10 min Xylenes), and infiltration with paraplast at 58° C (20 min in 1:1 Xylenes:paraplast, 20 min paraplast, and 20 min paraplast). Embryos were embedded parasagittally in paraffin wax, and then moved to a cold block for the paraplast to solidify. Embryos were cured at 4°C for seven days before sectioning.

2.6.3 Histology

Whole, cured, embedded embryos were exhaustively sectioned parasagittally using a standard microtome set to 18µm thickness per section with 5 sections per single slide. Sections were kept on a slide warmer at approximately 37° C overnight, and then were melted for one hour at 55° C the next day to ensure that sections adhered to the glass slide. Sections were further processed by CitriSolv (Fisher Scientific, Kalamazoo, MI) washes (4 min, repeated three times or until all wax was removed) to remove excess paraplast, ethanol clearing (2 min in 100% ethanol, repeated once, 1 min in 95% ethanol, and 1 min in 70% ethanol), counterstaining with 0.1% Eosin (Fisher Scientific, Kalamazoo, MI) in 100% ethanol (3-4 dips in solution, then 2 min), ethanol for clearing and excess

stain removal (10 sec in 95% ethanol, 15 sec in 95% ethanol, 1 min in 100% ethanol, repeated once), and CitriSolv washes for final processing (3 min, repeated three times). Slides were then coverslipped with 24 X 60 mm glass coverslips and DPX mountant (VWR, West Chester, PA) and were allowed to cure one week at room temperature.

2.6.4 Stereological Analysis

Fully processed embryos were assessed for proper orientation and visibility of the PA1 using a dissecting microscope and were then subjected to unbiased stereology. Sections were sampled as follows: the PA1 was assessed sampling every third section containing PA1 starting with a randomly generated number between one and three; embryonic volume and assessed sampling every fourth section starting with a randomly generated number between one and four. Parameters for the study were as follows established through the principles outlined in Mouton, 2002: for PA1 volume measurement, every third section with arch tissue was analyzed by stereology starting at a random start point chosen by a random number generator. Cells in the PA1 were counted using dissectors spaced at intervals of 60 µm with dimensions of 150 μm^2 area and 8 µm depth with a 2 µm guard height. Average CE for all volumes and cell counts was ≤ 0.10. Statistical differences were determined using a one-tailed Student's t-test. Systematic random sampling was used to quantify the number of cells in the PA1 and Calvalieri-point counting was utilized from volumetric measurements (MOUTON 2002). Region point counting was utilized to quantify embryo volume. Embryo volume was assessed with the following parameters: a frame area of 25 μm^2, 10 µm frame height, 2

µm guard height, 200 µm from spacing, 8000 μm^2 area per point, and sampling from the top of the section. Average CE values for embryo volumes were ≤ 0.01. Statistical differences were determined using a one-tailed Student's t-test.

CHAPTER 3. RESULTS: GENETIC DYSREGULATION AND MODIFICATION *IN VITRO*

3.1 *Dyrk1a* and *Rcan1* Are Dysregulated in the Ts65Dn E9.25 and E9.5 PA1 and NT

Dysregulation of *Dyrk1a* and *Rcan1*, independently and in concert, are hypothesized to influence craniofacial phenotypes via dysregulation of the transcription factor, NFATc, in its localization in the cell (ARRON *et al.* 2006). In order to determine the extent of their dysregulation on the craniofacial phenotypes observed in Ts65Dn, PA1 and NT tissues (Figure 3.1A) from E9.25 and E9.5 embryos were collected and RNA was extracted for analysis through qPCR. Samples run in duplicate showed downregulation of *Dyrk1a* and upregulation of *Rcan1* in the E9.25 PA1 and NT (Figure 3.1B). Interestingly, *Dyrk1a* relative expression (relative Ts65Dn expression to euploid expression) was upregulated and *Rcan1* was downregulated in the E9.5 PA1 and NT (Figure 3.1C). Furthermore, at E13.5 relative expression levels of *Dyrk1a* and *Rcan1* are upregulated in the PA1 (Figure 3.1D). The fluctuations in gene expression of these two genes relative to one another suggest an inverse relationship of regulation (Figure 3.2). Due to the relationship between *Dyrk1a* and *Rcan1* regulation and their hypothesized role in the developing embryonic mandible, the role of *Dyrk1a* in many DS phenotypes including cognition and brain development, and the availability of *Dyrk1a* modifiers, we

hypothesized that altering the activity of Dyrk1a could ameliorate the known cellular deficit in the PA1 at E9.5.

3.2 *Dyrk1a* and *Rcan1* Are Dysregulated in the Ts1Rhr E9.5 PA1

Ts1Rhr mice display a large, dysmorphic mandible as adults (OLSON *et al.* 2004a) and these alterations can be traced back to the developing PA1 at E9.5 (DEITZ and ROPER 2011). In order to determine what molecular changes occurred in the PA1 to cause these alterations at E9.5, the expression of *Dyrk1a*, *Rcan1*, and the transcription factor *Ets2* were studied for at E9.5 in the PA1 of Ts1Rhr embryos (Figure 3.3). Though strain-specific differences were present, *Dyrk1a* was upregulated in the PA1 and *Ets2* was downregulated in the PA1 (DEITZ and ROPER 2011). Dependent on strain, *Rcan1* was either up- or downregulated, however (DEITZ and ROPER 2011). The changes in regulation of these genes compared to that of the same structure and time point in Ts65Dn presents an interesting paradigm to study craniofacial alterations stemming from cellular alterations in proliferation and migration in the PA1 and NT tissues.

3.3 Ts65Dn Embryo PA1 and NT Display Proliferation and Migration Deficits *In Vitro*

Ts65Dn embryos at E9.5 display a smaller PA1 with fewer NCC than their somite-matched euploid littermates and fewer NCCs appear to migrate from the NT to the PA1 prior to this time point (ROPER *et al.* 2009). We cultured E9.5 PA1 and NT cells and assessed their propensity for proliferation and migration *in vitro* to confirm the reproducibility of previously published results and improve assay conditions (ROPER *et al.*

2009). Using a colorimetric assay of confluent, untreated trisomic and euploid E9.5 PA1 and NT cells to quantify proliferation revealed a proliferation deficit in trisomic PA1 and a similar proliferation level in trisomic NT when compared to euploid cells of the corresponding tissues (Figure 3.4). Previous methodologies utilized to measure proliferation and originally classify the proliferation deficit included the use of previously embedded E9.5 embryos which were stained with cresyl violet to mark mitotic and apoptotic cells (ROPER *et al.* 2009). Results previously published described a reduction in NCC in the PA1 of Ts65Dn E9.5 embryos compared to euploid littermates. In addition, these investigators also examined proliferation at E9.25 by culturing cell suspensions derived from a single PA1 each, and found fewer cells in wells containing cells from trisomic PA1 tissue compared to cells from euploid PA1 tissue.

To assess the migratory abilities of cells in the E9.5 PA1 and NT, cells were isolated as described and subjected to a migration assay using fibronectin-coated coverslips. Images taken at 24, 48, and 72 hours revealed that trisomic cells took longer to reach a state of confluency compared to euploid cells. Figure 3.5, panel 1 shows images taken at identical time points post plating, which illustrates the initial cellular deficit and growth delay indicated by slower overall migration of the confluent layer of cells into the scratch.

3.4 Ts1Rhr Embryos Do Not Display Proliferation or Migration Deficits *In Vitro*

Ts1Rhr cell culture assays were employed to better understand the molecular mechanism of action for EGCG. Ts1Rhr E9.5 PA1 and NT cells were subjected to proliferation and migration assays independently. Ts1Rhr cells proliferated similarly to euploid cells in both the PA1 and NT and appeared to display no significant alterations in proliferation rate. Cells from the E9.5 PA1 and NT of Ts1Rhr embryos were also cultured for migratory potential as previously described. Ts1Rhr cells displayed no initial migration deficit when compared to euploid cells over a culture period of 72 hours (Figure 3.6).

3.5 EGCG Ameliorates Ts65Dn Embryo Proliferation and Migration Deficits *In Vitro*

Untreated trisomic and trisomic treated with EGCG proliferation rates were compared to euploid rates in order to derive a fold change in proliferation between the cell populations. Trisomic cells derived from the Ts65Dn PA1 treated with DMSO proliferated significantly less than euploid cells in both the PA1 and NT at E9.5. Treatment of PA1 cells with 10 µM EGCG led to a significant increase in proliferation of cells in the PA1, but also a significant decrease in the proliferation of cells from the NT. Changes in trisomic PA1 proliferation were not sufficient to reach euploid levels at this concentration of EGCG, however. Treatment with 25 µM EGCG was sufficient to ameliorate the trisomic PA1 proliferation deficit without altering NT proliferation significantly. Lastly, treatment with 100 µM EGCG led to an overabundance of proliferation in both PA1 and NT cells to significant levels above euploid proliferation

(Figure 3.7). Interestingly, no initial proliferation deficit was seen in trisomic cells derived from the NT of E9.5 Ts65Dn embryos and this was maintained at the 25 µM EGCG dosage. A dose-dependent response to EGCG was thus observed in cells derived from the PA1, showing an optimal treatment dosage, but also indicating excessive EGCG on proliferation rates *in vitro*. Treatment of cells derived from the NT with EGCG showed a similar response in trend to that of treated cells from the PA1 (Figure 3.7).

Migration assessment of Ts65Dn and euploid PA1 and NT cells was performed using the scratch assay followed by treatment with DMSO or EGCG treatment for four hours. Ts65Dn PA1 cells treated with 10 µM EGCG showed a significant increase in migration compared to DMSO treatment, leading to euploid levels of migration over the 72 hours of the assay. This concentration of EGCG treatment led to an increase in migration of Ts65Dn NT cells, also, which reached near euploid levels after 72 hours in culture (still a significant increase over trisomic cell migration with DMSO treatment). Optimal migration was observed with 25 µM EGCG treatment of PA1 and NT cells when compared with migration rates of cells from euploid samples (Figure 3.8A and 3.8B). As with EGCG treatment in proliferation, a dose-dependent response was observed in migration rates for EGCG treated trisomic cells.

3.6 EGCG Does Not Alter Ts1Rhr Embryo Proliferation or Migration *In Vitro*

Proliferation of Ts1Rhr cells isolated from the PA1 and NT were also assessed using treatment with DMSO, 10 µM EGCG, or 25 µM EGCG. Analysis of cells treated with DMSO revealed significantly higher levels of proliferation in Ts1Rhr E9.5 PA1 cells

compared to euploid cells, but a proliferation deficit was observed in DMSO treated trisomic NT cells compared to euploid cells. Upon addition of 10 μM EGCG, Ts1Rhr cells from the PA1 and NT proliferated similarly to euploid cells but these proliferation rates were not significantly different from untreated trisomic cell proliferation rates. Treatment of Ts1Rhr PA1 and NT cells with 25 μM EGCG led to euploid levels of proliferation in both tissue types, established by a significant decrease in PA1 proliferation and a significant increase in NT proliferation. Treatment of E9.5 Ts1Rhr PA1 and NT cells with 100 μM led to a slight increase in PA1 cell proliferation (not significantly different from DMSO treated cells) and an increase in NT cell proliferation (not significant). Thus, no dose-dependent trends are observed in E9.5 Ts1Rhr PA1 and NT cells as were seen in cells derived from the E9.5 Ts65Dn PA1 and NT (Figure 3.9).

Ts1Rhr cells from the PA1 and NT treated with DMSO showed slight but not significant decreases in migration after initiation of the scratch assay; however, this alteration was ameliorated by the end of the 72 hour assay. Treatment of trisomic PA1 and NT cells with 10 μM EGCG led to a significant increase in PA1 cells to above euploid levels and a significant increase of NT cells to euploid levels with a slight decrease occurring over the 72 hour assay. Significant increases of migration to euploid levels also occurred in both PA1 and NT cells from Ts1Rhr E9.5 embryos. EGCG treatment appeared to alter migration only slightly over time, but values did not reach significance when compared to baseline migration in most treatment conditions (Figure 3.10).

3.7 Harmine Ameliorates Ts65Dn Embryo Proliferation Deficits *In Vitro*

Harmine, a small molecule inhibitor of Dyrk1a which binds the ATP binding pocket of the protein (ADAYEV *et al.* 2011), was also assessed for the same parameters of EGCG in cells from E9.5 Ts65Dn PA1 and NT. After establishing the deficits previously described in Ts65Dn cell culture with DMSO treatment, Ts65Dn PA1 and NT were cultured with 1 μM harmine, resulting in a significant increase in proliferation of PA1 cells to euploid levels and a slight increase in NT proliferation. Interestingly, euploid cells treated with 1 μM harmine displayed an increase in PA1 and NT proliferation to above euploid levels and those in trisomic cells treated with the same concentration of harmine. Treatment of Ts65Dn PA1 and NT cells with 10 μM harmine led to euploid like proliferation in trisomic PA1 and NT cells and an increased level of proliferation of euploid PA1 and NT cells above normal levels. Figure 3.11 shows a dose-dependent response of PA1 and NT cells to increasing concentrations of harmine, with optimal proliferation occurring at 1μM. Included in these figures and worthy of mention is the increase in proliferation observed in euploid samples in the presence of harmine.

3.8 Harmine Does Not Alter Ts1Rhr E9.5 Embryo PA1 Proliferation *In Vitro*

Assessment of proliferation in E9.5 Ts1Rhr PA1 and NT with DMSO or harmine treatment showed similar trends to EGCG in the NT. Treatment of E9.5 Ts1Rhr PA1 and NT cells with 1 μM harmine led to no change in proliferation in the PA1, while trisomic NT proliferation was rescued to euploid levels shown by a significant difference from

initially deficient proliferation of DMSO treated cells. Euploid cells treated with harmine showed a vigorous increase in proliferation compared with trisomic cells from the PA1 and NT and euploid cells from the PA1.

CHAPTER 4. RESULTS: THE EFFECTS OF EGCG *IN VIVO*

4.1 *In Vivo* EGCG Treatment Does Not Affect Litter Size

Litter sizes produced by E9.5 from pregnant females receiving EGCG or the equivalent volume of PBS on P7 and P8 of embryonic gestation were analyzed among four treatment groups using a preliminary cohort of animals: Ts65Dn mothers receiving EGCG, Ts65Dn mothers receiving PBS, euploid mothers receiving EGCG, and euploid mothers receiving PBS. Litter sizes were variable both among treatment groups and within the groups themselves. Overall, treatment did not adversely impact litter size, as euploid mothers receiving EGCG and Ts65Dn mothers receiving EGCG produced equivalent or larger litter sizes, respectively, than Ts65Dn mothers receiving PBS and as previously published (ROPER *et al.* 2006b), and produced similar litter sizes to euploid mothers receiving PBS (Figure 4.1).

4.2 *In Vivo* EGCG Treatment Does Alter Embryonic Developmental Stage at E9.5

Embryos from Ts65Dn and euploid pregnant females receiving EGCG and PBS were analyzed for developmental stage by somite number. Average somite numbers from each treatment group were quantified and no differences were found in average somites between embryo genotypes and treatment (Figure 4.2). Furthermore, a distribution of somite number for each litter from each treatment group indicated no

apparent alterations in average somite number, but an increased range of somites occurring in litters from mothers receiving EGCG (Figure 4.3).

4.3 EGCG Increases PA1 Cell Number in Trisomic and Euploid Embryos *In Vivo*

Embryos derived from pregnant females receiving EGCG and PBS were subjected to quantification using unbiased stereology of sections from whole mount embryos. Analysis of the number of cells in the PA1 of trisomic and euploid embryos from the two treatments revealed a cellular deficit in the trisomic PA1 compared to euploid, somite-matched littermates receiving PBS, as previously established (Figure 4.4) (ROPER *et al.* 2009). Trisomic embryos receiving EGCG showed an increase in cell number in the PA1 to euploid levels. In addition, euploid embryos receiving EGCG also displayed an increase in cell number in the PA1 above that of euploid embryos receiving PBS.

4.4 EGCG Increases PA1 and Embryo Volume *In Vivo*

Embryos receiving EGCG and PBS treatment were also assessed for PA1 and embryonic volume. Analysis of PA1 volumes revealed a smaller PA1 in trisomic embryos receiving PBS compared to euploid embryos receiving PBS, as previously established (ROPER *et al.* 2009). When receiving EGCG, trisomic PA1 volumes increased significantly compared to trisomic embryos receiving PBS, but not to the level of euploid PA1 receiving PBS. Furthermore, euploid embryos receiving EGCG showed a significant increase in PA1 volume compared to euploid embryos receiving PBS (Figure 4.5).

Analysis of embryonic volume of treatment groups reveled similar relationships. Trisomic embryos receiving PBS were significantly smaller than euploid embryos receiving PBS, and the addition of EGCG was not sufficient to change this relationship. However, euploid embryos receiving EGCG displayed an increased embryo volume significantly different from that of euploid embryos receiving PBS (Figure 4.6).

4.5 EGCG Alters Expression of Genes in Pathways Implicated in Craniofacial Development *In Vivo*

Embryos obtained from mothers receiving EGCG or equivalent volume PBS on E7 and E8 were utilized for gene expression analysis. Using qPCR to analyze relative expression of *Dyrk1, Rcan1, Shh, Gli1, Ptch1,* and *Ets2*, all of which are implicated in craniofacial or developmental pathways (ARRON *et al.* 2006; HILL *et al.* 2009; HU and HELMS 1999), in the PA1 of embryos receiving EGCG or PBS, we found that EGCG exposure leads to altered relative expression of several of these genes in the PA1. Baseline expression of these genes (relative expression of Ts PA1/Eu PA1) was as follows: 1.54 fold *Dyrk1,* 0.57 fold *Rcan1,* 0.55 fold *Shh,* 1.32 fold *Gli1,* 1.16 fold *Ptch1,* and 1.41 fold *Ets2* expression (Figure 4.7). Treatment of Ts65Dn embryos with EGCG revealed significant decreases in *Ptch* and *Ets2* expression in the PA1 and significant increases in *Rcan1* and *Shh* expression relative to original baseline expression values in the PA1 were observed (Figure 4.7). Other permutations of relative expression were also analyzed to better understand the effects of EGCG on the expression of these genes (Figure 4.7).

CHAPTER 5. DISCUSSION

5.1 Dysregulation of *Dyrk1a* and *Rcan1* at E9.5 May Lead to Altered NFAT Activity and Bone Development

Craniofacial alterations are present in all individuals with DS and interfere with daily functions of these individuals when combined with other DS phenotypes (such as hypotonia), leading to secondary health issues, such as failure to thrive and sleep apnea. These secondary phenotypes can lead to additional health concerns in a perpetuating cycle, such as long-term cognitive deficits (HALBOWER *et al.* 2006) and poor school performance (GOZAL 1998). Using the Ts65Dn mouse model, an origin of the cell deficit which leads to a deficient mandible in individuals with DS and this mouse model was traced to midgestation of mouse development, E9.5. From this information, we confirmed both a cellular deficit in proliferation and migration at this time point as described in Ts65Dn embryos (ROPER *et al.* 2009). Analysis of the PA1 which contributes to the mandible, as well at the NT from which neural crest cells which populate the PA1 are derived, using qPCR revealed genetic dysregulation of two genes known to regulate the transcription factor Nfatc, *Dyrk1a* and *Rcan1*. At E9.25, Ts65Dn display a downregulation of *Dyrk1a* and upregulation of *Rcan1* in the PA1, but an inverse in expression levels in the PA1 at E9.5. The continued changes in the cycling of *Dyrk1a* and *Rcan1* throughout various stages of development in the Ts65Dn PA1 also appear to

correlate with changes in the PA1 size relative to euploid littermates. At E9.25, no changes appear in the PA1 relative to euploid, stage-matched littermates and *Dyrk1a* is slightly downregulated, while *Rcan1* is upregulated. At E9.5, Ts65Dn embryos display a smaller PA1 than euploid littermates, but display upregulation of *Dyrk1a* and downregulation of *Rcan1*. At E13.5, *Dyrk1a* is highly downregulated, while *Rcan1* is highly upregulated in the PA1 where a smaller mandibular precursor is present with regard to the embryonic size. Interestingly, the tongue is of similar size in trisomic and euploid embryos, leading to a relative macroglossia in trisomic embryos. Information provided here indicates that dysregulation of these genes appears to initiate changes in the PA1 with genetic dysregulation traced back to E9.25, leading to the changes observed at E9.5 through E13.5 in development. This data may indicate the key roles for *Dyrk1a* and *Rcan1* regulation of NFAT in the proliferation and migration of NCC from the NT to the PA1 in this critical time window around E9.5.

Regulation of NFAT localization is particularly important in the PA1 (which contributes to the mandible and other facial bones) due to its ties to bone development. Members of the NFAT family of transcription factors are known to control bone homeostasis, including bone resorption and formation by osteoclasts and osteoblasts, respectively (SITARA and ALIPRANTIS 2010). Furthermore, *Dyrk1a* has been shown to inhibit Nfatc1 and transgenic mice overexpressing *Dyrk1a* have been shown to display significantly reduced bone mass reminiscent of the osteoporotic bone phenotype seen in individuals with DS (LEE *et al.* 2009). In addition, harmine, the Dyrk1a inhibitor also used in the cell culture experiments described here, has been shown to lead to

dephosphorylation of Nfatc1, disruption of events mediating osteoclastogenesis, and repression of bone resorption (EGUSA *et al.* 2011; YONEZAWA *et al.* 2011). Considering the evidence presented here, it is likely that dysregulation of NFAT localization due to dysregulation of *Dyrk1a*, *Rcan1*, or both, may lead to alterations in bone phenotypes not only in the developing craniofacial skeleton, but throughout the body.

5.2 Gene Dysregulation is Temporally Altered through Midgestation in the PA1

The condition of Down syndrome (DS), or Trisomy 21, leads to the dosage imbalance of genes on Hsa 21, and theoretically should lead to an approximately 1.5 fold relative expression of trisomic genes compared to euploid genes or the same genes from normosomic samples. However, several investigators have published evidence suggesting that genomic imbalance does not necessarily translate to transcript level, and thus other mechanisms regulate this process (KAHLEM *et al.* 2004; LYLE *et al.* 2004). In order to quantify regulation of trisomic genes *Dyrk1a* and *Rcan1* at the early stages of PA1 development, we performed qPCR on the PA1 or mandibular precursor of E9.25, E9.5, E10, and E13.5 embryos. Expression level of the two genes oscillated over the course of these time points with values upregulated for one gene and downregulated for the other at every time point except E13.5, when both genes are upregulated in the PA1. This regulation is reminiscent of the patterns of a feedback loop and may be indicative of a mechanism of regulation between the two genes. A recent study published the direct interaction of Dykr1a and Rcan1 via the phosphorylation of Rcan1 at Ser(112) and Thr(192) by Dyrk1a, increasing the ability of Rcan1 to inhibit the

phosphatase activity of calcineurin, causing reduced Nfat activity (JUNG *et al.* 2011). In addition, a brief inquiry into the regulation of these two genes when one is altered in copy number was undertaken by our laboratory. PA1 and NT tissue from *Dyrk1a* heterozygous embryos (mice with a normal genetic complement but just a single copy of Dykr1a) was used for qPCR analysis to better understand the effects of altering the copy number of one gene in this system on the other. This brief study revealed an upregulation of *Rcan1* in the presence of fixed downregulated *Dyrk1a* in the PA1 and NT. It is important to note, however, that *Dyrk1a* heterozygous mice are bred on an alternative background to that of Ts65Dn and Ts1Rhr mice and care should be taken in making comparisons in relative expression of genes between models (DEITZ and ROPER 2011). This data compiled with previously published studies suggests a feedback loop which maintains expression levels opposite in directionality of expression (upregulated versus downregulated), but in equal magnitude (Figure 5.1).

5.3 EGCG and Harmine Ameliorate Proliferation and Migration Deficits in Ts65Dn PA1 and NT Tissues *In Vitro*

Ts65Dn embryos at E9.5 display a proliferation and migration deficit in the PA1 and NT, respectively. *Dyrk1a*, a gene trisomic in Ts65Dn and in individuals with DS, is upregulated in the PA1 of Ts65Dn embryos at E9.5. Since EGCG and harmine are known Dyrk1a inhibitors, with much more known about the specific actions of harmine on Dyrk1a, we investigated the effects of these inhibitors *in vitro* on cells derived from the Ts65Dn PA1 and NT. Treatment with 25 μMM EGCG was sufficient to ameliorate

proliferation and migration deficits in Ts65Dn PA1 and NT cells, respectively, but lower levels of EGCG were not sufficient to produce euploid levels of proliferation and migration in Ts65Dn cells.

Treatment of Ts65Dn cells with harmine led to similar results with 1 µM and 10 µM concentrations, ameliorating proliferation and migration deficits in the PA1 and NT of Ts65Dn embryos, respectively. Interestingly, harmine treatment led to excessive euploid cell proliferation in both and tissue types.

5.4 EGCG and Harmine Alter Proliferation and Migration in Ts1Rhr PA1 and NT Tissues *In Vitro*

Ts1Rhr embryos display a mild proliferation deficit in the NT. *Dyrk1a* is also trisomic in Ts1Rhr mice and is upregulated in the PA1 of Ts1Rhr embryos at E9.5. Since EGCG and harmine are known Dyrk1a inhibitors, we also investigated the effects of these inhibitors *in vitro* on cells derived from the Ts1Rhr PA1 and NT in order to examine the effects of these inhibitors in a system with slight gene copy number differences and dramatic craniofacial differences. Treatment of cells with 10 µM, 25 µM, and 100 µM EGCG was able to improve NT proliferation to euploid levels in Ts1Rhr and without affecting PA1 proliferation. All concentrations of EGCG tested on PA1 and NT cells from euploid samples derived from Ts1Rhr litters displayed nominal effects.

Treatment of Ts1Rhr PA1 and NT cells with 1 µM harmine ameliorated NT proliferation deficits in Ts1Rhr embryos, but also led to excessive euploid cell proliferation in both tissue types. Though this was not specifically studied in cells

treated with EGCG, post hoc testing also showed an increase in EGCG treated euploid cells compared to those receiving DMSO. Proliferation increases in both euploid and trisomic cells may be indicative of later phenotypic changes occurring as a result of treatment with harmine and this change may also be indicative of underlying genetic alterations, as was hypothesized.

Of relevance in the context of these results are the mechanisms known or hypothesized for these two compounds. Harmine acts through a specific mechanism in which it inhibits Dyrk1a activity by interacting with the residues of the ATP binding pocket (BECKER and SIPPL 2011). In addition, it has been shown to have no adverse effects on cell viability in culture (GOCKLER *et al.* 2009). EGCG on the other hand has primarily only been studied in cancer systems, and in this case, expression of metastasis-associated 68-kDa laminin receptor confers EGCG responsiveness. However, one study performed using a mouse transgenic for Dyrk1a revealed that mice receiving green tea polyphenols displayed a correction of brain morphogenesis alterations and improvements in long term memory (GUEDJ *et al.* 2009). Despite the general lack of information regarding the effects of EGCG, we can hypothesize from the results provided here that EGCG and harmine act on Dyrk1a similarly, likely leading to a reduction in Dyrk1a activity or expression to produce these effects in vitro.

5.5 EGCG Does Not Negatively Impact Embryonic Development *In Vivo*

In preparing for an *in vivo* study, careful consideration was taken to determine which Dyrk1a inhibitor, EGCG or harmine, would be most appropriate as a gavage

treatment for pregnant Ts65Dn mothers. Despite a well-known mechanism of action for harmine on Dyrk1a, it is also known to act as an inhibitor for monoamine oxidase A (KIM *et al.* 1997; RIBA *et al.* 2003). Monoamine oxidase A functions continuously to catalyze the deamination of amines, such as norepinephrine, epinephrine, dopamine, and serotonin, in the brain and peripheral tissues by producing hydrogen peroxide as a byproduct (SHIH 1991; THORPE *et al.* 1987). Inhibiting this enzyme through use of harmine in an *in vivo* treatment could cause a toxic buildup of neurotransmitters throughout the body. Furthermore, EGCG is known to have the ability to cross the blood-brain and placental barriers (CHU *et al.* 2007) and has been used in previous *in vivo* studies through oral gavage, intraperitoneal injections, and ad libitum feedings (AMIN *et al.* 2010; GUEDJ *et al.* 2009; LONG *et al.* 2010). It is also widely available already to the public and, after water, tea is the most common beverage consumed in the world, having been a part of the Chinese diet for over 5000 years (MAK 2012; SARTIPPOUR *et al.* 2002). Therefore, due to its low toxicity, well-characterized health impacts, and potential for translational uses in humans, EGCG was chosen for the *in vivo* studies investigating the effects of Dyrk1a inhibition on NCC population of the PA1 and embryonic size.

Analysis of litter size produced from Ts65Dn and euploid mothers treated with EGCG and PBS revealed no negative impacts of EGCG on litter. In fact, litter sizes showed improvement in Ts65Dn females treated with EGCG compared to Ts65Dn females treated with PBS. Since EGCG has previously been shown to be effective in oral gavage techniques in the aim to have treatment reach developing embryos in pregnant females (LONG *et al.* 2010), there was little concern for toxic effects on the embryos. However, it

should be noted that several females were sacrificed on E9.5 that appeared to have been pregnant on E7 according to weight gain (2 grams or more), but contained only resorbed embryos and a swollen, vascularized uterus (Figure 5.2). We hypothesize that the physical stress of the gavage may have deterred pregnant females from consuming a regular intake of food and water as well as added an additional stress to their environment, causing a loss of pups between E7 and E9.5 of embryonic development.. Due to the lack of adverse impact of EGCG on litter size in Ts65Dn females, we have hypothesized that the concentration of EGCG itself is not the cause of these aborted litters, but rather the stress or volume of the treatment may be causing this artifact.

5.6 EGCG Ameliorates the PA1 Cell Deficit at E9.5 and May be Therapeutic for other DS Phenotypes

In order to understand the effects of EGCG on early mandibular development *in vivo*, Ts65Dn and euploid pregnant females treated with EGCG or PBS were analyzed using unbiased stereology under three parameters: NCC number, PA1 volume, and embryo volume. Ts65Dn embryos displayed a neural crest cell deficit at E9.5 which could be overcome with EGCG treatment on E7 and E8 of development. Interestingly, euploid embryos also treated with EGCG showed an increase in NCC number in the PA1. Results provided here indicate that similar effects occur in the developing PA1 regardless of genotype, suggesting EGCG acts similarly in both systems. Due to the knowledge presented regarding the ability of EGCG to inhibit Dyrk1a, we hypothesize that inhibition of Dyrk1a in the PA1 at E7 and E8 with EGCG treatment is sufficient to

cause alterations leading to increased NCCs proliferation to euploid levels observed at E9.5. Since *Dyrk1a* overexpression has been tied with NFAT cytoplasmic localization, a decrease in Dyrk1a activity or expression should theoretically lead to more nuclear NFAT and thus more transcriptional activity by NFAT. NFAT has many downstream targets, some of which include genes tied with homeostasis between proliferation and differentiation of cells (HUANG *et al.* 2011). Therefore, we hypothesize that this inhibition of Dyrk1a is sufficient to allow appropriate re-entry of NFAT into the nucleus, permitting euploid levels of proliferation of NCC and migration from the NT to PA1.

Though *Dyrk1a* has not been specifically studied in other proliferative disorders, it may serve as an interesting point of study in the future, in conjunction with investigations into NFAT localization. In addition, Dyrk1a inhibitors may also have a far-reaching effect on DS phenotypes. *DYRK1A* has also been highly implicated in DS brain pathology, including neuronal differentiation and maturation, spatial learning and memory deficits, and alterations in brain size and structure (AHN *et al.* 2006; ALTAFAJ *et al.* 2001; CANZONETTA *et al.* 2008; FOTAKI *et al.* 2002) and normalization of DYRK1A activity has been postulated as a therapy in DS (MAZUR-KOLECKA *et al.* 2012). Additionally, harmine has been tested on neural progenitor cells from Ts65Dn newborn mice in culture and has shown a prevention of premature neuronal maturation in trisomic cells (MAZUR-KOLECKA *et al.* 2012). Consequently, inhibition through the use of EGCG should lead to similar results and may be a valuable therapeutic in DS in the future.

5.7 EGCG Alters Expression of Genes Implicated in Craniofacial Development Pathways

EGCG is known to modify Dyrk1a activity and has been shown to decrease Dyrk1a protein levels in the presence of other green tea polyphenols (GUEDJ *et al.* 2009). Little has been established to this point, however, on the mechanism of action for EGCG and in particular, how it leads to alterations in the PA1 of the developing E9.5 Ts65Dn and euploid embryos. Relative expression analysis using qPCR revealed alterations in expression of six genes implicated alone or in part of a developmental pathway in craniofacial morphogenesis: *Dyrk1, Rcan1, Shh, Gli1, Ptch1,* and *Ets2.* Interestingly, relationships between some of these genes have been explored otherwise. For example, Dyrk1 can substantially enhance Gli1-dependent transcription (MAO *et al.* 2002), which has a function highly regulated in hedgehog signaling, known for its important role in cell proliferation and embryonic patterning (HAMMERSCHMIDT *et al.* 1997; INGHAM and MCMAHON 2001; VON OHLEN and HOOPER 1997). We hypothesize from the results presented that EGCG interacts with the feedback loop associated with *Dyrk1a* expression and signaling and also leads to alterations in expression of genes in the hedgehog pathway through alterations in *Dyrk1a* expression and/or Dyrk1a activity (Figure 5.3). Furthermore, EGCG may affect other genes through unknown mechanisms involved in craniofacial development. For example, *Ets2*, a gene triplicated in Ts65Dn mice encoding a transcription factor, has been shown to affect mesoderm-derived and neural crest-derived formative tissues which contribute to cranial skeletal elements when its gene dosage is altered in Ts65Dn mice (HILL *et al.* 2009).

5.8 Future Studies

Aside from its ability to inhibit Dyrk1a and rescue brain weight alteration in *Dyrk1a* transgenic mice (GUEDJ *et al.* 2009), little is known of the impact EGCG makes on the body of mice and embryos treated with the compound, aside from the data presented. In order to understand the broad spectrum of impact of EGCG in an *in vivo* system, an intensive evaluation of the mouse being treated, a pregnant female in this case, must be performed, including a thorough investigation for anomalies of the major organs, bones, and plasma levels of EGCG and in the case of oral gavage usage, and appearance of any physical stress of the esophagus. In addition, gross morphological evaluation should be performed of embryos throughout development. Current studies in our laboratory regarding the use of EGCG to overcome bone deficits in Ts65Dn adult mice provide compelling results in favor of EGCG treatment even after the abnormal phenotype has already been observed developmentally. Not only does this add to the application of use of EGCG treatments, but also reveals the potency of this compound.

Currently, several clinical trials are in place for DS treatments, including one using EGCG to reverse cognitive deficits observed in individuals with DS. The trial is in Phase II and will be assessing individuals between the ages of 14 and 29 years for alterations in memory and Dyrk1a activity, as well as psychomotor speed, attention, coordinator, and quality of life as secondary parameters for assessment. Individuals with be orally administered 9 mg/kg body weight of EGCG or a placebo daily for three months. The data collection phase of this trial has been completed, but not results are

currently available (ClinicalTrials.gov Identifier NCT01394796). Memantine is also currently under clinical trial for enhancement of cognitive abilities of young adults with DS, assessing neuropsychological parameters dependent on function of the hippocampus, as well as performance in a number of neuropsychological benchmarks and safety and tolerability assessments. Recruitment of individuals with DS ages 18 to 32 years to participate in a 5 mg/d week one, 5mg/BID week two, 5 and 10 mg/d divided dose week three, and 10 mg/BID week four treatment regimen is currently underway at The Children's Hospital in Colorado, U.S. (ClinicalTrials.gov Identifier NCT01112683).

Due to the potential translational impact of this research and its current use in clinical trials for other purposes, understanding what components of these compounds are producing the desired effects will be important in producing more effective and specific pharmaceuticals for treatment. While EGCG does appear to have valuable pharmaceutical properties, its specificity and impacts on other systems in the body are unknown and altering the structure or properties of this compound may allow for increased specificity with reproducible and predictable impacts throughout the body. This research will be crucial in steps toward advancing EGCG as a therapeutic by optimizing bioavailability, activity, and toxicity of various compounds. An understand the potential broad spectrum genetic effects of these compounds will also be vital, perhaps through the use of microarray of cells or various tissues exposed to EGCG treatment. Concomitantly, understanding the specific interactions of EGCG with other genes or protein produces aside from Dyrk1a should be investigated to appropriately define mechanisms of action for this compound.

LIST OF REFERENCES

LIST OF REFERENCES

ACLOQUE, H., M. S. ADAMS, K. FISHWICK, M. BRONNER-FRASER and M. A. NIETO, 2009 Epithelial-mesenchymal transitions: the importance of changing cell state in development and disease. J Clin Invest **119:** 1438-1449.

ADAYEV, T., M. C. CHEN-HWANG, N. MURAKAMI, J. WEGIEL and Y. W. HWANG, 2006 Kinetic properties of a MNB/DYRK1A mutant suitable for the elucidation of biochemical pathways. Biochemistry **45:** 12011-12019.

ADAYEV, T., J. WEGIEL and Y. W. HWANG, 2011 Harmine is an ATP-competitive inhibitor for dual-specificity tyrosine phosphorylation-regulated kinase 1A (Dyrk1A). Arch Biochem Biophys **507:** 212-218.

AGOPIAN, A. J., L. K. MARENGO and L. E. MITCHELL, 2012 Predictors of trisomy 21 in the offspring of older and younger women. Birth Defects Res A Clin Mol Teratol **94:** 31-35.

AHN, K. J., H. K. JEONG, H. S. CHOI, S. R. RYOO, Y. J. KIM *et al.*, 2006 DYRK1A BAC transgenic mice show altered synaptic plasticity with learning and memory defects. Neurobiol Dis **22:** 463-472.

ALDRIDGE, K., R. H. REEVES, L. E. OLSON and J. T. RICHTSMEIER, 2007 Differential effects of trisomy on brain shape and volume in related aneuploid mouse models. Am J Med Genet A **143A:** 1060-1070.

ALLEN, E. G., S. B. FREEMAN, C. DRUSCHEL, C. A. HOBBS, L. A. O'LEARY *et al.*, 2009 Maternal age and risk for trisomy 21 assessed by the origin of chromosome nondisjunction: a report from the Atlanta and National Down Syndrome Projects. Hum Genet **125:** 41-52.

ALTAFAJ, X., M. DIERSSEN, C. BAAMONDE, E. MARTI, J. VISA *et al.*, 2001 Neurodevelopmental delay, motor abnormalities and cognitive deficits in transgenic mice overexpressing Dyrk1A (minibrain), a murine model of Down's syndrome. Hum Mol Genet **10:** 1915-1923.

AMIN, A. R., D. WANG, H. ZHANG, S. PENG, H. J. SHIN *et al.*, 2010 Enhanced anti-tumor activity by the combination of the natural compounds (-)-epigallocatechin-3-gallate and luteolin: potential role of p53. J Biol Chem **285:** 34557-34565.

ANTONARAKIS, S. E., 1991 Parental origin of the extra chromosome in trisomy 21 as indicated by analysis of DNA polymorphisms. Down Syndrome Collaborative Group. N Engl J Med **324:** 872-876.

ANTONARAKIS, S. E., R. LYLE, E. T. DERMITZAKIS, A. REYMOND and S. DEUTSCH, 2004 Chromosome 21 and down syndrome: from genomics to pathophysiology. Nat Rev Genet **5:** 725-738.

ARAI, Y., T. IJUIN, T. TAKENAWA, L. E. BECKER and S. TAKASHIMA, 2002 Excessive expression of synaptojanin in brains with Down syndrome. Brain Dev **24:** 67-72.

AREOSA, S. A., and F. SHERRIFF, 2003 Memantine for dementia. Cochrane Database Syst Rev**:** CD003154.

ARRON, J. R., M. M. WINSLOW, A. POLLERI, C. P. CHANG, H. WU *et al.*, 2006 NFAT dysregulation by increased dosage of DSCR1 and DYRK1A on chromosome 21. Nature **441:** 595-600.

BAIN, J., L. PLATER, M. ELLIOTT, N. SHPIRO, C. J. HASTIE *et al.*, 2007 The selectivity of protein kinase inhibitors: a further update. Biochem J **408:** 297-315.

BAPTISTA, F., A. VARELA and L. B. SARDINHA, 2005 Bone mineral mass in males and females with and without Down syndrome. Osteoporos Int **16:** 380-388.

BAXTER, L. L., T. H. MORAN, J. T. RICHTSMEIER, J. TRONCOSO and R. H. REEVES, 2000 Discovery and genetic localization of Down syndrome cerebellar phenotypes using the Ts65Dn mouse. Hum Mol Genet **9:** 195-202.

BEALS, C. R., N. A. CLIPSTONE, S. N. HO and G. R. CRABTREE, 1997 Nuclear localization of NF-ATc by a calcineurin-dependent, cyclosporin-sensitive intramolecular interaction. Genes Dev **11:** 824-834.

BECKER, W., and W. SIPPL, 2011 Activation, regulation, and inhibition of DYRK1A. FEBS J **278:** 246-256.

BELICHENKO, N. P., P. V. BELICHENKO, A. M. KLESCHEVNIKOV, A. SALEHI, R. H. REEVES *et al.*, 2009 The "Down syndrome critical region" is sufficient in the mouse model to confer behavioral, neurophysiological, and synaptic phenotypes characteristic of Down syndrome. J Neurosci **29:** 5938-5948.

BELICHENKO, P. V., A. M. KLESCHEVNIKOV, A. SALEHI, C. J. EPSTEIN and W. C. MOBLEY, 2007 Synaptic and cognitive abnormalities in mouse models of Down syndrome: exploring genotype-phenotype relationships. J Comp Neurol **504:** 329-345.

BERG, J. M., and M. KOROSSY, 2001 Down syndrome before Down: a retrospect. Am J Med Genet **102:** 205-211.

BLAZEK, J. D., A. GADDY, R. MEYER, R. J. ROPER and J. LI, 2011 Disruption of bone development and homeostasis by trisomy in Ts65Dn Down syndrome mice. Bone **48:** 275-280.

BOEIRA, J. M., J. DA SILVA, B. ERDTMANN and J. A. HENRIQUES, 2001 Genotoxic effects of the alkaloids harman and harmine assessed by comet assay and chromosome aberration test in mammalian cells in vitro. Pharmacol Toxicol **89:** 287-294.

CALISSANO, P., C. MATRONE and G. AMADORO, 2010 Nerve growth factor as a paradigm of neurotrophins related to Alzheimer's disease. Dev Neurobiol **70:** 372-383.

CANZONETTA, C., C. MULLIGAN, S. DEUTSCH, S. RUF, A. O'DOHERTY *et al.*, 2008 DYRK1A-dosage imbalance perturbs NRSF/REST levels, deregulating pluripotency and embryonic stem cell fate in Down syndrome. Am J Hum Genet **83:** 388-400.

CATALDO, A. M., S. PETANCESKA, C. M. PETERHOFF, N. B. TERIO, C. J. EPSTEIN *et al.*, 2003 App gene dosage modulates endosomal abnormalities of Alzheimer's disease in a segmental trisomy 16 mouse model of down syndrome. J Neurosci **23:** 6788-6792.

CHAKRABARTI, L., Z. GALDZICKI and T. F. HAYDAR, 2007 Defects in embryonic neurogenesis and initial synapse formation in the forebrain of the Ts65Dn mouse model of Down syndrome. J Neurosci **27:** 11483-11495.

CHANG, K. T., and K. T. MIN, 2009 Upregulation of three Drosophila homologs of human chromosome 21 genes alters synaptic function: implications for Down syndrome. Proc Natl Acad Sci U S A **106:** 17117-17122.

CHAOUI, R., K. S. HELING, N. SARIOGLU, M. SCHWABE, A. DANKOF *et al.*, 2005 Aberrant right subclavian artery as a new cardiac sign in second- and third-trimester fetuses with Down syndrome. Am J Obstet Gynecol **192:** 257-263.

CHEN, D., S. B. WAN, H. YANG, J. YUAN, T. H. CHAN *et al.*, 2011 EGCG, green tea polyphenols and their synthetic analogs and prodrugs for human cancer prevention and treatment. Adv Clin Chem **53:** 155-177.

CHIU, R. W., R. AKOLEKAR, Y. W. ZHENG, T. Y. LEUNG, H. SUN *et al.*, 2011 Non-invasive prenatal assessment of trisomy 21 by multiplexed maternal plasma DNA sequencing: large scale validity study. BMJ **342:** c7401.

CHIU, R. W., H. SUN, R. AKOLEKAR, C. CLOUSER, C. LEE *et al.*, 2010 Maternal plasma DNA analysis with massively parallel sequencing by ligation for noninvasive prenatal diagnosis of trisomy 21. Clin Chem **56:** 459-463.

CHRIST, B., and C. P. ORDAHL, 1995 Early stages of chick somite development. Anat Embryol (Berl) **191:** 381-396.

CHRISTMAN, J. K., G. SHEIKHNEJAD, M. DIZIK, S. ABILEAH and E. WAINFAN, 1993 Reversibility of changes in nucleic acid methylation and gene expression induced in rat liver by severe dietary methyl deficiency. Carcinogenesis **14:** 551-557.

CHU, K. O., C. C. WANG, C. Y. CHU, K. W. CHOY, C. P. PANG *et al.*, 2007 Uptake and distribution of catechins in fetal organs following in utero exposure in rats. Hum Reprod **22:** 280-287.

CLARKE, M. J., D. A. THOMSON, M. J. GRIFFITHS, J. G. BISSENDEN, A. AUKETT *et al.*, 1989 An unusual case of mosaic Down's syndrome involving two different Robertsonian translocations. J Med Genet **26:** 198-201.

CONTESTABILE, A., T. FILA, R. BARTESAGHI and E. CIANI, 2009a Cell cycle elongation impairs proliferation of cerebellar granule cell precursors in the Ts65Dn mouse, an animal model for Down syndrome. Brain Pathol **19:** 224-237.

CONTESTABILE, A., T. FILA, A. CAPPELLINI, R. BARTESAGHI and E. CIANI, 2009b Widespread impairment of cell proliferation in the neonate Ts65Dn mouse, a model for Down syndrome. Cell Prolif **42:** 171-181.

CONTESTABILE, A., T. FILA, C. CECCARELLI, P. BONASONI, L. BONAPACE *et al.*, 2007 Cell cycle alteration and decreased cell proliferation in the hippocampal dentate gyrus and in the neocortical germinal matrix of fetuses with Down syndrome and in Ts65Dn mice. Hippocampus **17:** 665-678.

CORDERO, D. R., S. BRUGMANN, Y. CHU, R. BAJPAI, M. JAME *et al.*, 2010 Cranial neural crest cells on the move: Their roles in craniofacial development. Am J Med Genet A **2:** 270-279.

COSTA, A. C., J. J. SCOTT-MCKEAN and M. R. STASKO, 2008 Acute injections of the NMDA receptor antagonist memantine rescue performance deficits of the Ts65Dn mouse model of Down syndrome on a fear conditioning test. Neuropsychopharmacology **33:** 1624-1632.

COULY, G., S. CREUZET, S. BENNACEUR, C. VINCENT and N. M. LE DOUARIN, 2002 Interactions between Hox-negative cephalic neural crest cells and the foregut endoderm in patterning the facial skeleton in the vertebrate head. Development **129:** 1061-1073.

CREMONA, O., G. DI PAOLO, M. R. WENK, A. LUTHI, W. T. KIM *et al.*, 1999 Essential role of phosphoinositide metabolism in synaptic vesicle recycling. Cell **99:** 179-188.

DAS, I., and R. H. REEVES, 2011 The use of mouse models to understand and improve cognitive deficits in Down syndrome. Dis Model Mech **4:** 596-606.

DAVISSON, M. T., C. SCHMIDT, R. H. REEVES, N. G. IRVING, E. C. AKESON *et al.*, 1993 Segmental trisomy as a mouse model for Down syndrome. Prog Clin Biol Res **384:** 117-133.

DE, A. M. L. M., A. SAN JUAN, P. S. PEREIRA and C. S. DE SOUZA, 2000 A case of mosaic trisomy 21 with Down's syndrome signs and normal intellectual development. J Intellect Disabil Res **44 (Pt 1):** 91-96.

DEITZ, S. L., and R. J. ROPER, 2011 Trisomic and allelic differences influence phenotypic variability during development of Down syndrome mice. Genetics **189:** 1487-1495.

DELABAR, J. M., D. THEOPHILE, Z. RAHMANI, Z. CHETTOUH, J. L. BLOUIN *et al.*, 1993 Molecular mapping of twenty-four features of Down syndrome on chromosome 21. Eur J Hum Genet **1:** 114-124.

DELOM, F., E. BURT, A. HOISCHEN, J. VELTMAN, J. GROET *et al.*, 2009 Transchromosomic cell model of Down syndrome shows aberrant migration, adhesion and proteome response to extracellular matrix. Proteome Sci **7:** 31.

DOWN, J. L., 1866 Observation on an ethnic classification of idiots. Mental retardation (Washington) **33:** 54.

DUFRESNE, C. J., and E. R. FARNWORTH, 2001 A review of latest research findings on the health promotion properties of tea. J Nutr Biochem **12:** 404-421.

DUPIN, E., and L. SOMMER, 2012 Neural crest progenitors and stem cells: From early development to adulthood. Dev Biol.

EGUSA, H., M. DOI, M. SAEKI, S. FUKUYASU, Y. AKASHI *et al.*, 2011 The small molecule harmine regulates NFATc1 and Id2 expression in osteoclast progenitor cells. Bone **49:** 264-274.

EHRICH, M., C. DECIU, T. ZWIEFELHOFER, J. A. TYNAN, L. CAGASAN *et al.*, 2011 Noninvasive detection of fetal trisomy 21 by sequencing of DNA in maternal blood: a study in a clinical setting. Am J Obstet Gynecol **204:** 205 e201-211.

ELLINGER, S., N. MULLER, P. STEHLE and G. ULRICH-MERZENICH, 2011 Consumption of green tea or green tea products: is there an evidence for antioxidant effects from controlled interventional studies? Phytomedicine **18:** 903-915.

EPSTEIN, C. J., 2001 Down Syndrome (Trisomy 21). The Metabolic & Molecular Basis of Inherited Diease**:** 1223-1256.

EPSTEIN, C. J., 2006 Down's syndrome: critical genes in a critical region. Nature **441:** 582-583.

ESCORIHUELA, R. M., I. F. VALLINA, C. MARTINEZ-CUE, C. BAAMONDE, M. DIERSSEN *et al.*, 1998 Impaired short- and long-term memory in Ts65Dn mice, a model for Down syndrome. Neurosci Lett **247:** 171-174.

FERNANDEZ, F., and C. C. GARNER, 2007 Object recognition memory is conserved in Ts1Cje, a mouse model of Down syndrome. Neurosci Lett **421:** 137-141.

FOTAKI, V., M. DIERSSEN, S. ALCANTARA, S. MARTINEZ, E. MARTI *et al.*, 2002 Dyrk1A haploinsufficiency affects viability and causes developmental delay and abnormal brain morphology in mice. Mol Cell Biol **22:** 6636-6647.

FREEMAN, S. B., L. F. TAFT, K. J. DOOLEY, K. ALLRAN, S. L. SHERMAN *et al.*, 1998 Population-based study of congenital heart defects in Down syndrome. Am J Med Genet **80:** 213-217.

FREI, M., 2011 Cell Viability and Proliferation, pp. 17-21 in *BioFiles*.

FROST, D., B. MEECHOOVET, T. WANG, S. GATELY, M. GIORGETTI *et al.*, 2011 beta-carboline compounds, including harmine, inhibit DYRK1A and tau phosphorylation at multiple Alzheimer's disease-related sites. PLoS One **6:** e19264.

FUENTES, J. J., L. GENESCA, T. J. KINGSBURY, K. W. CUNNINGHAM, M. PEREZ-RIBA *et al.*, 2000 DSCR1, overexpressed in Down syndrome, is an inhibitor of calcineurin-mediated signaling pathways. Hum Mol Genet **9:** 1681-1690.

GOCKLER, N., G. JOFRE, C. PAPADOPOULOS, U. SOPPA, F. J. TEJEDOR *et al.*, 2009 Harmine specifically inhibits protein kinase DYRK1A and interferes with neurite formation. FEBS J **276:** 6324-6337.

GONZALEZ-AGUERO, A., G. VICENTE-RODRIGUEZ, L. A. MORENO and J. A. CASAJUS, 2011 Bone mass in male and female children and adolescents with Down syndrome. Osteoporos Int **22:** 2151-2157.

GOZAL, D., 1998 Sleep-disordered breathing and school performance in children. Pediatrics **102:** 616-620.

GRAEF, I. A., F. CHEN and G. R. CRABTREE, 2001 NFAT signaling in vertebrate development. Curr Opin Genet Dev **11:** 505-512.

GUEDJ, F., C. SEBRIE, I. RIVALS, A. LEDRU, E. PALY *et al.*, 2009 Green tea polyphenols rescue of brain defects induced by overexpression of DYRK1A. PLoS One **4:** e4606.

GUIDI, S., E. CIANI, P. BONASONI, D. SANTINI and R. BARTESAGHI, 2011 Widespread proliferation impairment and hypocellularity in the cerebellum of fetuses with down syndrome. Brain Pathol **21:** 361-373.

GUIHARD-COSTA, A. M., S. KHUNG, K. DELBECQUE, F. MENEZ and A. L. DELEZOIDE, 2006 Biometry of face and brain in fetuses with trisomy 21. Pediatr Res **59:** 33-38.

GUIMARAES, C. V., L. F. DONNELLY, S. R. SHOTT, R. S. AMIN and M. KALRA, 2008 Relative rather than absolute macroglossia in patients with Down syndrome: implications for treatment of obstructive sleep apnea. Pediatr Radiol **38:** 1062-1067.

GWACK, Y., S. SHARMA, J. NARDONE, B. TANASA, A. IUGA *et al.*, 2006 A genome-wide Drosophila RNAi screen identifies DYRK-family kinases as regulators of NFAT. Nature **441:** 646-650.

HALBOWER, A. C., M. DEGAONKAR, P. B. BARKER, C. J. EARLEY, C. L. MARCUS *et al.*, 2006 Childhood obstructive sleep apnea associates with neuropsychological deficits and neuronal brain injury. PLoS Med **3:** e301.

HAMMERLE, B., E. VERA-SAMPER, S. SPEICHER, R. ARENCIBIA, S. MARTINEZ *et al.*, 2002 Mnb/Dyrk1A is transiently expressed and asymmetrically segregated in neural progenitor cells at the transition to neurogenic divisions. Dev Biol **246:** 259-273.

HAMMERSCHMIDT, M., A. BROOK and A. P. MCMAHON, 1997 The world according to hedgehog. Trends Genet **13:** 14-21.

HARA, Y., 2011 Tea catechins and their applications as supplements and pharmaceutics. Pharmacol Res **64:** 100-104.

HASLE, H., 2001 Pattern of malignant disorders in individuals with Down's syndrome. Lancet Oncol **2:** 429-436.

HATTORI, M., A. FUJIYAMA, T. D. TAYLOR, H. WATANABE, T. YADA *et al.*, 2000 The DNA sequence of human chromosome 21. Nature **405:** 311-319.

HELMS, J. A., and R. A. SCHNEIDER, 2003 Cranial skeletal biology. Nature **423:** 326-331.

HERRERA, F., Q. CHEN, W. H. FISCHER, P. MAHER and D. R. SCHUBERT, 2009 Synaptojanin-1 plays a key role in astrogliogenesis: possible relevance for Down's syndrome. Cell Death Differ **16:** 910-920.

HILL, C. A., T. E. SUSSAN, R. H. REEVES and J. T. RICHTSMEIER, 2009 Complex contributions of Ets2 to craniofacial and thymus phenotypes of trisomic "Down syndrome" mice. Am J Med Genet A **149A:** 2158-2165.

HITZLER, J. K., 2007 Acute megakaryoblastic leukemia in Down syndrome. Pediatr Blood Cancer **49:** 1066-1069.

HODGSON, J. M., and K. D. CROFT, 2010 Tea flavonoids and cardiovascular health. Mol Aspects Med **31:** 495-502.

HU, D., and J. A. HELMS, 1999 The role of sonic hedgehog in normal and abnormal craniofacial morphogenesis. Development **126:** 4873-4884.

HUANG, T., Z. XIE, J. WANG, M. LI, N. JING *et al.*, 2011 Nuclear factor of activated T cells (NFAT) proteins repress canonical Wnt signaling via its interaction with Dishevelled (Dvl) protein and participate in regulating neural progenitor cell proliferation and differentiation. J Biol Chem **286:** 37399-37405.

HUETHER, C. A., J. IVANOVICH, B. S. GOODWIN, E. L. KRIVCHENIA, V. S. HERTZBERG *et al.*, 1998 Maternal age specific risk rate estimates for Down syndrome among live births in whites and other races from Ohio and metropolitan Atlanta, 1970-1989. J Med Genet **35:** 482-490.

INGHAM, P. W., and A. P. MCMAHON, 2001 Hedgehog signaling in animal development: paradigms and principles. Genes Dev **15:** 3059-3087.

JAMES, S. J., M. POGRIBNA, I. P. POGRIBNY, S. MELNYK, R. J. HINE *et al.*, 1999 Abnormal folate metabolism and mutation in the methylenetetrahydrofolate reductase gene may be maternal risk factors for Down syndrome. Am J Clin Nutr **70:** 495-501.

JUNG, M. S., J. H. PARK, Y. S. RYU, S. H. CHOI, S. H. YOON *et al.*, 2011 Regulation of RCAN1 Protein Activity by Dyrk1A Protein-mediated Phosphorylation. J Biol Chem **286:** 40401-40412.

KAHLEM, P., M. SULTAN, R. HERWIG, M. STEINFATH, D. BALZEREIT *et al.*, 2004 Transcript level alterations reflect gene dosage effects across multiple tissues in a mouse model of down syndrome. Genome Res **14:** 1258-1267.

KENTRUP, H., W. BECKER, J. HEUKELBACH, A. WILMES, A. SCHURMANN *et al.*, 1996 Dyrk, a dual specificity protein kinase with unique structural features whose activity is dependent on tyrosine residues between subdomains VII and VIII. J Biol Chem **271:** 3488-3495.

KIM, H., S. O. SABLIN and R. R. RAMSAY, 1997 Inhibition of monoamine oxidase A by beta-carboline derivatives. Arch Biochem Biophys **337:** 137-142.

KIMURA, M., X. CAO, J. SKURNICK, M. CODY, P. SOTEROPOULOS *et al.*, 2005 Proliferation dynamics in cultured skin fibroblasts from Down syndrome subjects. Free Radic Biol Med **39:** 374-380.

KIMURA, R., K. KAMINO, M. YAMAMOTO, A. NURIPA, T. KIDA *et al.*, 2007 The DYRK1A gene, encoded in chromosome 21 Down syndrome critical region, bridges between beta-amyloid production and tau phosphorylation in Alzheimer disease. Hum Mol Genet **16:** 15-23.

KIRBY, M., and D. STEWART, 1984 Adrenergic innervation of the developing chick heart: neural crest ablations to produce sympathetically aneural hearts. Am J Anat **171:** 295-305.

KIRBY, M. L., 1991 Neural crest and the morphogenesis of Down syndrome with special emphasis on cardiovascular development. Prog Clin Biol Res **373:** 215-225.

KLESCHEVNIKOV, A. M., P. V. BELICHENKO, A. J. VILLAR, C. J. EPSTEIN, R. C. MALENKA *et al.*, 2004 Hippocampal long-term potentiation suppressed by increased inhibition in the Ts65Dn mouse, a genetic model of Down syndrome. J Neurosci **24:** 8153-8160.

KNIGHT, R. D., and T. F. SCHILLING, 2006 Cranial neural crest and development of the head skeleton. Adv Exp Med Biol **589:** 120-133.

KORBEL, J. O., T. TIROSH-WAGNER, A. E. URBAN, X. N. CHEN, M. KASOWSKI *et al.*, 2009 The genetic architecture of Down syndrome phenotypes revealed by high-resolution analysis of human segmental trisomies. Proc Natl Acad Sci U S A **106:** 12031-12036.

KORENBERG, J. R., X. N. CHEN, R. SCHIPPER, Z. SUN, R. GONSKY *et al.*, 1994 Down syndrome phenotypes: the consequences of chromosomal imbalance. Proc Natl Acad Sci U S A **91:** 4997-5001.

KOTZOT, D., and A. SCHINZEL, 2000 Paternal meiotic origin of der(21;21)(q10;q10) mosaicism [46,XX/46, XX,der(21;21)(q10;q10),+21] in a girl with mild Down syndrome. Eur J Hum Genet **8:** 709-712.

KUBAS, C., 1999 Noninvasive means of identifying fetuses with possible Down syndrome: a review. J Perinat Neonatal Nurs **13:** 27-46.

LARSEN, C. A., R. H. DASHWOOD and W. H. BISSON, 2010 Tea catechins as inhibitors of receptor tyrosine kinases: mechanistic insights and human relevance. Pharmacol Res **62:** 457-464.

LEE, Y., J. HA, H. J. KIM, Y. S. KIM, E. J. CHANG *et al.*, 2009 Negative feedback Inhibition of NFATc1 by DYRK1A regulates bone homeostasis. J Biol Chem **284:** 33343-33351.

LEJEUNE, J., R. TURPIN and M. GAUTIER, 1959a [Chromosomic diagnosis of mongolism]. Arch Fr Pediatr **16:** 962-963.

LEJEUNE, J., R. TURPIN and M. GAUTIER, 1959b [Mongolism; a chromosomal disease (trisomy)]. Bull Acad Natl Med **143:** 256-265.

LIANG, C. C., A. Y. PARK and J. L. GUAN, 2007 In vitro scratch assay: a convenient and inexpensive method for analysis of cell migration in vitro. Nat Protoc **2:** 329-333.

LOCKROW, J., H. BOGER, H. BIMONTE-NELSON and A. C. GRANHOLM, 2011 Effects of long-term memantine on memory and neuropathology in Ts65Dn mice, a model for Down syndrome. Behav Brain Res **221:** 610-622.

LONG, L., Y. LI, Y. D. WANG, Q. Y. HE, M. LI *et al.*, 2010 The preventive effect of oral EGCG in a fetal alcohol spectrum disorder mouse model. Alcohol Clin Exp Res **34:** 1929-1936.

LORENZI, H. A., and R. H. REEVES, 2006 Hippocampal hypocellularity in the Ts65Dn mouse originates early in development. Brain Res **1104:** 153-159.

LUMSDEN, A., N. SPRAWSON and A. GRAHAM, 1991 Segmental origin and migration of neural crest cells in the hindbrain region of the chick embryo. Development **113:** 1281-1291.

LYLE, R., F. BENA, S. GAGOS, C. GEHRIG, G. LOPEZ *et al.*, 2009 Genotype-phenotype correlations in Down syndrome identified by array CGH in 30 cases of partial trisomy and partial monosomy chromosome 21. Eur J Hum Genet **17:** 454-466.

LYLE, R., C. GEHRIG, C. NEERGAARD-HENRICHSEN, S. DEUTSCH and S. E. ANTONARAKIS, 2004 Gene expression from the aneuploid chromosome in a trisomy mouse model of down syndrome. Genome Res **14:** 1268-1274.

MAK, J. C., 2012 Potential role of green tea catechins in various disease therapies: Progress and promise. Clin Exp Pharmacol Physiol **39:** 265-273.

MAO, J., P. MAYE, P. KOGERMAN, F. J. TEJEDOR, R. TOFTGARD *et al.*, 2002 Regulation of Gli1 transcriptional activity in the nucleus by Dyrk1. J Biol Chem **277:** 35156-35161.

MAZUR-KOLECKA, B., A. GOLABEK, E. KIDA, A. RABE, Y. W. HWANG *et al.*, 2012 Effect of DYRK1A activity inhibition on development of neuronal progenitors isolated from Ts65Dn mice. J Neurosci Res **90:** 999-1010.

MCELHINNEY, D. B., M. STRAKA, E. GOLDMUNTZ and E. H. ZACKAI, 2002 Correlation between abnormal cardiac physical examination and echocardiographic findings in neonates with Down syndrome. Am J Med Genet **113:** 238-241.

MEGARBANE, A., A. RAVEL, C. MIRCHER, F. STURTZ, Y. GRATTAU *et al.*, 2009 The 50th anniversary of the discovery of trisomy 21: the past, present, and future of research and treatment of Down syndrome. Genet Med **11:** 611-616.

MOORE, C. S., 2006 Postnatal lethality and cardiac anomalies in the Ts65Dn Down syndrome mouse model. Mamm Genome **17:** 1005-1012.

MOORE, C. S., J. S. LEE, B. BIRREN, G. STETTEN, L. L. BAXTER *et al.*, 1999 Integration of cytogenetic with recombinational and physical maps of mouse chromosome 16. Genomics **59:** 1-5.

MOUTON, P. R., 2002 Principles and Practices of Unbiased Stereology: An Introduction for Bioscientists. Johns Hopkins University Press, Baltimore.

MULLER, F., M. REBIFFE, A. TAILLANDIER, J. F. OURY and E. MORNET, 2000 Parental origin of the extra chromosome in prenatally diagnosed fetal trisomy 21. Hum Genet **106:** 340-344.

MURAL, R. J., M. D. ADAMS, E. W. MYERS, H. O. SMITH, G. L. MIKLOS *et al.*, 2002 A comparison of whole-genome shotgun-derived mouse chromosome 16 and the human genome. Science **296:** 1661-1671.

NAGLE, D. G., D. FERREIRA and Y. D. ZHOU, 2006 Epigallocatechin-3-gallate (EGCG): chemical and biomedical perspectives. Phytochemistry **67:** 1849-1855.

NERI, G., and J. M. OPITZ, 2009 Down syndrome: comments and reflections on the 50th anniversary of Lejeune's discovery. Am J Med Genet A **149A:** 2647-2654.

NOONAN, J. A., 1968 Hypertelorism with Turner phenotype. A new syndrome with associated congenital heart disease. Am J Dis Child **116:** 373-380.

O'DOHERTY, A., S. RUF, C. MULLIGAN, V. HILDRETH, M. L. ERRINGTON *et al.*, 2005 An aneuploid mouse strain carrying human chromosome 21 with Down syndrome phenotypes. Science **309:** 2033-2037.

O'RAHILLY, R., and F. MULLER, 2007 The development of the neural crest in the human. J Anat **211:** 335-351.

OGAWA, Y., Y. NONAKA, T. GOTO, E. OHNISHI, T. HIRAMATSU *et al.*, 2010 Development of a novel selective inhibitor of the Down syndrome-related kinase Dyrk1A. Nat Commun **1:** 86.

OKUI, M., T. IDE, K. MORITA, E. FUNAKOSHI, F. ITO *et al.*, 1999 High-level expression of the Mnb/Dyrk1A gene in brain and heart during rat early development. Genomics **62:** 165-171.

OLSON, L. E., J. T. RICHTSMEIER, J. LESZL and R. H. REEVES, 2004a A chromosome 21 critical region does not cause specific Down syndrome phenotypes. Science **306:** 687-690.

OLSON, L. E., R. J. ROPER, L. L. BAXTER, E. J. CARLSON, C. J. EPSTEIN *et al.*, 2004b Down syndrome mouse models Ts65Dn, Ts1Cje, and Ms1Cje/Ts65Dn exhibit variable severity of cerebellar phenotypes. Dev Dyn **230:** 581-589.

OLSON, L. E., R. J. ROPER, C. L. SENGSTAKEN, E. A. PETERSON, V. AQUINO *et al.*, 2007 Trisomy for the Down syndrome 'critical region' is necessary but not sufficient for brain phenotypes of trisomic mice. Hum Mol Genet **16:** 774-782.

PALMEIRIM, I., S. RODRIGUES, J. K. DALE and M. MAROTO, 2008 Development on time. Adv Exp Med Biol **641:** 62-71.

PALOMAKI, G. E., E. M. KLOZA, G. M. LAMBERT-MESSERLIAN, J. E. HADDOW, L. M. NEVEUX *et al.*, 2011 DNA sequencing of maternal plasma to detect Down syndrome: an international clinical validation study. Genet Med **13:** 913-920.

PARK, J., Y. OH, L. YOO, M. S. JUNG, W. J. SONG *et al.*, 2010 Dyrk1A phosphorylates p53 and inhibits proliferation of embryonic neuronal cells. J Biol Chem **285:** 31895-31906.

PARKER, S. E., C. T. MAI, M. A. CANFIELD, R. RICKARD, Y. WANG *et al.*, 2010 Updated National Birth Prevalence estimates for selected birth defects in the United States, 2004-2006. Birth Defects Res A Clin Mol Teratol **88:** 1008-1016.

PEREIRA, P. L., L. MAGNOL, I. SAHUN, V. BRAULT, A. DUCHON *et al.*, 2009 A new mouse model for the trisomy of the Abcg1-U2af1 region reveals the complexity of the combinatorial genetic code of down syndrome. Hum Mol Genet **18:** 4756-4769.

PETERSEN, M. B., S. E. ANTONARAKIS, T. J. HASSOLD, S. B. FREEMAN, S. L. SHERMAN *et al.*, 1993 Paternal nondisjunction in trisomy 21: excess of male patients. Hum Mol Genet **2:** 1691-1695.

PHELPS, P. D., D. POSWILLO and G. A. LLOYD, 1981 The ear deformities in mandibulofacial dysostosis (Treacher Collins syndrome). Clin Otolaryngol Allied Sci **6:** 15-28.

POGRIBNY, I. P., B. J. MILLER and S. J. JAMES, 1997 Alterations in hepatic p53 gene methylation patterns during tumor progression with folate/methyl deficiency in the rat. Cancer Lett **115:** 31-38.

POSWILLO, D., 1975 The pathogenesis of the Treacher Collins syndrome (mandibulofacial dysostosis). Br J Oral Surg **13:** 1-26.

REEVES, R. H., N. G. IRVING, T. H. MORAN, A. WOHN, C. KITT *et al.*, 1995 A mouse model for Down syndrome exhibits learning and behaviour deficits. Nat Genet **11:** 177-184.

REINHOLDT, L. G., Y. DING, G. T. GILBERT, A. CZECHANSKI, J. P. SOLZAK *et al.*, 2011 Molecular characterization of the translocation breakpoints in the Down syndrome mouse model Ts65Dn. Mamm Genome **22:** 685-691.

RIBA, J., M. VALLE, G. URBANO, M. YRITIA, A. MORTE *et al.*, 2003 Human pharmacology of ayahuasca: subjective and cardiovascular effects, monoamine metabolite excretion, and pharmacokinetics. J Pharmacol Exp Ther **306:** 73-83.

RICHARDS, B. W., 1969 Mosaic mongolism. J Ment Defic Res **13:** 66-83.

RICHTSMEIER, J. T., L. L. BAXTER and R. H. REEVES, 2000 Parallels of craniofacial maldevelopment in Down syndrome and Ts65Dn mice. Dev Dyn **217:** 137-145.

RICHTSMEIER, J. T., A. ZUMWALT, E. J. CARLSON, C. J. EPSTEIN and R. H. REEVES, 2002 Craniofacial phenotypes in segmentally trisomic mouse models for Down syndrome. Am J Med Genet **107:** 317-324.

ROPER, R. J., L. L. BAXTER, N. G. SARAN, D. K. KLINEDINST, P. A. BEACHY *et al.*, 2006a Defective cerebellar response to mitogenic Hedgehog signaling in Down [corrected] syndrome mice. Proc Natl Acad Sci U S A **103:** 1452-1456.

ROPER, R. J., and R. H. REEVES, 2006 Understanding the basis for Down syndrome phenotypes. PLoS Genet **2:** e50.

ROPER, R. J., H. K. ST JOHN, J. PHILIP, A. LAWLER and R. H. REEVES, 2006b Perinatal loss of Ts65Dn Down syndrome mice. Genetics **172:** 437-443.

ROPER, R. J., J. F. VANHORN, C. C. CAIN and R. H. REEVES, 2009 A neural crest deficit in Down syndrome mice is associated with deficient mitotic response to Sonic hedgehog. Mech Dev **126:** 212-219.

ROUBERTOUX, P. L., and M. CARLIER, 2010 Mouse models of cognitive disabilities in trisomy 21 (Down syndrome). Am J Med Genet C Semin Med Genet **154C:** 400-416.

RUEDA, N., J. FLOREZ and C. MARTINEZ-CUE, 2008 Chronic pentylenetetrazole but not donepezil treatment rescues spatial cognition in Ts65Dn mice, a model for Down syndrome. Neurosci Lett **433:** 22-27.

RUEDA, N., M. LLORENS-MARTIN, J. FLOREZ, E. VALDIZAN, P. BANERJEE *et al.*, 2010 Memantine normalizes several phenotypic features in the Ts65Dn mouse model of Down syndrome. J Alzheimers Dis **21:** 277-290.

RYOO, S. R., H. K. JEONG, C. RADNAABAZAR, J. J. YOO, H. J. CHO *et al.*, 2007 DYRK1A-mediated hyperphosphorylation of Tau. A functional link between Down syndrome and Alzheimer disease. J Biol Chem **282:** 34850-34857.

SAGO, H., E. J. CARLSON, D. J. SMITH, J. KILBRIDGE, E. M. RUBIN *et al.*, 1998 Ts1Cje, a partial trisomy 16 mouse model for Down syndrome, exhibits learning and behavioral abnormalities. Proc Natl Acad Sci U S A **95:** 6256-6261.

SALEHI, A., J. D. DELCROIX, P. V. BELICHENKO, K. ZHAN, C. WU *et al.*, 2006 Increased App expression in a mouse model of Down's syndrome disrupts NGF transport and causes cholinergic neuron degeneration. Neuron **51:** 29-42.

SALEHI, A., M. FAIZI, P. V. BELICHENKO and W. C. MOBLEY, 2007 Using mouse models to explore genotype-phenotype relationship in Down syndrome. Ment Retard Dev Disabil Res Rev **13:** 207-214.

SALEHI, A., M. FAIZI, D. COLAS, J. VALLETTA, J. LAGUNA *et al.*, 2009 Restoration of norepinephrine-modulated contextual memory in a mouse model of Down syndrome. Sci Transl Med **1:** 7ra17.

SANTAGATI, F., and F. M. RIJLI, 2003 Cranial neural crest and the building of the vertebrate head. Nat Rev Neurosci **4:** 806-818.

SARTIPPOUR, M. R., Z. M. SHAO, D. HEBER, P. BEATTY, L. ZHANG *et al.*, 2002 Green tea inhibits vascular endothelial growth factor (VEGF) induction in human breast cancer cells. J Nutr **132:** 2307-2311.

SATGE, D., and M. VEKEMANS, 2011 Down syndrome patients are less likely to develop some (but not all) malignant solid tumours. Clin Genet **79:** 289-290; author reply 291-282.

SAVAGE, A. R., M. B. PETERSEN, D. PETTAY, L. TAFT, K. ALLRAN *et al.*, 1998 Elucidating the mechanisms of paternal non-disjunction of chromosome 21 in humans. Hum Mol Genet **7:** 1221-1227.

SCOTT-MCKEAN, J. J., and A. C. COSTA, 2011 Exaggerated NMDA mediated LTD in a mouse model of Down syndrome and pharmacological rescuing by memantine. Learn Mem **18:** 774-778.

SEO, H., and O. ISACSON, 2005 Abnormal APP, cholinergic and cognitive function in Ts65Dn Down's model mice. Exp Neurol **193:** 469-480.

SHANAFELT, T. D., T. G. CALL, C. S. ZENT, B. LAPLANT, D. A. BOWEN *et al.*, 2009 Phase I trial of daily oral Polyphenon E in patients with asymptomatic Rai stage 0 to II chronic lymphocytic leukemia. J Clin Oncol **27:** 3808-3814.

SHERMAN, S. L., S. B. FREEMAN, E. G. ALLEN and N. E. LAMB, 2005 Risk factors for nondisjunction of trisomy 21. Cytogenet Genome Res **111:** 273-280.

SHIH, J. C., 1991 Molecular basis of human MAO A and B. Neuropsychopharmacology **4:** 1-7.

SHOTT, S. R., 2006 Down syndrome: common otolaryngologic manifestations. Am J Med Genet C Semin Med Genet **142C:** 131-140.

SIAREY, R. J., J. STOLL, S. I. RAPOPORT and Z. GALDZICKI, 1997 Altered long-term potentiation in the young and old Ts65Dn mouse, a model for Down Syndrome. Neuropharmacology **36:** 1549-1554.

SIAREY, R. J., A. J. VILLAR, C. J. EPSTEIN and Z. GALDZICKI, 2005 Abnormal synaptic plasticity in the Ts1Cje segmental trisomy 16 mouse model of Down syndrome. Neuropharmacology **49:** 122-128.

SINGH, B. N., S. SHANKAR and R. K. SRIVASTAVA, 2011 Green tea catechin, epigallocatechin-3-gallate (EGCG): mechanisms, perspectives and clinical applications. Biochem Pharmacol **82:** 1807-1821.

SITARA, D., and A. O. ALIPRANTIS, 2010 Transcriptional regulation of bone and joint remodeling by NFAT. Immunol Rev **233:** 286-300.

SMITH, D. J., M. E. STEVENS, S. P. SUDANAGUNTA, R. T. BRONSON, M. MAKHINSON *et al.*, 1997 Functional screening of 2 Mb of human chromosome 21q22.2 in transgenic mice implicates minibrain in learning defects associated with Down syndrome. Nat Genet **16:** 28-36.

SUSSAN, T. E., A. YANG, F. LI, M. C. OSTROWSKI and R. H. REEVES, 2008 Trisomy represses Apc(Min)-mediated tumours in mouse models of Down's syndrome. Nature **451:** 73-75.

TATTI, S., E. STOCKFLETH, K. R. BEUTNER, H. TAWFIK, U. ELSASSER *et al.*, 2010 Polyphenon E: a new treatment for external anogenital warts. Br J Dermatol **162:** 176-184.

TEBER, O. A., G. GILLESSEN-KAESBACH, S. FISCHER, S. BOHRINGER, B. ALBRECHT *et al.*, 2004 Genotyping in 46 patients with tentative diagnosis of Treacher Collins syndrome revealed unexpected phenotypic variation. Eur J Hum Genet **12:** 879-890.

TEJEDOR, F., X. R. ZHU, E. KALTENBACH, A. ACKERMANN, A. BAUMANN *et al.*, 1995 minibrain: a new protein kinase family involved in postembryonic neurogenesis in Drosophila. Neuron **14:** 287-301.

THORPE, L. W., K. N. WESTLUND, L. M. KOCHERSPERGER, C. W. ABELL and R. M. DENNEY, 1987 Immunocytochemical localization of monoamine oxidases A and B in human peripheral tissues and brain. J Histochem Cytochem **35:** 23-32.

THREADGILL, D. S., J. P. KRAUS, S. A. KRAWETZ and J. E. WOMACK, 1991 Evidence for the evolutionary origin of human chromosome 21 from comparative gene mapping in the cow and mouse. Proc Natl Acad Sci U S A **88:** 154-158.

TIAN, L., R. GUO, X. YUE, Q. LV, X. YE *et al.*, 2012 Intranasal administration of nerve growth factor ameliorate beta-amyloid deposition after traumatic brain injury in rats. Brain Res **1440:** 47-55.

TRAINOR, P. A., 2010 Craniofacial birth defects: The role of neural crest cells in the etiology and pathogenesis of Treacher Collins syndrome and the potential for prevention. Am J Med Genet A **152A:** 2984-2994.

TRAZZI, S., V. M. MITRUGNO, E. VALLI, C. FUCHS, S. RIZZI *et al.*, 2011 APP-dependent up-regulation of Ptch1 underlies proliferation impairment of neural precursors in Down syndrome. Hum Mol Genet **20:** 1560-1573.

VAN CLEVE, S. N., S. CANNON and W. I. COHEN, 2006 Part II: Clinical Practice Guidelines for adolescents and young adults with Down Syndrome: 12 to 21 Years. J Pediatr Health Care **20:** 198-205.

VAN CLEVE, S. N., and W. I. COHEN, 2006 Part I: clinical practice guidelines for children with Down syndrome from birth to 12 years. J Pediatr Health Care **20:** 47-54.

VENAIL, F., Q. GARDINER and M. MONDAIN, 2004 ENT and speech disorders in children with Down's syndrome: an overview of pathophysiology, clinical features, treatments, and current management. Clin Pediatr (Phila) **43:** 783-791.

VENTERS, S. J., M. L. HULTNER and C. P. ORDAHL, 2008 Somite cell cycle analysis using somite-staging to measure intrinsic developmental time. Dev Dyn **237:** 377-392.

VON OHLEN, T., and J. E. HOOPER, 1997 Hedgehog signaling regulates transcription through Gli/Ci binding sites in the wingless enhancer. Mech Dev **68:** 149-156.

WANG, D., F. WANG, Y. TAN, L. DONG, L. CHEN *et al.*, 2012 Discovery of potent small molecule inhibitors of DYRK1A by structure-based virtual screening and bioassay. Bioorg Med Chem Lett **22:** 168-171.

WATERSTON, R. H., K. LINDBLAD-TOH, E. BIRNEY, J. ROGERS, J. F. ABRIL *et al.*, 2002 Initial sequencing and comparative analysis of the mouse genome. Nature **420:** 520-562.

WESSELS, M. W., F. J. LOS, I. M. FROHN-MULDER, M. F. NIERMEIJER, P. J. WILLEMS *et al.*, 2003 Poor outcome in Down syndrome fetuses with cardiac anomalies or growth retardation. Am J Med Genet A **116A:** 147-151.

WILLIAMS, A. D., C. H. MJAATVEDT and C. S. MOORE, 2008 Characterization of the cardiac phenotype in neonatal Ts65Dn mice. Dev Dyn **237:** 426-435.

WILLIAMS, C. A., J. L. FRIAS, M. K. MCCORMICK, S. E. ANTONARAKIS and E. S. CANTU, 1990 Clinical, cytogenetic, and molecular evaluation of a patient with partial trisomy 21 (21q11-q22) lacking the classical Down syndrome phenotype. Am J Med Genet Suppl **7:** 110-114.

WILLIAMSON, G., P. COPPENS, L. SERRA-MAJEM and T. DEW, 2011 Review of the efficacy of green tea, isoflavones and aloe vera supplements based on randomised controlled trials. Food Funct **2:** 753-759.

WINSLOW, M. M., M. PAN, M. STARBUCK, E. M. GALLO, L. DENG *et al.*, 2006 Calcineurin/NFAT signaling in osteoblasts regulates bone mass. Dev Cell **10:** 771-782.

WISNIEWSKI, K. E., H. M. WISNIEWSKI and G. Y. WEN, 1985 Occurrence of neuropathological changes and dementia of Alzheimer's disease in Down's syndrome. Ann Neurol **17:** 278-282.

WOODS, Y. L., G. RENA, N. MORRICE, A. BARTHEL, W. BECKER *et al.*, 2001 The kinase DYRK1A phosphorylates the transcription factor FKHR at Ser329 in vitro, a novel in vivo phosphorylation site. Biochem J **355:** 597-607.

YABUT, O., J. DOMOGAUER and G. D'ARCANGELO, 2010 Dyrk1A overexpression inhibits proliferation and induces premature neuronal differentiation of neural progenitor cells. J Neurosci **30:** 4004-4014.

YAMAGISHI, C., H. YAMAGISHI, J. MAEDA, T. TSUCHIHASHI, K. IVEY *et al.*, 2006 Sonic hedgehog is essential for first pharyngeal arch development. Pediatr Res **59:** 349-354.

YONEZAWA, T., S. HASEGAWA, M. ASAI, T. NINOMIYA, T. SASAKI *et al.*, 2011 Harmine, a beta-carboline alkaloid, inhibits osteoclast differentiation and bone resorption in vitro and in vivo. Eur J Pharmacol **650:** 511-518.

YU, T., Z. LI, Z. JIA, S. J. CLAPCOTE, C. LIU *et al.*, 2010a A mouse model of Down syndrome trisomic for all human chromosome 21 syntenic regions. Hum Mol Genet **19:** 2780-2791.

YU, T., C. LIU, P. BELICHENKO, S. J. CLAPCOTE, S. LI *et al.*, 2010b Effects of individual segmental trisomies of human chromosome 21 syntenic regions on hippocampal long-term potentiation and cognitive behaviors in mice. Brain Res **1366:** 162-171.

ZHANG, X., H. ZHANG, M. TIGHIOUART, J. E. LEE, H. J. SHIN *et al.*, 2008 Synergistic inhibition of head and neck tumor growth by green tea (-)-epigallocatechin-3-gallate and EGFR tyrosine kinase inhibitor. Int J Cancer **123:** 1005-1014.

ZHAO, H., P. BRINGAS, JR. and Y. CHAI, 2006 An in vitro model for characterizing the post-migratory cranial neural crest cells of the first branchial arch. Dev Dyn **235:** 1433-1440.

TABLES

Table 1.1 Higher prevalence of DS births to advanced age women. Advanced maternal age is a risk factor for DS. Despite more children with DS being born to younger mothers, prevalence of DS births is higher in older women due to lower overall birth rates in older women. Data were collected from white individuals with DS, total live births, reported risk rates per 1000 live births, and rates corrected for birth certification under-reporting in Ohio 1970-1983. Corrected rates were obtained by dividing the reported rates by the percentage of reporting: 0.367. Modified from Huether et al., 1998 (HUETHER *et al.* 1998).

Maternal Age	Down syndrome	Live births	Rate/1000 births	Corrected rate
≤ 15	4.69	14,361	0.33	0.89
16	4.00	31,556	0.13	0.35
17	11.39	58,718	0.19	0.53
18	11.69	86,648	0.14	0.37
19	27.08	113,332	0.24	0.65
20	28.40	126,094	0.23	0.61
21	41.60	137,010	0.30	0.83
22	35.60	147,035	0.24	0.66
23	33.00	154,182	0.21	0.58
24	47.22	153,738	0.31	0.84
25	45.55	148,831	0.31	0.83
26	46.79	140,365	0.33	0.91
27	47.55	128,241	0.37	1.01
28	32.76	113,829	0.29	0.79
29	39.27	97,647	0.40	1.10
30	37.56	80,573	0.47	1.27
31	31.78	64,795	0.49	1.34
32	30.33	50,963	0.60	1.62

Table 1.1 Continued

33	25.71	40,161	0.64	1.74
34	24.29	31,496	0.77	2.10
35	27.21	24,136	1.13	3.07
36	23.12	18,611	1.24	3.38
37	24.66	13,936	1.77	4.82
38	36.33	10,737	3.38	9.22
39	24.36	8167	2.98	8.13
40	33.34	5963	5.59	15.23
41	14.09	4185	3.37	9.17
42	15.62	2834	5.51	15.02
43	12.12	1708	7.09	19.33
44	14.93	962	15.52	42.29
45	6.95	467	14.88	40.56
46	5.95	220	27.05	73.71
47	1.22	90	13.60	37.06
48	0.00	21	0.00	0.00
≥49	1.00	22	45.46	123.86

FIGURES

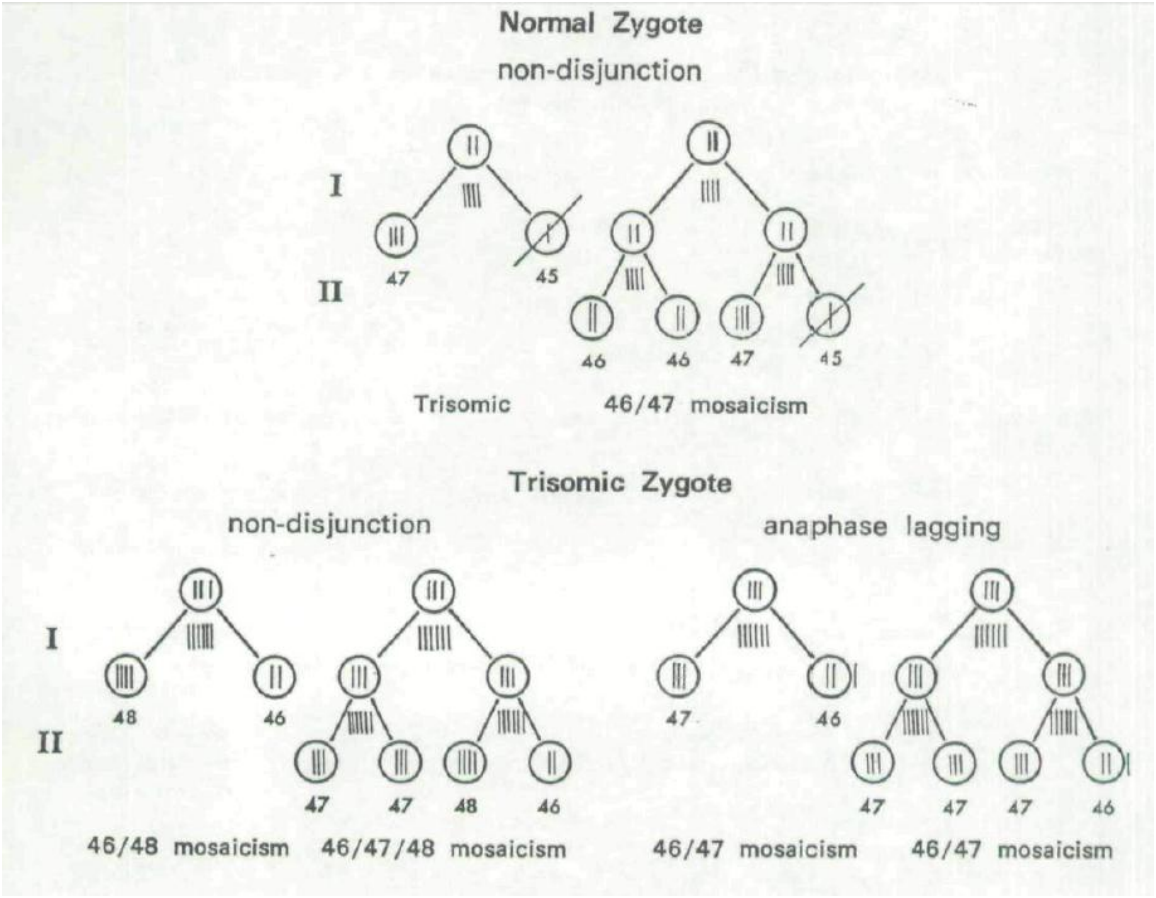

Figure 1.1: Mosaicism may result from a genetically normal or trisomic zygote due to mitotic errors. Mosaicism can occur through numerous mechanisms including nondisjunction from the normal zygote during the second division or in the trisomic zygote in either the first or second divisions. Modified from Richards, 1969 (RICHARDS 1969).

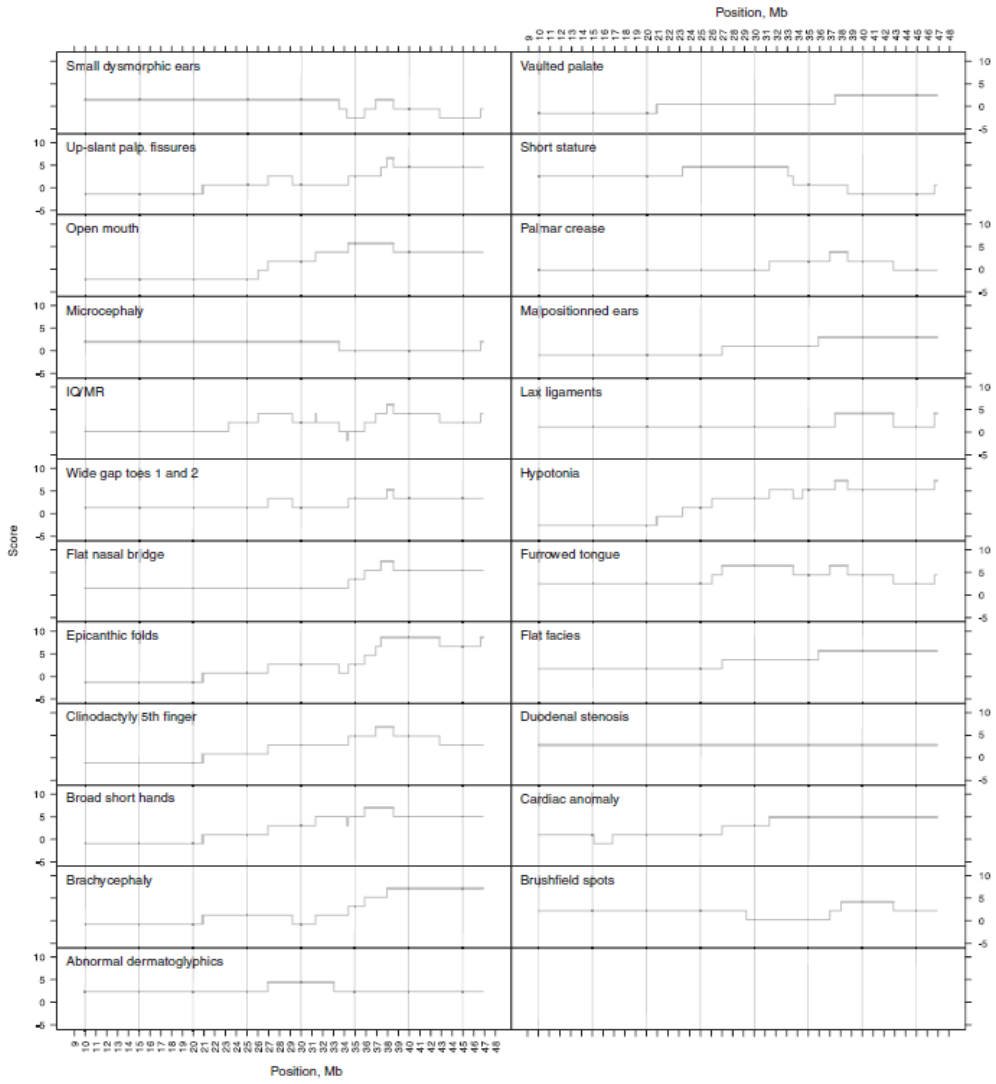

Figure 1.2: Susceptibility regions for various phenotypes have been developed from phenotypic mapping. Using 30 cases of partial trisomy to map phenotypes of these individuals, Lyle and colleagues developed regions of Hsa 21 which likely play a role in the development of a single phenotype. As outlined above, phenotypes including craniofacial phenotypes, cardiac anomalies, hypotonia, and ID have all been mapped to various regions of Hsa 21 and termed 'susceptibility regions.' Each phenotype described is represented by a score (y-axis) designating the likelihood of a feature mapping to a position on Hsa 21 (x-axis). Modified from Lyle et al., 2009
(LYLE *et al.* 2009).

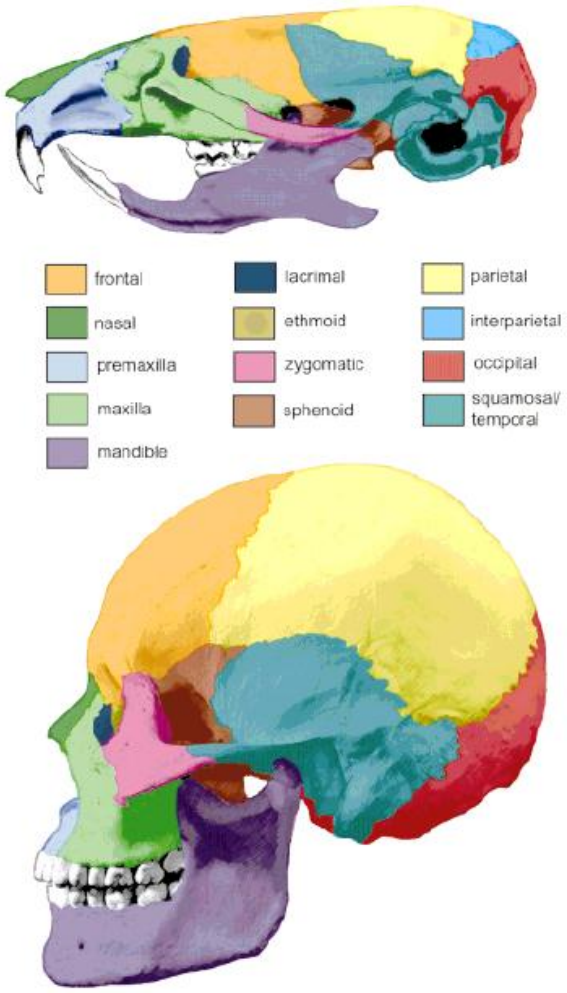

Figure 1.3: Mice display a high level of homology with humans in craniofacial bones. Placement of craniofacial bones and the proximity of these bones with respect to one another in mice are highly reflective of that in humans. The location of these bones is crucial to maintain homology in signaling pathways to which the developing form of these structures are exposed. The similarities in the craniofacial skeletons between humans and mice allow for comparisons to be made between the developmental precursor to the mandible in the Ts65Dn mouse model of DS and that of individuals with DS in order to better understand the genotype-phenotype relationships occurring in the facial skeleton. Modified from Richtsmeier et al., 2000 (RICHTSMEIER *et al.* 2000).

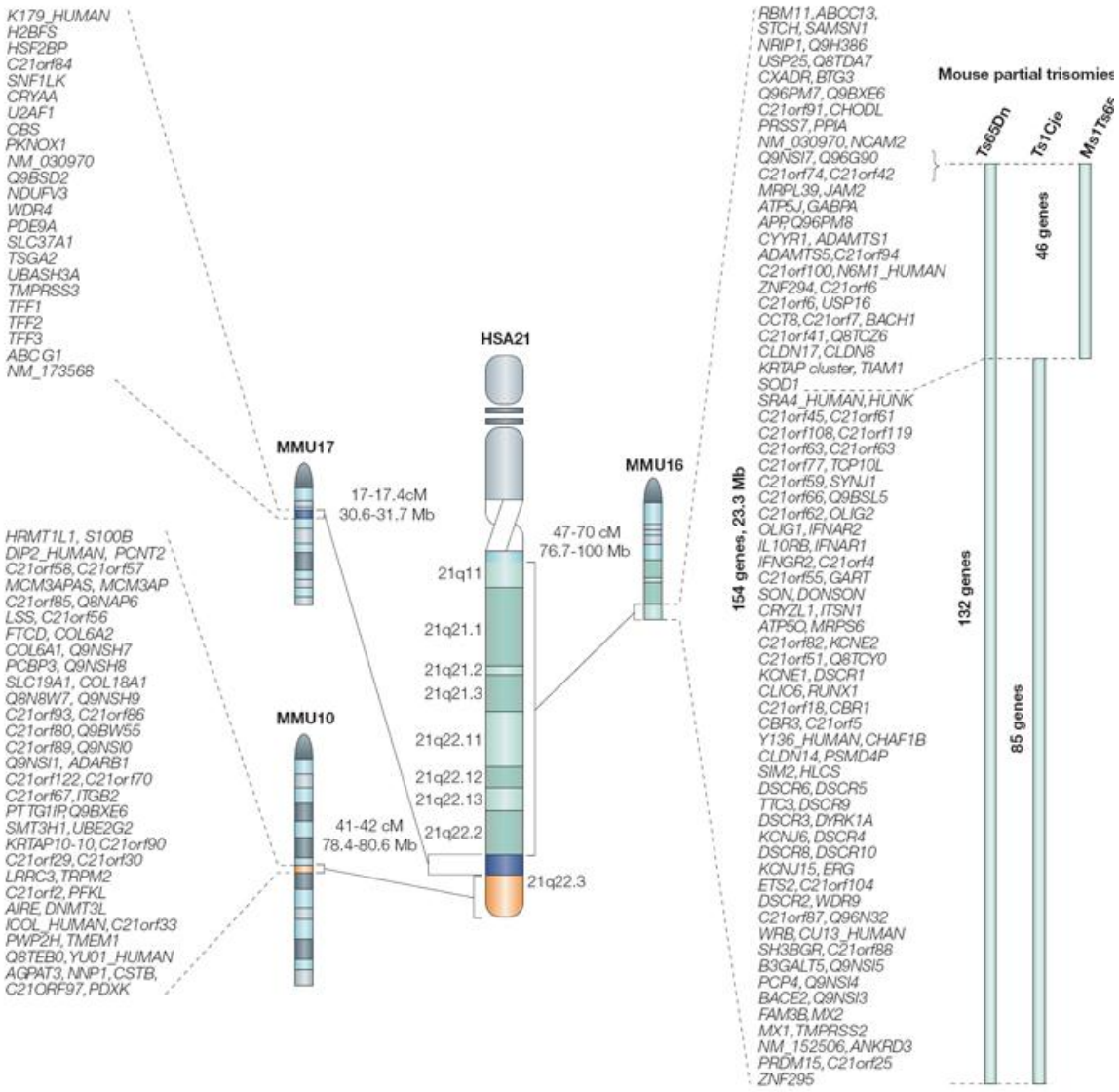

Figure 1.4: Hsa 21 genes can be found on Mmu 10, 16, and 17 with differing contributions of genes from each Mmu chromosome. The genes found on Hsa 21 can be found on Mmu 16, Mmu 10, and Mmu 17. Mmu 10 and 17 contain a multitude of genes other than those found on Hsa 21, compounding the difficulty of chromosomal engineering for only Hsa 21 genes in mouse models. Modified from Antonarakis et al., 2004 (ANTONARAKIS *et al.* 2004).

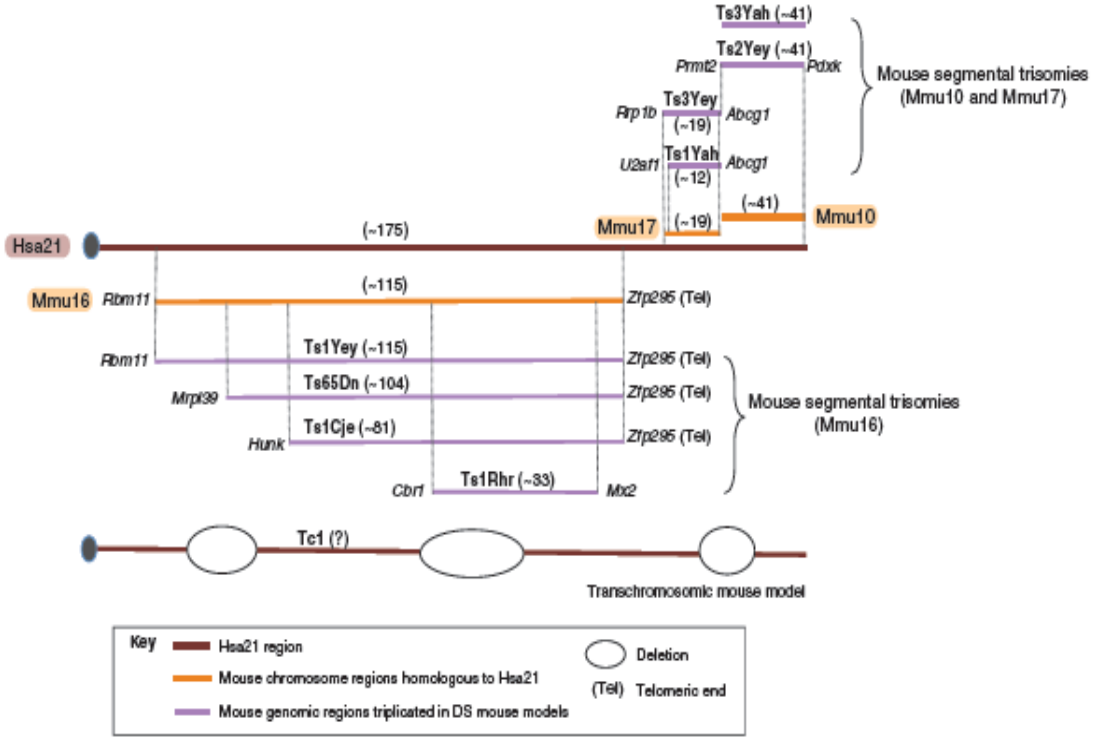

Figure 1.5: Mouse models of Down syndrome. Mouse models trisomic for orthologs from Hsa 21 have been developed to better understand how specific genes contribute to a number of DS phenotypes. The Ts65Dn mouse is the most commonly used model and contains a triplication for about half of the Hsa 21 orthologs; Ts1Rhr mice are trisomic for approximately 33 of the genes triplicated in Ts65Dn mice; and Tc1 mice are transchromosomic, containing the most Hsa 21 orthologs in three copies of all DS mouse models currently developed. Several other mouse models have been developed to better understand the contribution of specific chromosomes and regions associated with DS, including Ts1Cje, Ts1Yey, Ts1Yah and other small segmentally trisomic mice. Modified from Das and Reeves, 2011 (DAS and REEVES 2011).

A

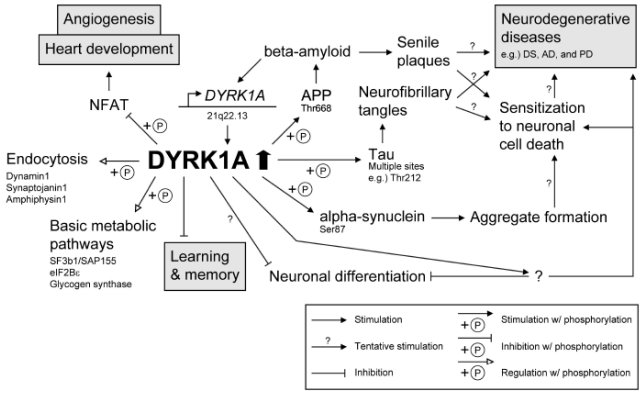

B

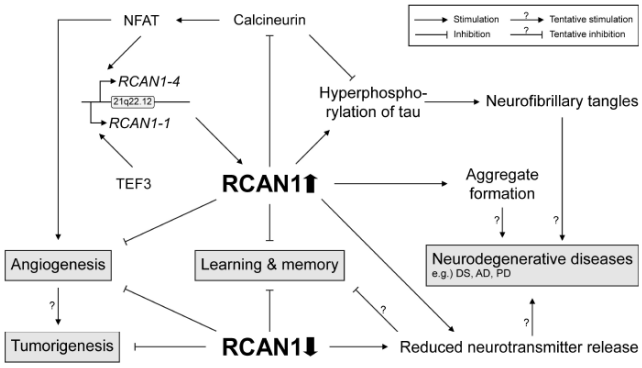

Figure 1.6: *DYRK1A* and *RCAN1* are involved in multiple biological processes and pathways.(A) *DYRK1A* is involved in multiple cellular pathways including biochemical processes and genetic regulation of several genes implicated in DS, including APP, the transcription factor NFAT and itself. (B) *RCAN1* is also involved in numerous biological processes including angiogenesis, tumorigenesis, learning and memory and regulation of neurotransmitter release. RCAN1 indirectly effects NFAT localization through calcineurin, leading to a link between DYRK1A and RCAN1 in their regulation of NFAT. Modified from Park et al., 2009 (PARK *et al.* 2009).

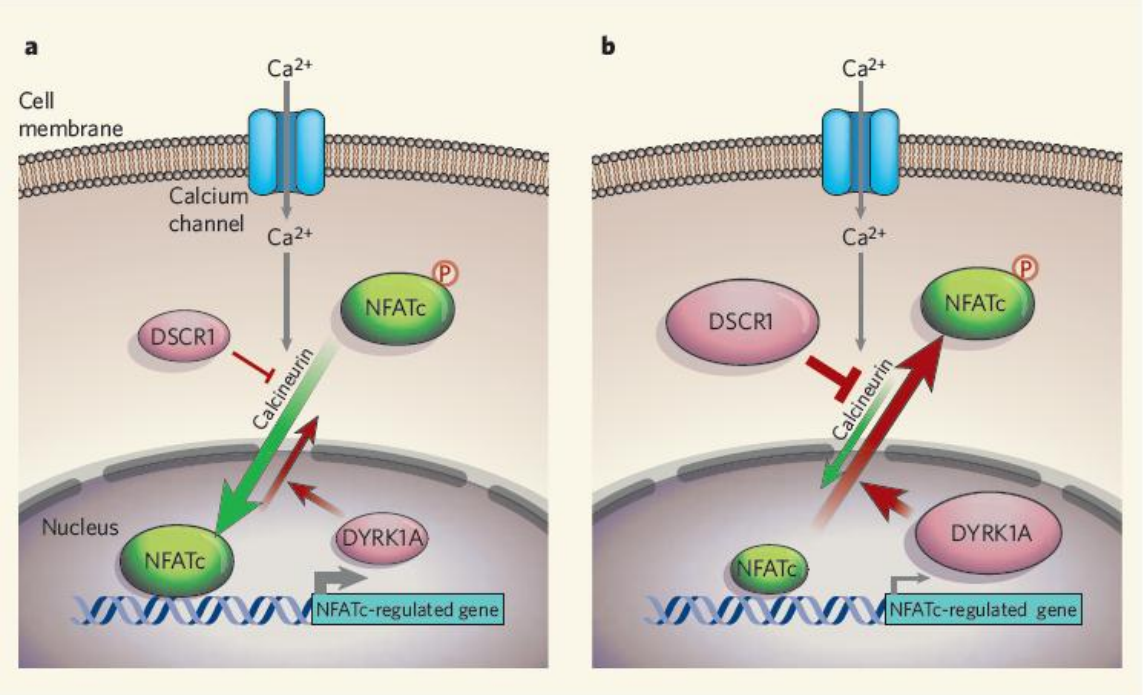

Figure 1.7: Regulation of NFAT localization by *DYRK1A* and *RCAN1*.(A) *DYRK1A* and *DSCR1 (RCAN1)* when expressed at euploid levels, regulate the localization of NFAT through phosphorylation or inhibition of the phosphatase calcineurin, respectively. (B) When *DYRK1A* and *RCAN1* are in three copies, such as in the case of trisomy 21, it is hypothesized that increased phosphorylation of NFAT leads to increased cytoplasmic localization, coupled with increase inhibition of calcineurin, leading to a synergistic cytoplasmic localization of NFAT. The overexpression of *DYRK1A* and *DSCR1 (RCAN1*) would thus lead to decreased expression of genes which rely on transcriptional activation from NFAT. Modified from Epstein 2006 (EPSTEIN 2006).

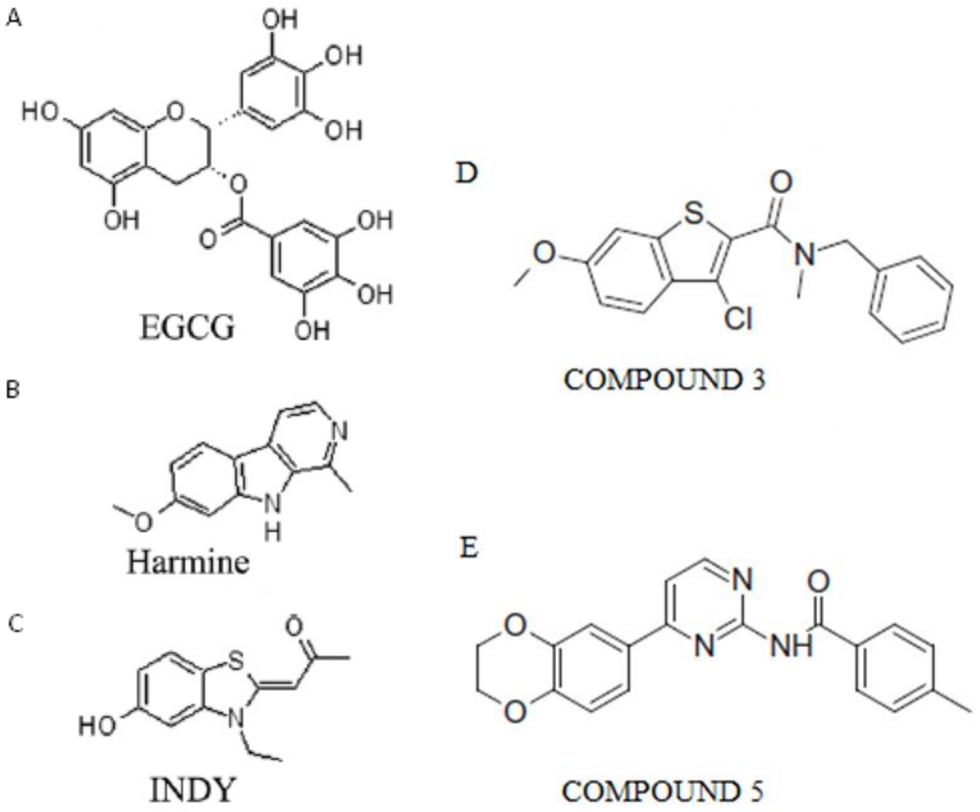

Figure 1.8: Natural and synthetic DYRK1A inhibitors.(A) Epigallocatechin-3-gallate (EGCG) and (B) harmine exist naturally as plant-derived substances known to strongly inhibit DYRK1A. (C) INDY has undergone very little study, but has profound impacts on DYRK1A expression and an ability to rescue NFAT signaling. Screening for novel DYRK1A inhibitors revealed six novel compounds of which compounds 3 (D) and 5 (E) were selected for further study. Modified from Wang et al., 2011. (WANG *et al.* 2011)

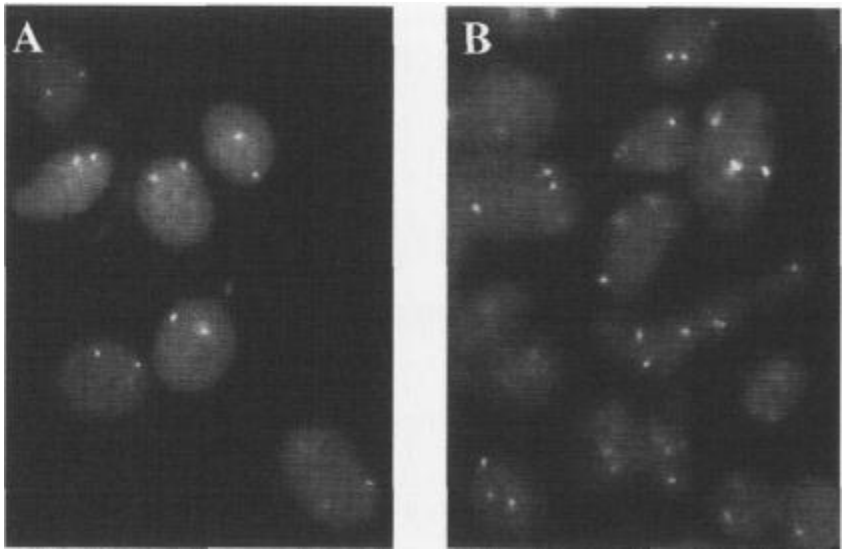

Figure 2.1: The use of fluorescence in situ hybridization (FISH) to genotype Ts65Dn mice and embryos. Prior to the development of primers to amplify the breakpoint between the Mmu 16 and Mmu 17 centromere segment in Ts65Dn, FISH was utilized. (A) Euploid fibroblasts provide two fluorescent signals, while (B) trisomic fibroblasts show three fluorescent signals per cell. Modified from Strovel et al., 1999 (STROVEL *et al.* 1999).

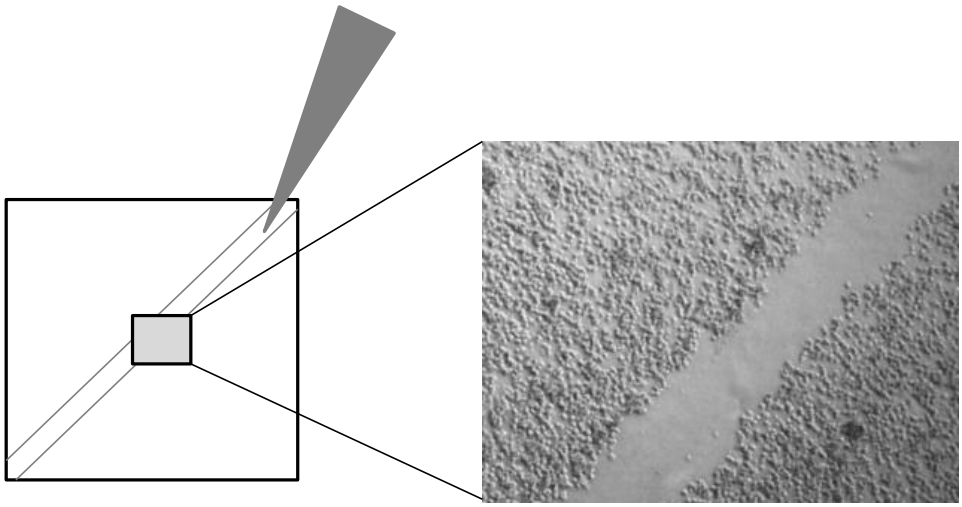

Figure 2.2: Utilization of the scratch test for quantification of migration. Cells grown to confluency on fibronectin-coated coverslips were subjected to the scratch test assay as described by Liang and colleagues (LIANG *et al.* 2007). For each sample, a diagonal scratch was made across the cell surface using a pipet tip as illustrated. Media was changed after the scratch was made to remove any debris and cells remaining in the scratch were quantified to be eliminated from subsequent counts.

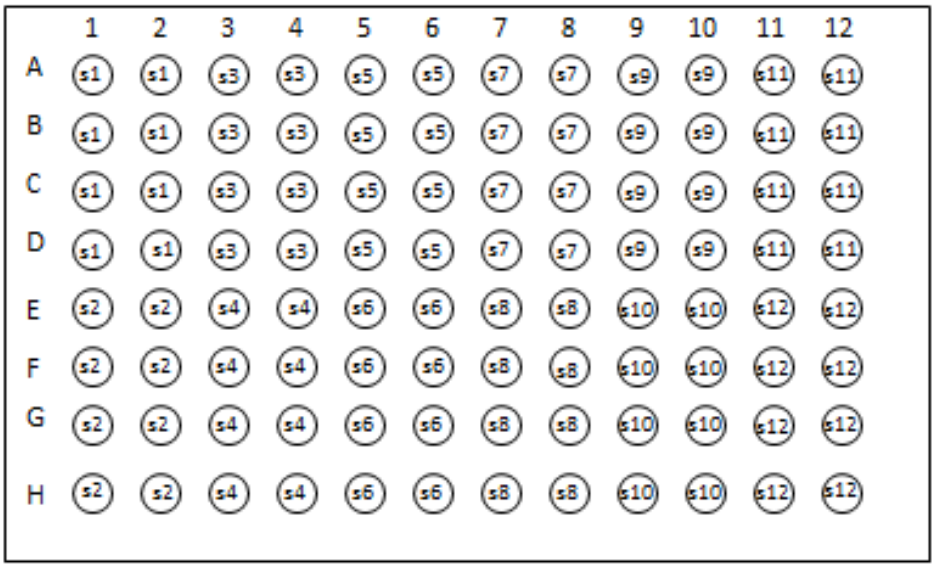

Figure 2.3: A plate schematic for qPCR analysis of RNA. For qPCR analysis of RNA derived from the PA1 and NT, plates were set up as shown above. Rows A and E were used for the reference gene probe, rows B and F for target gene 1, rows C and G for target gene 2, and rows D and H for target gene 3. Samples were divided as shown with trisomic samples (s1, s3, s5, s7, s9, and s11) on the top half of the plate and euploid samples (s2, s4, s6, s8, s10, and s12) on the bottom half of the plate. For each well, 15 µl of probe master mix corresponding to the appropriate gene were used, then 5 µl of the corresponding sample cDNA.

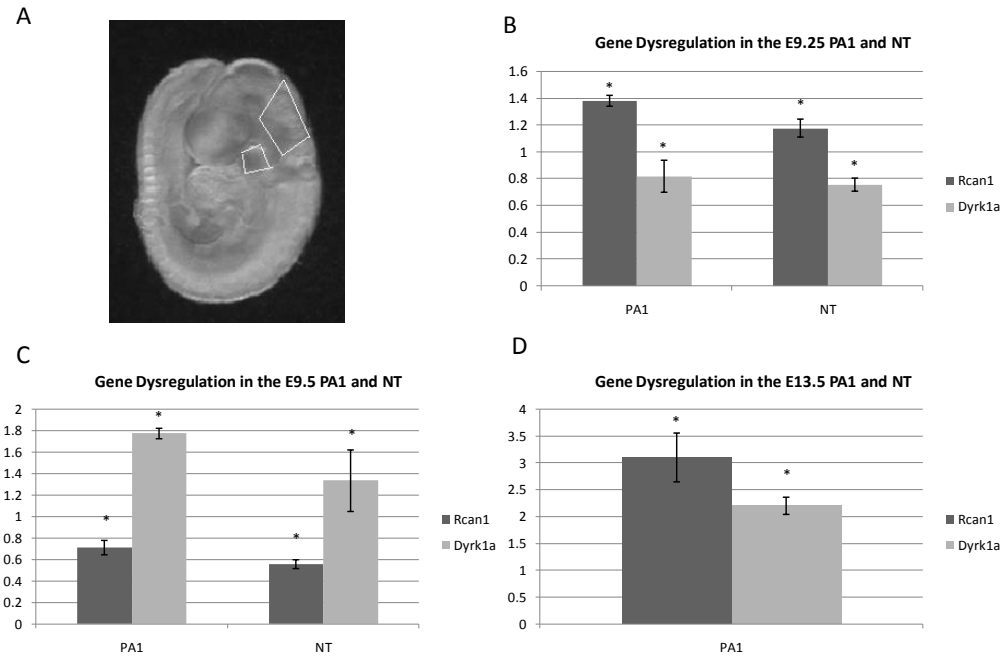

Figure 3.1: Dysregulation of Hsa 21 genes found in three copies in Ts65Dn mice occurs in the PA1 and NT early in development. (A) For RNA extraction from E9.25 (15-18 somites) and E9.5 (21-24 somites), the PA1 and NT were dissected as shown and analyzed for each embryo. (B) Similar trends of *Rcan1* and *Dyrk1a* regulation in the E9.25 PA1 and NT, including increased expression of Rcan1 ($p \leq 0.05$, PA1 and NT) and a slight decrease in expression of *Dyrk1a* ($p \leq 0.05$, PA1 and NT) (N = 5 Eu, 5 Ts PA1; 5 Eu, 5 Ts NT). (C) A complete reversal in relative expression to increased expression of *Dyrk1a* ($p \leq 0.05$, PA1 and NT) and decreased expression of *Rcan1* ($p \leq 0.05$, PA1 and NT) compared to euploid levels characterizes E9.5 PA1 and NT genetic regulation when compared to values at E9.25. *Dyrk1a* is highly expressed in both structures ($p \leq 0.05$, PA1 and NT), while *Rcan1* is downregulated ($p \leq 0.05$, PA1 and NT) (N = 7 Eu, 7 Ts PA1; 5 Eu, 5 Ts NT). (D) Keeping with this trend, RNA in the E13.5 PA1 reveals an upregulation of *Rcan1* ($p \leq 0.01$) and downregulation of *Dyrk1a* ($p \leq 0.05$) (N= 9 Eu, 9 Ts). Expected euploid levels of expression are equal to 1 for relative expression comparisons. For statistical analysis, 2-tailed Students t-tests were used and are shown in the graph as * for $p \leq 0.05$.

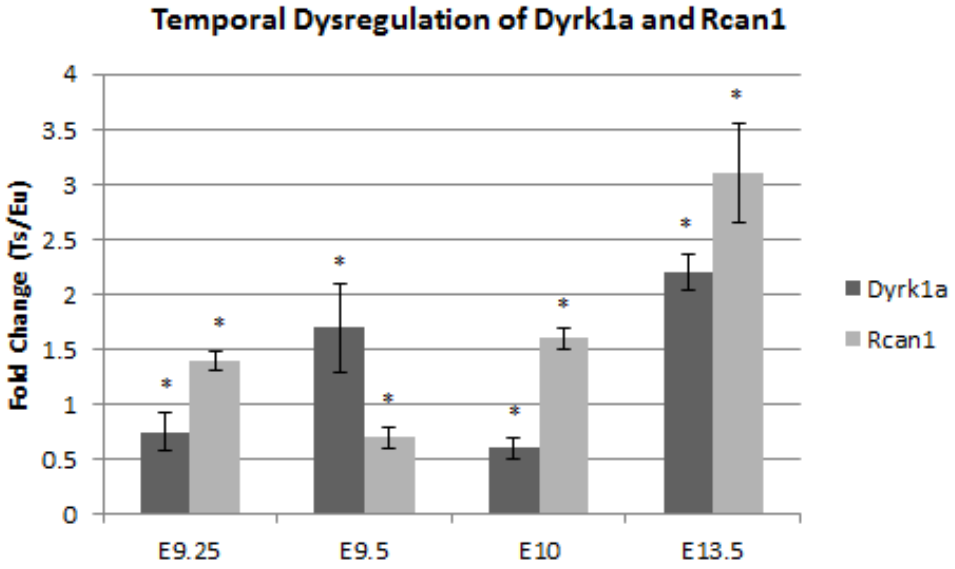

Figure 3.2: Trisomic genes *Dyrk1a* and *Rcan1* display alterations in expression dependent on time in the PA1. Changes in over- and underexpression of expression of *Dyrk1a* and *Rcan1* appear to occur over time, especially around midgestation of the developing Ts65Dn mouse embryo. At E9.25, *Dyrk1a* is downregulated ($p \leq 0.05$), while *Rcan1* is upregulated ($p \leq 0.05$) (N = 5 Eu, 5 Ts). At E9.5, *Dyrk1a* is then upregulated ($p \leq 0.05$) and *Rcan1* is downregulated ($p \leq 0.05$) from euploid levels (N = 7 Eu, 7 Ts). At E10, this relationship again switches and *Dryk1a* is downregulated ($p \leq 0.05$), while *Rcan1* is upregulated ($p \leq 0.05$) (N = 5 Eu, 5 Ts). Later in development at E13.5, *Dyrk1a* and *Rcan1* are both upregulated ($p \leq 0.01$ for both genes) (N = 9 Eu, 9 Ts), continuing to show that alterations in the expression of these two changes occur frequently throughout midgestation. Expected euploid levels of expression are equal to 1 for relative expression comparisons. For statistical analysis, 2-tailed Students t-tests were used and are shown in the graph as * for $p \leq 0.05$. Error bars indicate standard error of the mean.

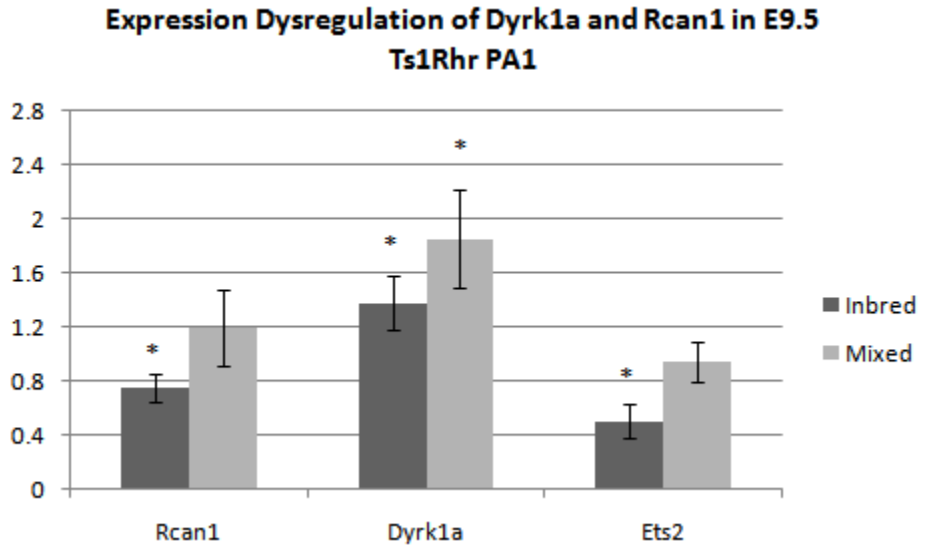

Figure 3.3: Expression Dysregulation of *Dyrk1a* and *Rcan1* in the E9.5 Ts1Rhr PA1. Expression of Rcan1, Dyrk1a, and Ets2, three genes hypothesized or known to be involved in craniofacial development were assessed for relative expression in the Ts1Rhr E9.5 PA1. Ts1Rhr mice were bred on two genetically different backgrounds to account for differences between methodologies in several studies. Despite genetic differences in background, Ts1Rhr E9.5 PA1 display genetic dysregulation, including upregulation of *Dyrk1a*. Changes in *Rcan1* and *Ets2* also appear to be present, but differ by strain. Expected euploid levels of expression are equal to 1 for relative expression comparisons. For statistical analysis, 2-tailed Students t-tests were used and are shown in the graph as * for $p \leq 0.05$. Error bars indicate standard error of the mean.

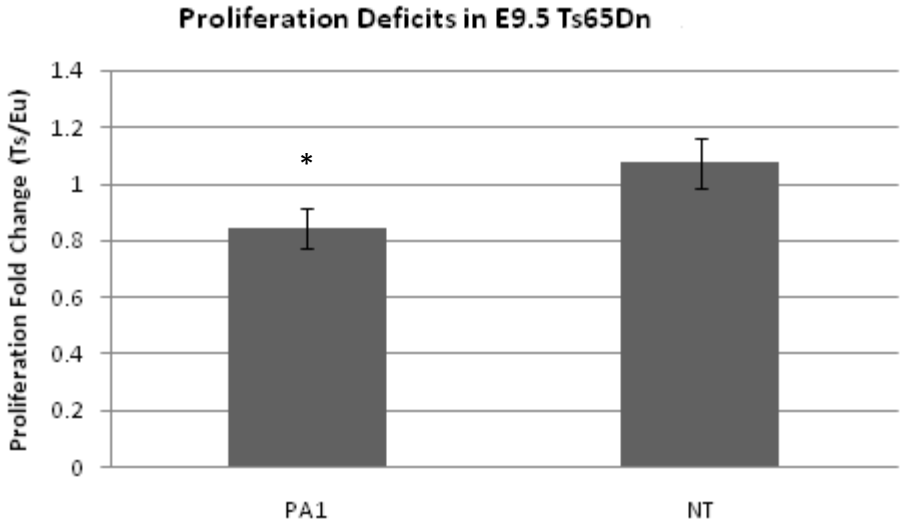

Figure 3.4: Ts65Dn PA1 are deficient in cellular proliferation. Modifications to improve methodology and precise data collection from that described in Roper *et al*., 2009 were made in this proliferation assay. Ts65Dn mice display reduced proliferation in the PA1 ($p \leq 0.05$) with respect to their euploid littermates (N = 7 Eu, 6 Ts). No alteration in proliferation of cells from the E9.5 NT was present ($p = 0.92$) (N = 7 Eu, 6 Ts). For statistical analysis, 1-tailed Students t-tests were used and are shown in the graph as * for $p \leq 0.05$. Error bars indicate standard error of the mean.

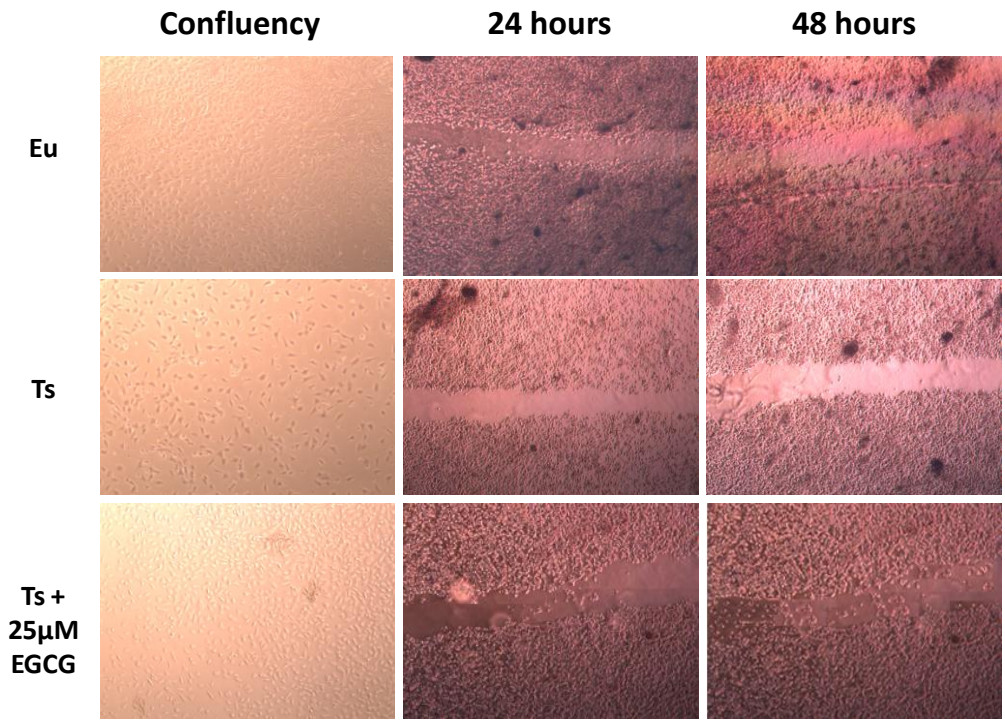

Figure 3.5: Ts65Dn proliferation and migration deficits observed in culture. When cells were observed on the same day after plating, dramatic differences in plate coverage were observed between trisomic and euploid samples. After growing each sample to confluency, the sample was subjected to the scratch assay. Dramatic differences can be observed in the decreased migration of Ts65Dn PA1 cells back into the scratch when compared with the euploid cells above. Treatment with 25µM EGCG appears to visibly rescue these deficiencies from confluency through the termination of the assay.

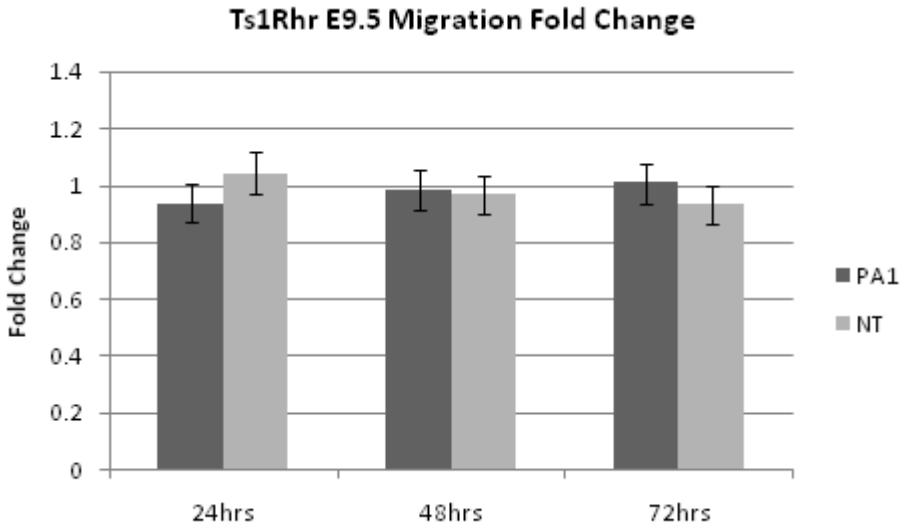

Figure 3.6: Ts1Rhr display no significant migration deficits in the PA1 or NT. PA1 (N = 11 Eu, 11 Ts) and NT cells (N = 11 Eu, 11 Ts) derived Ts1Rhr embryos migrate at euploid levels from 24 hours after the initiation of the scratch assay through the termination of the assay at 72 hours. No significant differences were found throughout the assay. For statistical analysis, 2-tailed Students t-tests were used ($p = 0.10$ PA1 24 hours; $p = 0.74$ PA1 48 hours; $p = 0.93$ PA1 72 hours; $p = 0.57$ NT 24 hours; $p = 0.63$ NT 48 hours; $p = 0.12$ NT 72 hours). Error bars indicate standard error of the mean.

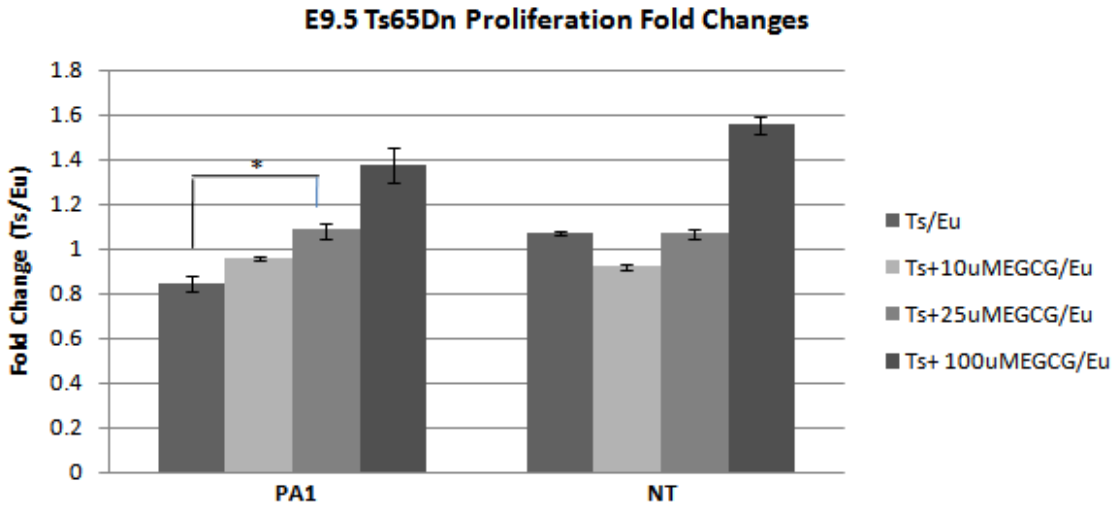

Figure 3.7: Ts65Dn PA1 cells display a proliferation deficit which can be overcome with EGCG treatment. Cells from the PA1 of E9.5 Ts65Dn embryos display impaired proliferation compared to euploid cells ($p \leq 0.01$) (N = 8 Eu, 7 Ts). These cells respond in a dose-dependent manner to treatment, with a significant increase in proliferation with the addition of 10µM EGCG ($p \leq 0.05$) and optimal proliferation occurring with 25µM EGCG treatment for 4 hours ($p \leq 0.001$) (N = 10 Ts, 10 Eu). Addition of 100µM EGCG led to an excessive increase in proliferation above euploid levels ($p \leq 0.001$). Interestingly, cell from the NT display no deficit in proliferation, but are still affected by EGCG treatment. A dose of 10µM (N = 10 Eu, 10 Ts) appears to adversely affect proliferation of cells from NT ($p \leq 0.01$), while 25µM EGCG produces no change from untreated trisomic cells ($p = 0.89$). A significant increase in proliferation can be seen, however, in treatment with 100µM EGCG (N = 10 Eu, 10 Ts) to above euploid levels ($p \leq 0.001$). For statistical analysis, a 2-tailed Students t-test was used and are shown in the graph as * for $p \leq 0.05$. Error bars indicate standard error of the mean.

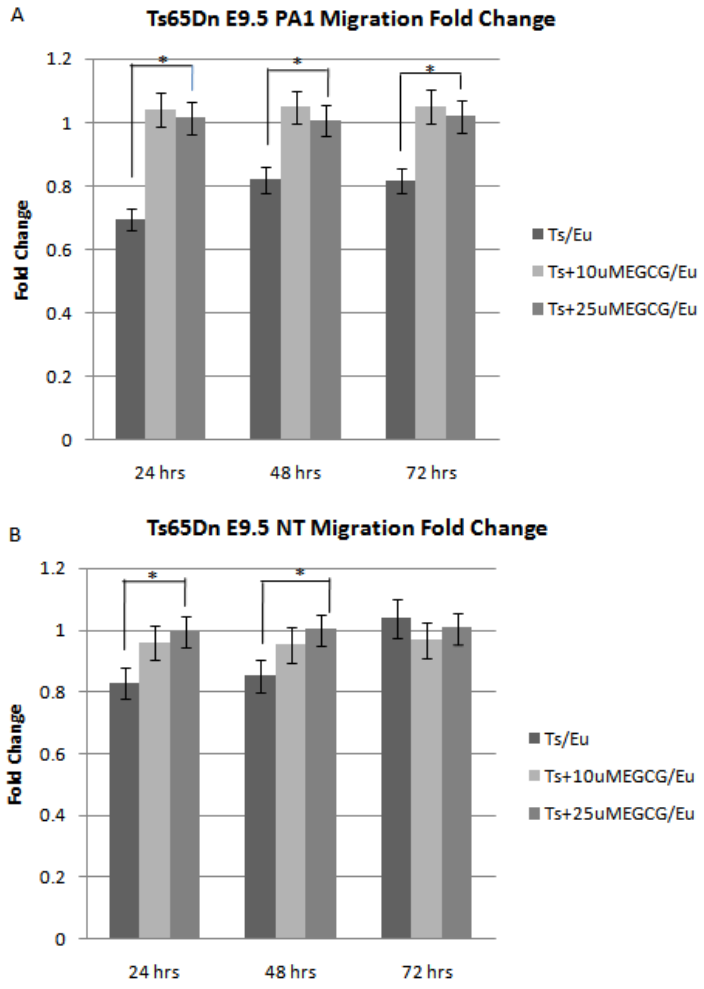

Figure 3.8: Ts65Dn PA1 and NT cells display migration deficits at E9.5 which can be overcome with EGCG treatment. Cells from the PA1 of Ts65Dn E9.5 embryos display an initial migration deficit ($p \leq 0.001$) which is not overcome through the progression of the scratch assay (N = 11 Eu, 8 Ts). However, treatment with both 10µM ($p \leq 0.001$) (N = 8 Eu, 8 Ts) and 25µM EGCG ($p \leq 0.001$) (N = 7 Eu, 7 Ts) is sufficient to rescue this deficit within 24 hours. Migration continues to be rescued in the PA1 at 48 and 72 hours ($p \leq 0.01$ for all conditions). Migration in the NT is deficient at 24 hours post assay initiation, but appears to reach euploid levels of migration by the completion of the assay. Treatment with 10µM ($p \leq 0.05$) and 25µM ($p \leq 0.05$) rescues this initial migration deficit and maintains cell migration using 25µM ($p \leq 0.05$) at euploid levels through the termination of the assay. For statistical analysis, 2-tailed Students t-tests were used and are shown in the graph as * for $p \leq 0.05$. Error bars indicate standard error of the mean.

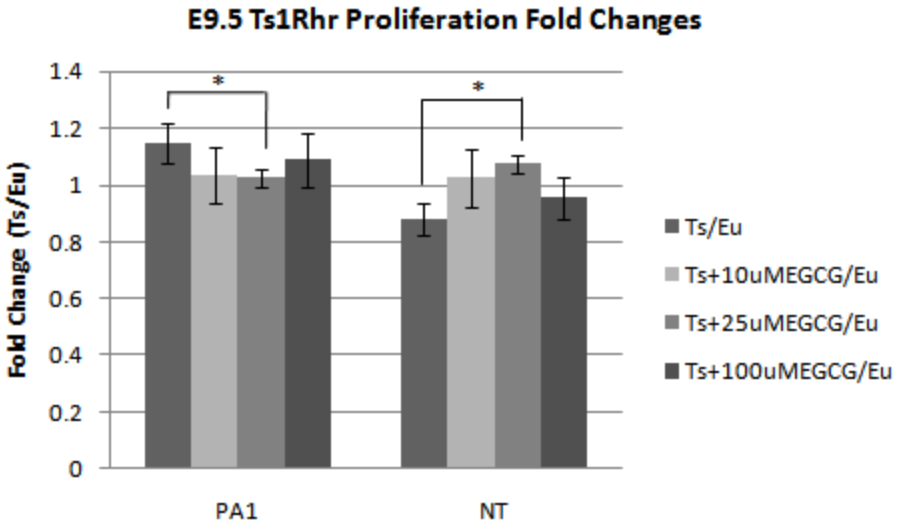

Figure 3.9: Ts1Rhr display no proliferation deficit in the PA1, but a slight deficit in NT at E9.5. Cells from the PA1 of E9.5 Ts1Rhr embryos display a slightly elevated level of proliferation (N = 8 Eu, 7 Ts PA1), mimicking their known phenotype of a larger PA1 than euploid littermates at this time point and as adults (DEITZ and ROPER 2011). Treatment with EGCG had no effect on the proliferation of PA1 cells at 10 µM (N = 8 Eu, 7 Ts), 25 µM (N = 8 Eu, 8 Ts), and 100 µM (N = 6 Eu, 6 Ts). Cells from the NT of these embryos displayed a slight decrease in proliferation (N = 8 Eu, 7 Ts) which was ameliorated with EGCG treatment at 10 µM (N = 8 Eu, 7 Ts), 25 µM (N = 8 Eu, 8 Ts), and 100µM (N = 6 Eu, 6 Ts). For statistical analysis, 2-tailed Students t-tests were used and are shown in the graph as * for $p \leq 0.05$. Error bars indicate standard error of the mean.

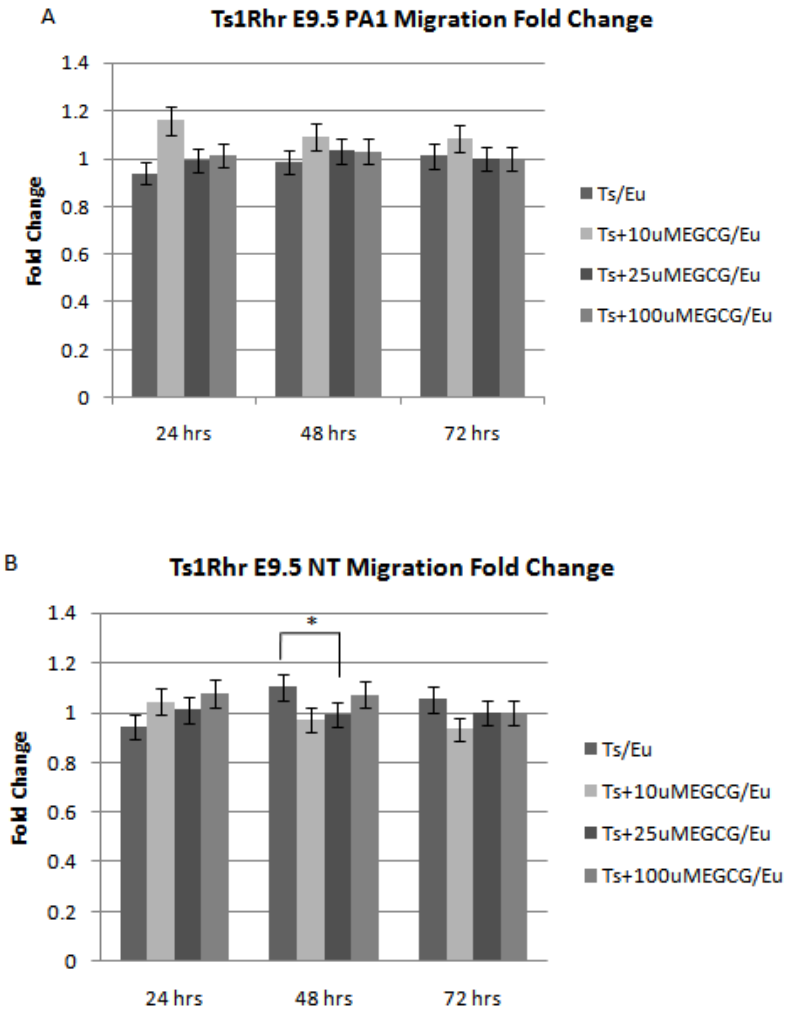

Figure 3.10: Ts1Rhr PA1 and NT migration is not significantly altered by EGCG. Assessment for migration of E9.5 Ts1Rhr PA1 and NT revealed no significant deficit in migration of cells from either structure ($p = 0.11$ PA1; $p = 0.12$ NT) (N = 10 Eu, 10 Ts PA1; 10 Eu, 10 Ts NT). While migration was slightly increased in PA1 cells treated with 10µM EGCG ($p \leq 0.05$), but not NT cells ($p = 0.31$) initially, treatment of NT cells with 10µM led to some decrease in proliferation at 48 ($p \leq 0.05$) and 72 hours ($p \leq 0.05$) (N = 10 Eu, 8 Ts PA1; 10 Eu, 8 Ts NT), treatment of PA1 and NT cells with 100µM EGCG had no effects ($p = 0.79$ PA1, $p = 0.55$) (N = 7 Eu, 7 Ts PA1; 10 Eu, 10 Ts NT) on migration. For statistical analysis, 2-tailed Students t-tests were used and are shown in the graph as * for $p \leq 0.05$. Error bars indicate standard error of the mean.

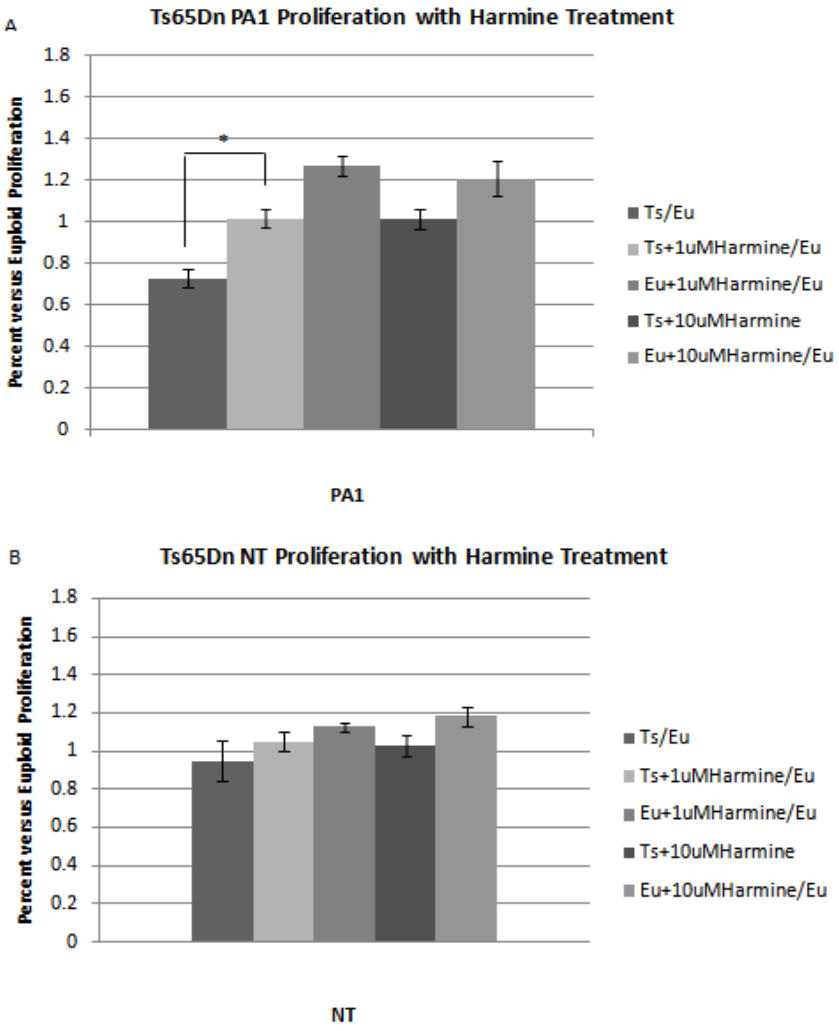

Figure 3.11: Harmine corrects the E9.5 Ts65Dn PA1 proliferation deficit and increases euploid proliferation. Treatment of PA1 cells with 1µM (N = 8 Eu, 8 Ts) and 10µM harmine (N = 8 Eu, 8 Ts) was sufficient to rescue proliferation to a euploid level ($p \leq 0.01$; $p \leq 0.01$, respectively). Assessment of euploid cells alone with the same treatment revealed dramatic increases in proliferation of PA1 cells ($p \leq 0.001$ for 1µM and 10µM treatments). A slight proliferation deficit seen in NT untreated cells ($p = 0.22$) can be altered to increase proliferation of trisomic and euploid cells, with significant increases in euploid cell proliferation at 1µM ($p \leq 0.05$) and 10µM ($p \leq 0.05$) (N = 8 Eu, 8 Ts at 1µM; N = 8 Eu, 8 Ts at 10µM). For statistical analysis, 2-tailed Students t-tests were used and are shown in the graph as * for $p \leq 0.05$. Error bars indicate standard error of the mean.

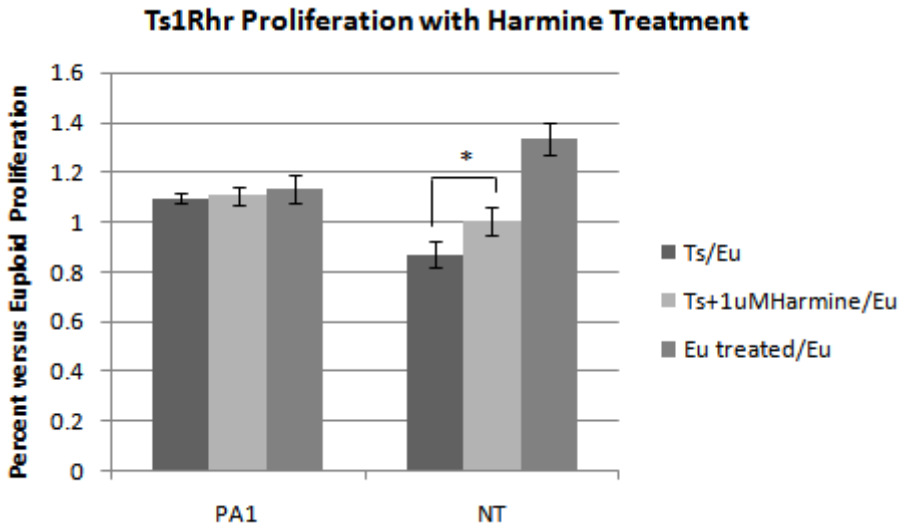

Figure 3.12: Harmine increases Ts1Rhr PA1 and NT proliferation in a dose-dependent manner. Slight decreases in NT proliferation ($p \leq 0.05$) (N = 7 Eu, 7 Ts) were overcome by 1µM harmine (N = 7 Eu, 7 Ts) to euploid levels in the NT ($p \leq 0.05$). Harmine treatment also increased the proliferation of euploid cells from the PA1 ($p \leq 0.05$) and the NT ($p \leq 0.001$). For statistical analysis, 2-tailed Students t-tests were used and are shown in the graph as * for $p \leq 0.05$. Error bars indicate standard error of the mean.

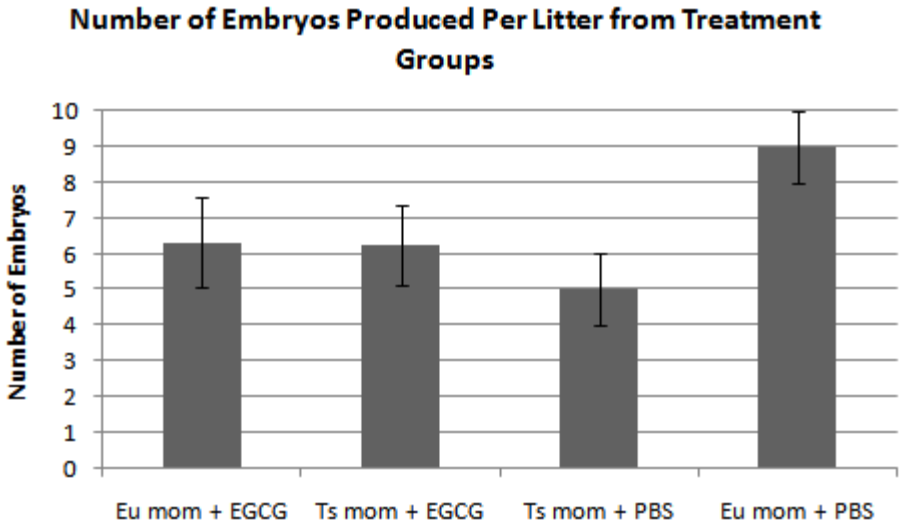

Figure 4.1: EGCG treatment does not adversely impact litter sizes. Embryos from pregnant euploid (N = 38 pups, 6; N = 18 pups, 2 litters for PBS) and Ts65Dn (N = 25 pups, 4 litters EGCG; N = 10 pups, 2 litters for PBS treatment) females treated by oral gavage twice daily on E7 and E8 with EGCG or PBS, and sacrificed on E9.5 were not adversely affected by EGCG treatment, as shown by no reduction in litter size. The number of embryos present in Ts65Dn mothers receiving EGCG did not differ significantly from euploid mothers receiving EGCG, though it appears that litter sizes increased with EGCG treatment. For statistical analysis, 1-tailed Students t-tests were used. Error bars indicate standard error of the mean.

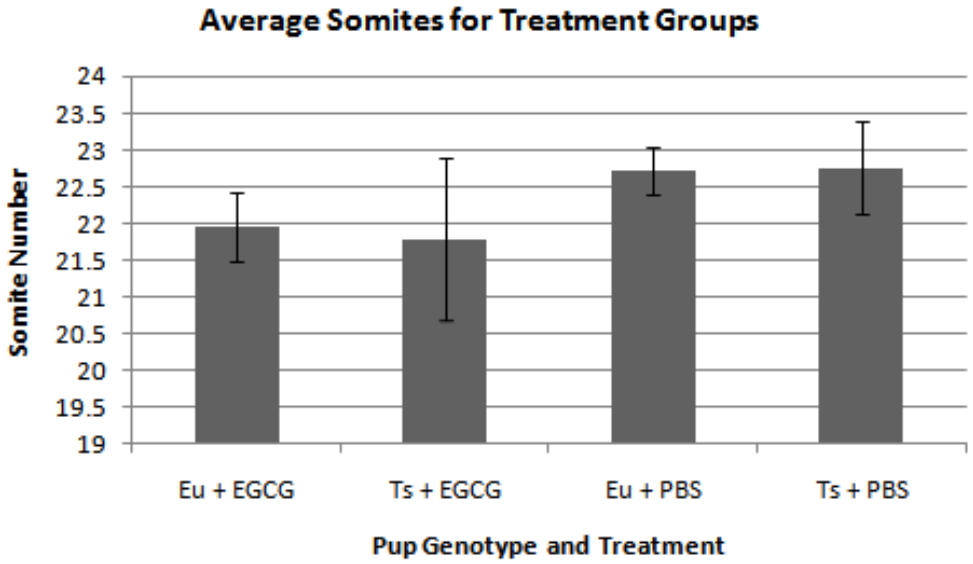

Figure 4.2: EGCG treatment does not adversely impact developmental staging among treatment groups or between genotypes. Pups from treated and untreated mothers were analyzed by genotype for somite stage to understand the impacts of EGCG on development. No differences were seen between EGCG or PBS treatment groups or trisomic or euploid genotype, indicating no overall developmental effects by EGCG *in vivo* (N = 43 pups Eu + EGCG; N = 9 pups Ts + EGCG; N = 14 pups Eu + PBS; N = 4 pups Ts + PBS). For statistical analysis, 1-tailed Students t-tests were used. Error bars indicate standard error of the mean.

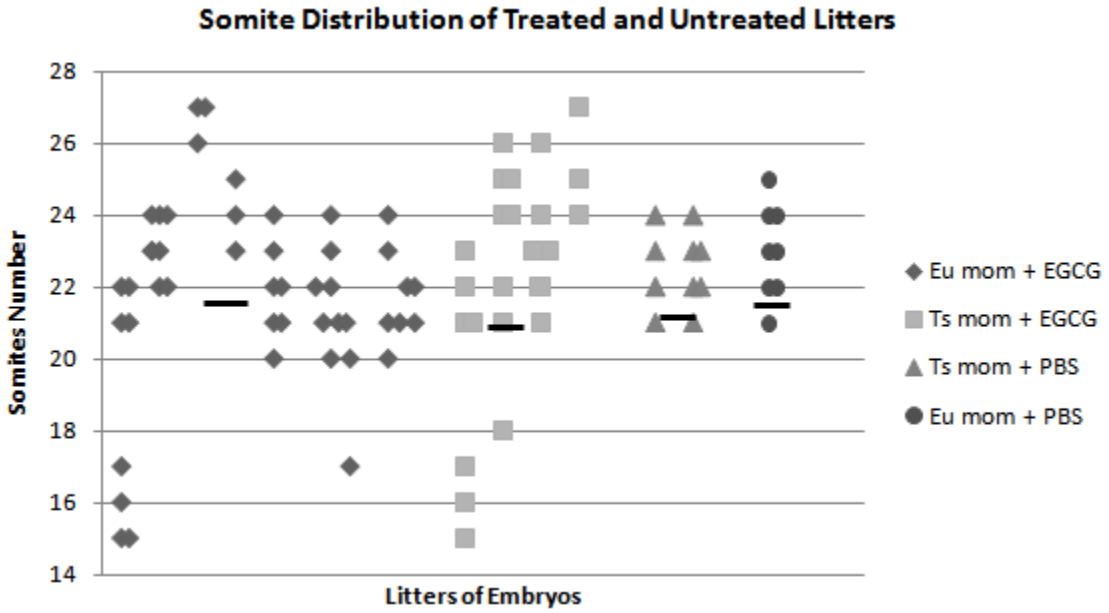

Figure 4.3: Developmental stage distribution is not altered by EGCG. Though increased variability appears to be present in litters receiving EGCG *in vivo*, median and average somite stages of E9.5 embryos receiving EGCG or PBS do not differ significantly between groups. Distributions are designated into four groups: by genotype of the mother combined with treatment. Each distribution group cluster indicates a single litter and the somite stages of the individual embryos in that litter (N = 8 litters, 47 pups for Eu mom + EGCG; N = 4 litters, 25 pups for Ts mom + EGCG; N = 2 litters, 10 pups for Ts mom + PBS; N = 1 litter, 8 pups for Eu mom + PBS).

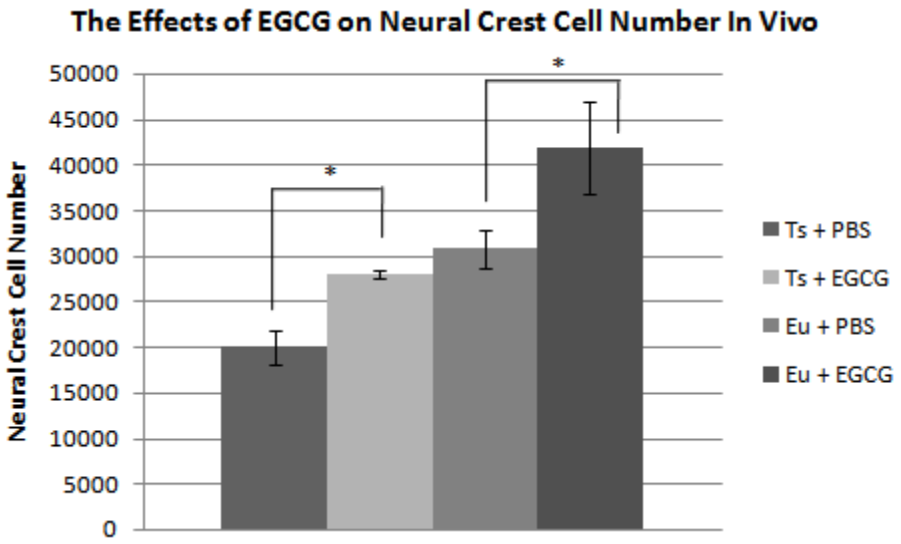

Figure 4.4: EGCG treatment leads to an increase in cell number in the trisomic and euploid PA1. Stereological analysis of E9.5 EGCG and PBS treated embryos revealed a NCC deficit in trisomic embryos treated with PBS (N = 4) compared to euploid embryos treated with PBS (N = 4) ($p \leq 0.01$). When trisomic embryos were treated with EGCG (N = 4), however, this deficit was ameliorated to euploid levels ($p = 0.082$). However, treatment of euploid embryos with EGCG (N = 4), led to an increase in NCC above euploid embryos treated with PBS ($p \leq 0.05$). For statistical analysis, 2-tailed Students t-tests were used and are shown in the graph as * for $p \leq 0.05$. Error bars indicate standard error of the mean.

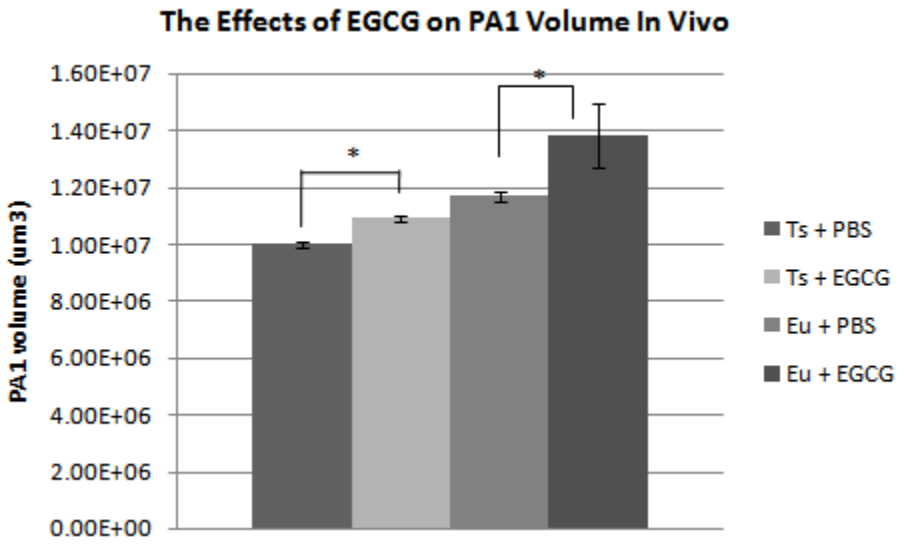

Figure 4.5: EGCG treatment increases PA1 volume in trisomic and euploid embryos. Trisomic PBS treated embryos (N = 4) display a smaller PA1 volume than euploid PBS treated embryos (N = 4) ($p \leq 0.001$). Treatment of Ts65Dn embryos with EGCG (N = 4) improves PA1 volume to above trisomic PBS PA1 volume ($p \leq 0.001$), but not to PBS treated euploid PA1 volume ($p \leq 0.01$). Treatment of euploid embryos with EGCG (N = 4) leads to increased PA1 above PBS treated euploid PA1 volume ($p \leq 0.05$). For statistical analysis, 2-tailed Students t-tests were used and are shown in the graph as * for $p \leq 0.05$. Error bars indicate standard error of the mean.

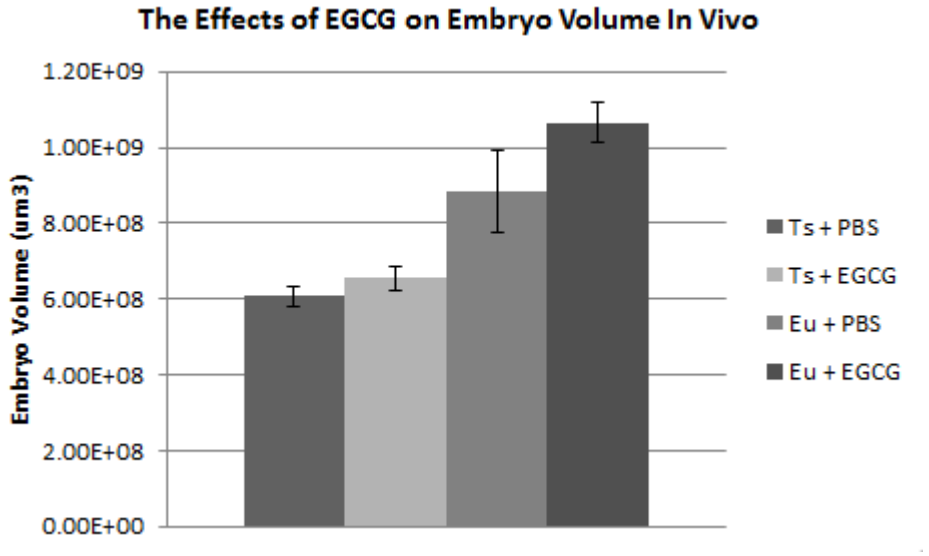

Figure 4.6: EGCG treatment increases embryo volume in euploid, but not trisomic embryos. Ts65Dn PBS treated embryos (N = 4) are smaller than euploid PBS treated embryos (N = 4) as measured through stereological analysis of embryonic volume ($p \leq 0.001$). Treatment of trisomic embryos with EGCG (N = 4) does not lead to a significant increase in volume compared to PBS treated euploid embryos, but does increase embryonic volume in comparison to PBS treated trisomic embryos. Euploid embryos treated with EGCG (N = 4) have a larger embryo volume than euploid treated PBS embryos, but this value is not significant ($p = 0.092$). For statistical analysis, 2-tailed Students t-tests were used. Error bars indicate standard error of the mean.

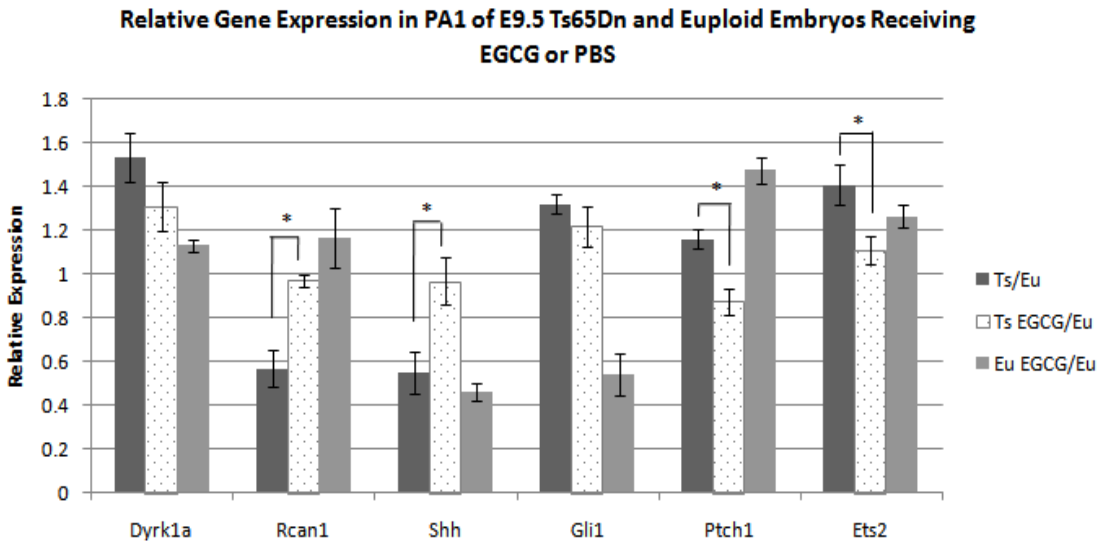

Figure 4.7: EGCG exposure leads to expression alterations of genes involved in pathways impacting craniofacial development. Baseline expression of *Dyrk1a, Rcan1, Shh, Gli1, Ptch1,* and *Ets2* reveals alterations in expression from euploid values (a value of 1). Expression of these genes is altered in several cases in trisomic PA1 receiving EGCG treatment with most achieving near euploid values of relative expression (N = 3 Ts receiving EGCG, 3Eu receiving EGCG, 3 Ts receiving PBS, and 3 Eu receiving PBS). Expected euploid levels of expression are equal to 1 for relative expression comparisons. For statistical analysis, 2-tailed Students t-tests were used and are shown in the graph as * for $p \leq 0.05$. Error bars indicate standard error of the mean.

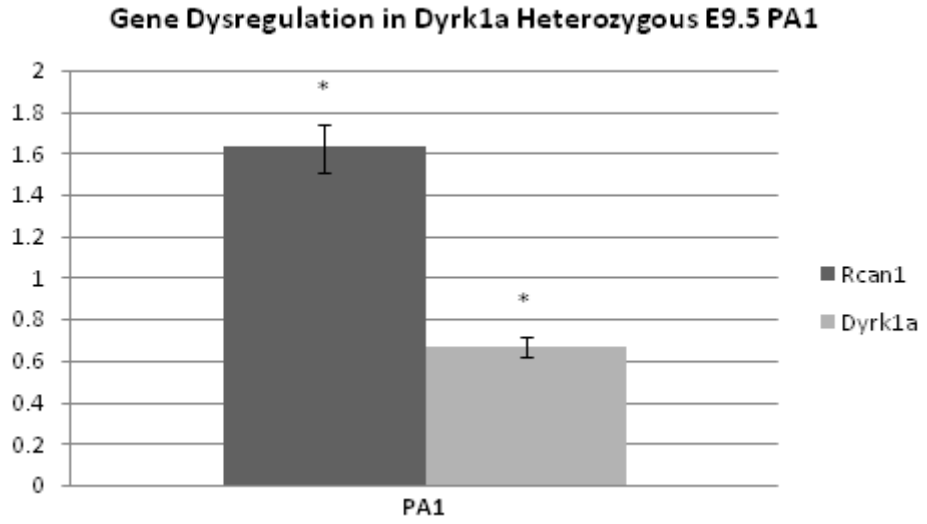

Figure 5.1: Loss of expression of *Dyrk1a* leads to upregulation of *Rcan1*. *Dyrk1a* and *Rcan1* are hypothesized to regulate the expression of one another. Using RNA extracted from the PA1 of a *Dyrk1a* heterozygous mouse, qPCR revealed a subsequent upregulation of *Rcan1* ($p \leq 0.05$) and downregulation of *Dyrk1a* ($p \leq 0.05$) due to deletion of one copy of the gene (N = 4 Eu, 4 Ts PA1; 4 Eu, 4 Ts NT). These two genes appear to regulate one another in the PA1 at midgestation. Expected euploid levels of expression are equal to 1 for relative expression comparisons. For statistical analysis, 2-tailed Students t-tests were used and are shown in the graph as * for $p \leq 0.05$. Error bars indicate standard error of the mean.

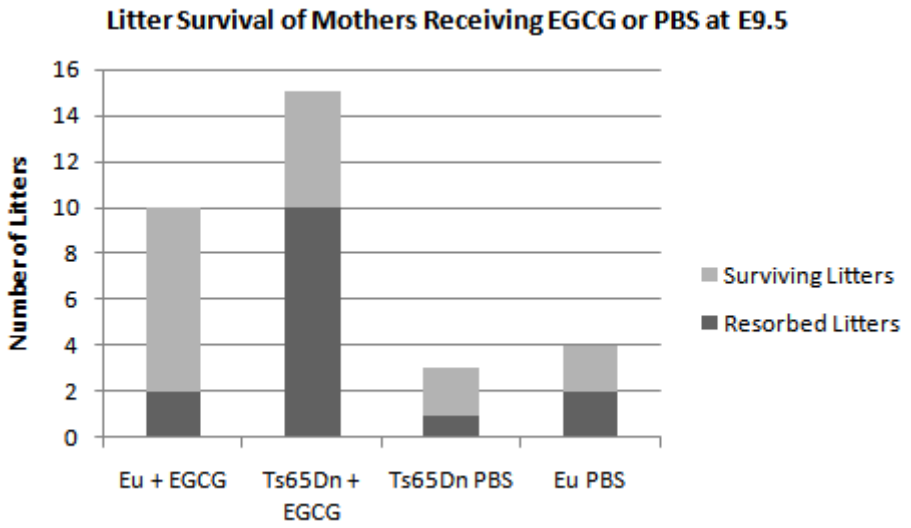

Figure 5.2: Litter survival in pregnant Ts65Dn and euploid mothers receiving EGCG is not altered by dosage. Litter sizes from pregnant females receiving EGCG or PBS on E7 and E8 were quantified at E9.5 when embryos were dissected. A lost litter (resorbed) was classified as the presence of uterine swelling with the appearance or presence of embryonic tissue either at the time of dissection or within the two days prior to the dissection. Proportionally, fewer litters were lost from euploid mothers receiving treatment than trisomic mothers receiving treatment overall.

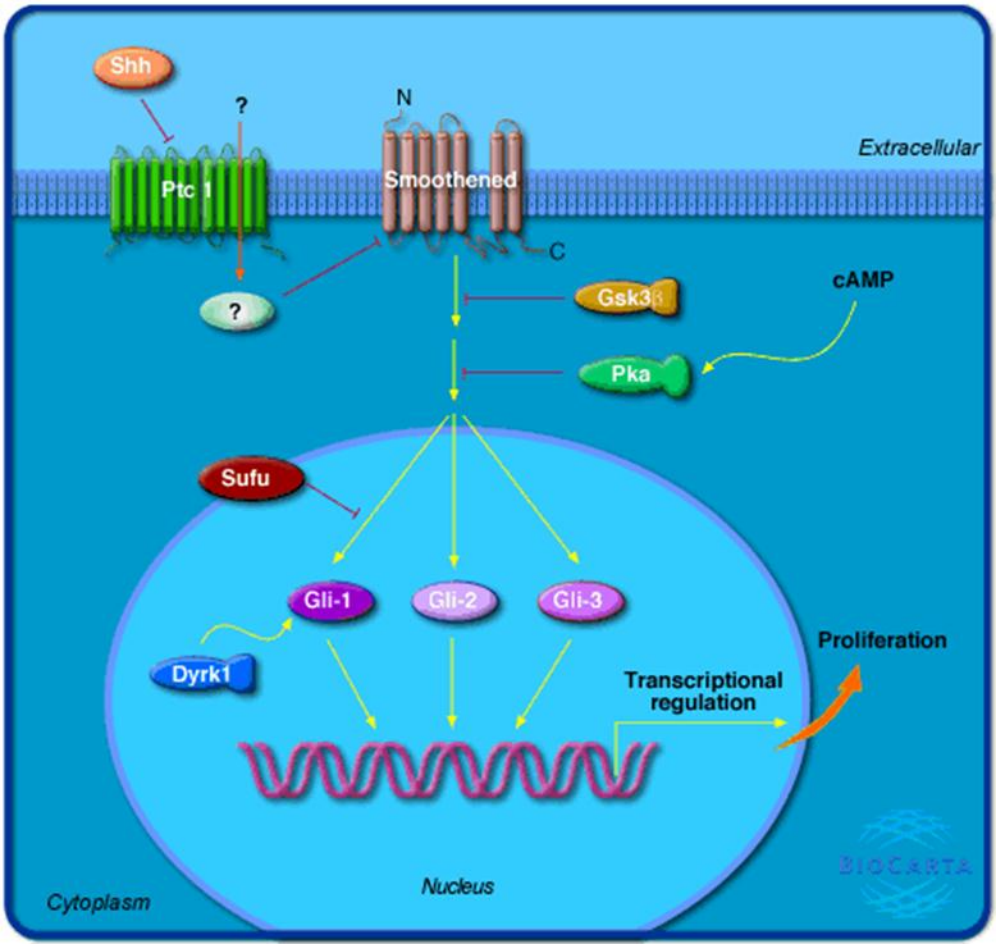

Figure 5.3: EGCG-related expression alterations of genes involved in pathways impacting craniofacial development may occur through changes in Dyrk1a activity. Expression of *Dyrk1a* is altered in the trisomic E9.5 PA1 and that activity of this gene is known to be altered by treatment with EGCG. As depicted, Dyrk1 interacts with Gli1, a transcription factor, which transcribes genes impacting proliferation. Hypothesized normalization of Dyrk1a activity may lead to normalization of this transcriptional pathway when EGCG is present, leading to normalization of proliferation in the E9.5 trisomic PA1. Image provided by Biocarta (http://cgap.nci.nih.gov/Pathways/BioCarta/m_shhPathway).

PUBLICATION

INVESTIGATION

Trisomic and Allelic Differences Influence Phenotypic Variability During Development of Down Syndrome Mice

Samantha L. Deitz and Randall J. Roper[1]
Department of Biology and Indiana University Center for Regenerative Biology and Medicine, Indiana University-Purdue University Indianapolis, Indiana 46202

ABSTRACT Individuals with full or partial Trisomy 21 (Ts21) present with clinical features collectively referred to as Down syndrome (DS), although DS phenotypes vary in incidence and severity between individuals. Differing genetic and phenotypic content in individuals with DS as well as mouse models of DS facilitate the understanding of the correlation between specific genes and phenotypes associated with Ts21. The Ts1Rhr mouse model is trisomic for 33 genes (the "Down syndrome critical region" or DSCR) hypothesized to be responsible for many clinical DS features, including craniofacial dysmorphology with a small mandible. Experiments with Ts1Rhr mice showed that the DSCR was not sufficient to cause all DS phenotypes by identifying uncharacteristic craniofacial abnormalities not found in individuals with DS or other DS mouse models. We hypothesized that the origins of the larger, dysmorphic mandible observed in adult Ts1Rhr mice develop from larger embryonic craniofacial precursors. Because of phenotypic variability seen in subsequent studies with Ts1Rhr mice, we also hypothesized that genetic background differences would alter Ts1Rhr developmental phenotypes. Using Ts1Rhr offspring from two genetic backgrounds, we found differences in mandibular precursor volume as well as total embryonic volume and postnatal body size of Ts1Rhr and nontrisomic littermates. Additionally, we observed increased relative expression of *Dyrk1a* and differential expression of *Ets2* on the basis of the genetic background in the Ts1Rhr mandibular precursor. Our results suggest that trisomic gene content and allelic differences in trisomic or nontrisomic genes influence variability in gene expression and developmental phenotypes associated with DS.

DOWN syndrome (DS) is caused by three copies of all or part of human chromosome 21 (Hsa21) and occurs in ~1 of 700–800 live births (Christianson *et al.* 2006). Individuals with DS display subsets of phenotypes with a spectrum of severities including cognitive impairment, facial dysmorphology, congenital heart defects, and behavioral anomalies (Richtsmeier *et al.* 2000; Epstein 2001; Van Cleve *et al.* 2006; Van Cleve and Cohen 2006). The precise genetic and molecular mechanisms causing specific traits associated with Trisomy 21 (Ts21) are not well defined. Early genotype–phenotype analyses based on individuals with partial Ts21 were used to define a "Down syndrome critical or chromosomal region" (DSCR), and trisomy of the DSCR was thought to be responsible for most of the major clinical features of DS (Korenberg *et al.* 1990; Delabar *et al.* 1993). Experiments in mice with segmental trisomy for the DSCR disproved the original DSCR hypothesis by demonstrating that genes in the DSCR were not sufficient to cause the craniofacial features associated with DS (Olson *et al.* 2004a). Advanced analyses of individuals with segmental Ts21 have presented evidence against a single critical region affecting all DS phenotypes and led to the hypothesis that three copies of a gene or genes on Hsa21 (not the entire DSCR or only the DSCR) may be an important factor for one or a few well-defined DS abnormalities (Korbel *et al.* 2009; Lyle *et al.* 2009).

The correlation between DS genotype and phenotype has been investigated using mouse models trisomic for Hsa21 homologs (Table 1) (Escorihuela *et al.* 1995; Siarey *et al.* 1997; Baxter *et al.* 2000; Olson *et al.* 2004a, 2007; Lorenzi and Reeves 2006; Aldridge *et al.* 2007; Belichenko *et al.* 2009). Ts65Dn mice, the most commonly used mouse model of DS, replicate many DS-like abnormalities, including

doi: 10.1534/genetics.111.131391
Manuscript received June 6, 2011; accepted for publication September 8, 2011
Supporting information is available online at http://www.genetics.org/content/suppl/2011/09/16/genetics.111.131391.DC1.
[1]Corresponding author: Department of Biology, Indiana University Center for Regenerative Biology and Medicine, Indiana University-Purdue University Indianapolis, 723 W. Michigan St., SL 306, Indianapolis, IN 46202. E-mail: rjroper@iupui.edu

Table 1 DS-associated phenotypes found in Ts65Dn and Ts1Rhr mice on different genetic backgrounds

Strain	Background	Trisomy	Body size	Brain	Cerebellum	Hippocampus	LTP	Functional tests	E9.5 PA1	*Ets2*	*Dyrk1a*	*Rcan1*
Ts65Dn	B6C3F$_n$	~104 genes	Smaller, shorter femur[a]	Similar[b]	Reduced[b]	Reduced[c]	Decreased[d]	Abnormal Morris water[e]	Reduced, fewer NCs[f]	3	3	3
Ts1Rhr	50% B6, 25% 129, 25% C3H	~33 genes	Larger,[a,g] longer femur[a]	Smaller[g]	Reduced[g]				Not significant but slightly large[h,i]	3	3	2
	50% B6, 50% 129		Larger[j]	Larger[j]	Reduced[h,i]	Similar[h,i]						
	100% B6						Normal (CA1)[j]	Normal Morris water[j]	Enlarged, more NCs[j]			
	B6C3F$_n$		Larger[k]	Larger[k]		Similar[k]	Decreased (fascia dentata)[k]	Impaired object recognition,[k] inferior T maze, thigmotaxic[k]				

[a] Olson *et al.* (2004).
[b] Baxter *et al.* (2000).
[c] Lorenzi and Reeves (2006).
[d] Siarey *et al.* (1997).
[e] Escorihuela *et al.* (1995).
[f] Roper *et al.* (2009).
[g] Aldridge *et al.* (2007).
[h] Normalized for size.
[i] This study.
[j] Olson *et al.* (2007).
[k] Belichenko *et al.* (2009).

a small mandible and other craniofacial phenotypes (Richtsmeier *et al.* 2000). The Dp(16Cbr1-ORF9)1Rhr (Ts1Rhr) mouse model, trisomic for the 33 genes orthologous to those in the DSCR (and triplicated in Ts65Dn mice), was developed to test the DSCR hypothesis by examining craniofacial phenotypes in mice. Ts1Rhr mice exhibited a larger overall size and craniofacial alterations, including a larger and morphologically different mandible than observed in Ts65Dn mice and individuals with DS (Olson *et al.* 2004a). Additional studies of Ts1Rhr mice and euploid littermates have shown differences in cerebellar and brain size, as well as neuronal long-term potentiation (LTP) and behavioral tests of learning and memory (Table 1) (Aldridge *et al.* 2007; Olson *et al.* 2007; Belichenko *et al.* 2009). Yet, some discrepancies exist between studies with Ts1Rhr mice, possibly due to differences in genetic background and experimental methodologies (Table 1). Taken together, these studies show Ts1Rhr mice may have alterations in similar structures as those affected in individuals with DS, although the resultant phenotype may not always replicate those seen in other DS mouse models or individuals with DS.

Candidate genes for craniofacial phenotypes associated with DS include *Dyrk1a*, *Rcan1 (Dscr1)*, and *Ets2*. *Dyrk1a* has been implicated in several DS phenotypes, including cognitive impairment, motor function, and craniofacial abnormalities (Altafaj *et al.* 2001; Hammerle *et al.* 2003; Arron *et al.* 2006). Although *Rcan1* may contribute to behavioral, neurophysiological, and suppression-of-tumor-growth phenotypes in DS, a third copy of only a small contiguous genetic segment including *RCAN1* in humans was not sufficient to cause DS craniofacial phenotypes (Baek *et al.* 2009; Belichenko *et al.* 2009; Eggermann *et al.* 2010). In mouse models, overexpression of *Ets2* has been implicated in craniofacial and tumorigenesis phenotypes (Sumarsono *et al.* 1996; Wolvetang *et al.* 2003; Sussan *et al.* 2008). Yet, reducing the *Ets2* copy number from three to two in Ts65Dn mice was not enough to normalize the DS-like craniofacial abnormalities with the exception of some mesoderm-derived elements of the skull (Hill *et al.* 2009). Ts1Rhr mice have three copies of *Dyrk1a* and *Ets2* but two copies of *Rcan1* and may be used in conjunction with other DS models to understand the effects of trisomic genes on craniofacial development (Table 1).

The origin of the small mandible associated with DS has been traced to a small first pharyngeal arch (PA1) with fewer neural crest cells in embryonic day 9.5 (E9.5) Ts65Dn as compared to euploid embryos (Roper *et al.* 2009). Additionally, perinatal Ts65Dn mice commonly display the reduced weight and small stature seen in infants with DS (Cronk *et al.* 1988; Roizen and Patterson 2003; Roper *et al.* 2006). We present evidence suggesting that trisomic gene content as well as allelic differences in trisomic and nontrisomic genes lead to phenotypic differences in mandibular precursor development and postnatal growth in Ts1Rhr mice and may significantly contribute to the developmental variability of Ts21 phenotypes.

Materials and Methods

Mice

Dp(16Cbr1-ORF9)1Rhr (Ts1Rhr) mice were obtained from Roger Reeves at The Johns Hopkins University School of Medicine (Baltimore). These mice had been backcrossed to C57BL/6J (B6) mice for 12 generations (N12) to establish the B6.Ts1Rhr line. 129S6/SvEv (129) mice were purchased from Taconic Laboratories (Germantown, NY). B6CBA-Tg(Wnt1-lacZ)206Amc/J mice were obtained from The Jackson Laboratory and backcrossed for 6 generations to B6 mice to create B6 mice carrying the Wnt1-lacZ transgene (B6.Wnt1-lacZ). B6.129S4-Gt(ROSA)26Sor^{tm1Sor}/J (B6.R26R) and C3H/HeJ (C3H) mice were purchased from The Jackson Laboratory and crossed to create B6C3F1 males. 129S6/SvEv (129) mice were bred to B6 mice, and the trisomic mice generated (B6129.Ts1Rhr) were then bred to B6C3F1 animals to produce offspring from B6129.Ts1Rhr × B6C3F1 and B6C3F1 × B6129.Ts1Rhr crosses. Both male and female Ts1Rhr mice are fertile and were used to generate additional mice. Offspring were genotyped at 6 days and weighed at 6 and 28 days to compare with previous analyses of Ts65Dn mice. Mice were maintained on the Lab Diet 5001 Rodent Diet (PMI Nutrition International, Brentwood, MO). All animal research was approved by the Indiana University-Purdue University Indianapolis (IUPUI) Institutional Animal Care and Use Committee and performed at IUPUI.

Generation of embryos from Ts1Rhr mothers

(B6.Ts1Rhr × B6.Wnt1-lacZ) and (B6129.Ts1Rhr × B6C3F1) matings were used to obtain E9.5 embryos with a B6 (henceforth referred to as "inbred") or ~50% B6, 25% C3H, 25% 129 (henceforth referred to as "mixed") genetic background, respectively. Female Ts1Rhr mice were introduced to male mice in the evening and subsequently checked for vaginal plugs the next morning, with E0.5 established at noon on the day the plug was found. Nine days following plug identification, pregnant Ts1Rhr mothers were killed, E9.5 embryos were dissected, and somites were counted. Embryos were processed as previously established (Roper *et al.* 2009), sectioned parasagitally at 18 μm and counterstained with 0.1% eosin, or used for gene expression analysis as described below. E9.5 embryos derived from 17 inbred [n = 34 trisomic (Ts), 73 euploid (Eu)] and 8 mixed (n = 31 Ts, 35 Eu) matings were used to quantify PA1 volume as previously done in E9.5 Ts65Dn offspring (Roper *et al.* 2009).

Gene expression analysis of Ts1Rhr embryonic tissue

RNA was isolated from the PA1 of each embryo using the PureLink RNA Micro Kit (Invitrogen) and analyzed for purity and concentration using the Nanodrop ND-1000 Spectrophotometer (Thermo Scientific). For each gene expression assay, RNA from somite and litter-matched samples was converted to cDNA using the TaqMan Reverse Transcription Reagents and quantitative PCR (qPCR) performed with the TaqMan Expression Master Mix (Applied Biosystems) and reference (*Ev1* or *Actin*) and target (*Dyrk1a*, *Rcan1*, and *Ets2*) gene probes. Crossing point (Cp) values from each probe (done in triplicate) were averaged for comparison of target to reference samples using the Applied Biosystems 7300 Real Time PCR System and software. Analysis of Cp values was performed as previously described (Pfaffl 2001).

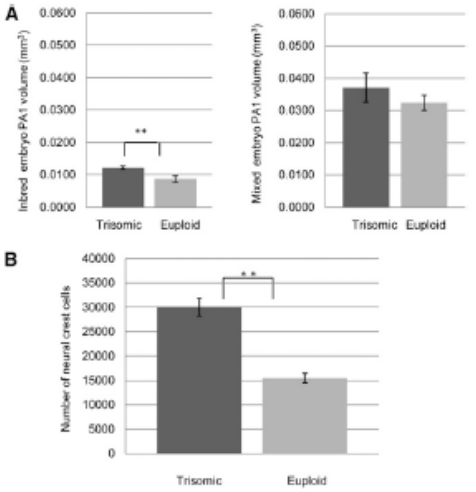

Figure 1 PA1 of E9.5 offspring from Ts1Rhr mice on inbred and mixed backgrounds. (A) PA1 volumes of trisomic embryos on an inbred background were significantly larger than those of euploid littermates of somite-matched embryos ($P < 0.01$, n = 12 trisomic and 12 euploid embryos), whereas PA1 volumes of embryos from a mixed background were not significantly different ($P = 0.37$, n = 11 trisomic and 12 euploid embryos). (B) PA1 of inbred Ts1Rhr embryos were composed of significantly more neural crest cells than euploid embryos ($P < 0.01$, n = 12 trisomic and 12 euploid embryos). Results are provided with error bars indicating standard error of the mean. $^{**}P < 0.01$.

Genotyping of Ts1Rhr embryos and mice

Embryonic and postnatal offspring were genotyped by PCR amplification of DNA isolated from yolk sacs and tissues taken at 6 days postnatal, respectively. Offspring from Ts1Rhr mice were genotyped by PCR using primers for Hyg (Olson *et al.* 2004a) (5′ CCGTCAGGACATTGTTGGA 3′) and (5′ CCGTAACCTCTGCCGTTCA 3′) amplified for 35 cycles (denaturation: 30 s at 94°; annealing: 60 s at 55°; and extension: 45 s at 72°) and the duplication junction (5′ GCCAGAGGCCACTTGTGTAG 3′) and (5′ TGTTGACCTC GAGGGACCTA 3′) amplified for 30 cycles (denaturation: 30 s at 94°; annealing: 30 s at 62.6°; and extension: 30 s at 72°) as well as the Tcrd DNA control primers (oIMR 8744 and 8745) (The Jackson Laboratory).

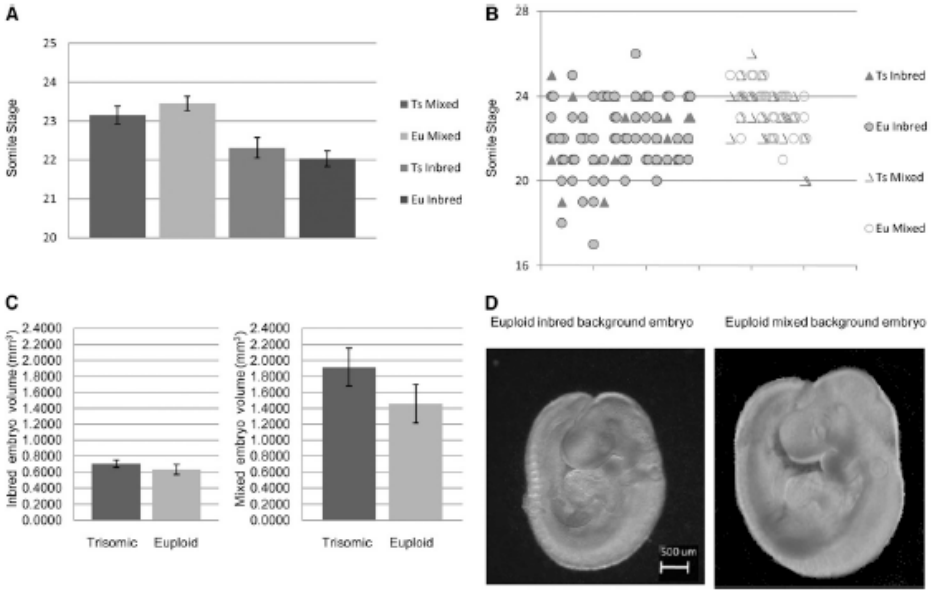

Figure 2 Average somite stage, somite variability, and volumes of E9.5 embryos by genotype and genetic background. (A) Embryos of mixed background displayed greater average somite stages than those of inbred background ($n = 11$ trisomic and 12 euploid and $n = 12$ trisomic and 12 euploid, respectively). (B) No overall difference in distribution of somite stage was seen in E9.5 euploid and Ts1Rhr embryos on either an inbred ($P = 0.61$, $n = 32$ trisomic and 69 euploid embryos) or mixed ($P = 0.26$, $n = 31$ trisomic and 35 euploid embryos) background. On the graph embryos are separated according to litter horizontally and somite number vertically. (C) Embryonic volumes (mm^3) of trisomic and euploid somite-matched embryos on inbred (left) and mixed backgrounds (right) were not significantly different at E9.5 ($P = 0.34$, $n = 12$ trisomic and 12 euploid and $P = 0.18$, $n = 11$ trisomic and 12 euploid, respectively). (D) Two somite-matched euploid embryos (23 somites: inbred-background embryo left, mixed-background embryo right) displayed apparent volumetric differences. Results in A and C are provided with error bars indicating standard error of the mean.

Quantitative morphological analysis of embryonic mice

Unbiased stereology was used to determine the volume and number of neural crest cells in the PA1 of Ts1Rhr and euploid littermate E9.5 embryos through systematic random sampling (Mouton 2002; Roper *et al.* 2009). PA1 volumes and neural crest cell numbers were obtained on every fourth and third section, respectively, as previously described (Roper *et al.* 2009). Twelve euploid and 12 trisomic embryos with an inbred background and 10 euploid and 10 trisomic embryos with a mixed background were used for stereological studies. Average coefficient of error (CE) was <0.01 for embryonic volume and <0.10 for PA1 volume and neural crest (NC) number. Scaling of the PA1 was performed by dividing the PA1 volume by the embryonic volume for each individual embryo.

Statistical analyses

All data were checked and did not significantly deviate from the expected normal distributions. Data analysis was performed using a two-tailed *t*-test and chi square analysis in Microsoft Excel. Differences between offspring on the inbred and mixed backgrounds were determined using ANOVA in PROC GLM (SAS, Cary, NC). Least significant difference post-hoc comparisons (contrasts) were used to determine differences between backgrounds for individual phenotypes. A significance level of $\alpha = 0.05$ was used in all multiple comparison tests. Raw data has been deposited as supporting information, File S1.

Results

Variability in mandibular development in the Ts1Rhr model of DS

The PA1 contains NC cells and is a developmental precursor to structures of the mid and lower face, including the mandible. We anticipated that the larger, more dysmorphic mandible found in adult Ts1Rhr mice would be predicated by a larger PA1 containing more NC cells in E9.5 Ts1Rhr as compared to euploid littermates. Somite-matched E9.5 Ts1Rhr trisomic and control mixed background embryos [similar background where craniofacial, mandibular, and body size changes were observed in adult Ts1Rhr mice

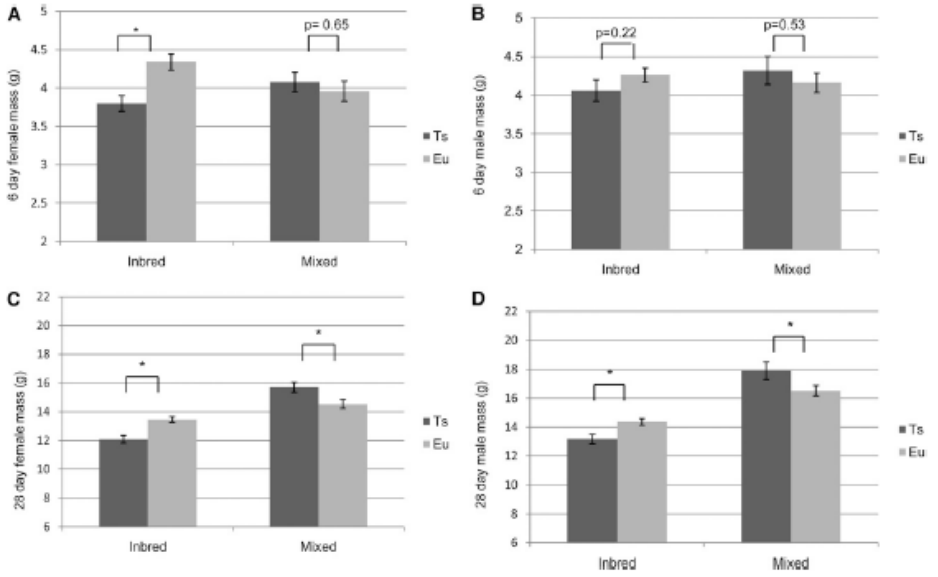

Figure 3 Weights of offspring from Ts1Rhr inbred and mixed background mating crosses. (A) Trisomic inbred P6 females were significantly smaller than euploid mice while no significant difference was seen in mixed background female P6 mice ($P < 0.05$, $n = 60$ trisomic and 75 euploid; $P = 0.65$, $n = 33$ trisomic and 40 euploid). (B) No significant differences in male mice at P6 were observed (inbred: $P = 0.22$, $n = 51$ trisomic and 94 euploid; mixed: $P = 0.53$, $n = 27$ trisomic and 46 euploid). (C) Trisomic inbred P28 females were significantly smaller than euploid littermates, while trisomic mixed P28 females were significantly larger than euploid littermates ($P < 0.05$, $n = 68$ trisomic and 83 euploid; $P < 0.05$, $n = 32$ trisomic and 41 euploid). (D) Weight differences were also apparent in males at P28 (inbred: $P < 0.05$, $n = 56$ trisomic and 100 euploid; mixed: $P < 0.05$, $n = 29$ trisomic and 46 euploid). *$P < 0.05$. Results are provided with error bars indicating standard error of the mean.

(Olson *et al.* 2004a)] did not exhibit a significant difference in PA1 volume (Figure 1A). To test the effect of allelic differences on the mandibular precursor phenotype, we examined PA1 volume in E9.5 Ts1Rhr and euploid embryos on an inbred C57BL/6J background. Both the PA1 volume ($P = 0.004$) and the NC number ($P < 0.001$) were greater in Ts1Rhr as compared to euploid somite-matched inbred embryos (Figure 1, A and B). Additionally, the PA1 from all inbred Ts1Rhr and euploid embryos was significantly smaller than those on a mixed background ($P = 0.004$) (Figure 1A).

Developmental size affected by trisomic and nontrisomic genes

Because the PA1 appeared smaller in all inbred as compared to mixed background embryos, we examined developmental body size and stage as potential contributors to the observed mandibular precursor phenotype. E9.5 Ts1Rhr as compared to euploid embryo littermates showed no significant difference in average number of somites or embryonic volume when compared within a single background (Figure 2, A–C). When all Ts1Rhr and euploid embryos were compared in a single ANOVA analysis, however, both trisomic and euploid embryo body sizes from a mixed background were larger than Ts1Rhr and euploid littermate embryo body sizes from an inbred background (Figure 2, C and D). Because there was a marked difference in overall embryonic volume between backgrounds, we scaled PA1 size to overall body volume within a single background and found the scaled PA1 volume remained significantly larger ($P = 0.0037$) in trisomic embryos from an inbred background and approached significance ($P = 0.063$) in trisomic embryos from a mixed background.

To understand how genetic background influences postnatal development as indicated by mass, we examined pup weights at postnatal day 6 (P6) and P28. At P6, there were significant differences in weight between all female offspring ($F_{3,204} = 5.03$, $P = 0.002$). A posthoc analysis revealed that female inbred Ts1Rhr mice weighed less than either their euploid littermates or female offspring from the mixed background cross (Figure 3A). No significant differences between male mice were seen at P6 (Figure 3B). However, at P28 both female and male inbred Ts1Rhr trisomic offspring weighed significantly less than their euploid littermates and all mixed background counterparts (Figure 3, C and D). In contrast, but in agreement with previously published data (Olson *et al.* 2004a), female and male trisomic offspring on a mixed

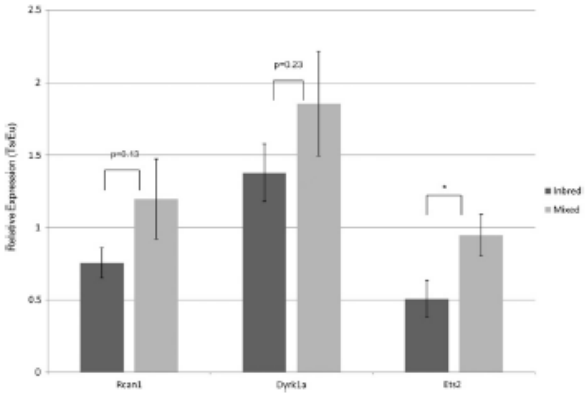

Figure 4 *Dyrk1a*, *Rcan1*, and *Ets2* gene expression alterations in the PA1 of inbred and mixed background mice. Slight but not significant differences in gene expression between inbred and mixed backgrounds in the PA1 of E9.5 embryos were seen in *Dyrk1a* and *Rcan1* ($P = 0.23$ and 0.13, respectively). A significant difference in expression levels was present between both backgrounds for *Ets2* (*$P < 0.05$). Expression levels of *Rcan1* and *Ets2* in the PA1 of E9.5 embryos on a mixed background did not differ significantly from euploid levels, while *Dyrk1a* was significantly upregulated ($n = 6$ trisomic and 6 euploid embryos from 3 litters). Expression of *Rcan1* was slightly downregulated in the PA1 of E9.5 embryos on an inbred background, *Dyrk1a* was upregulated, and *Ets2* was significantly downregulated in expression ($n = 7$ trisomic and 7 euploid embryos from three litters). Results are provided with error bars indicating standard error of the mean.

background weighed significantly more than euploid littermates (Figure 3, C and D). The data on embryonic and postnatal size, combined with previous results observed in Ts65Dn mice (Table 1) (Roper *et al.* 2006, 2009), indicate that differences in trisomic content as well as allelic differences in either trisomic or nontrisomic genes are responsible for some developmental phenotypic variability.

Expression of Dyrk1a, Rcan1, and Ets2 in PA1 of Ts1Rhr E9.5 embryos

To identify how allelic differences affect trisomic gene expression in the developing PA1, the expression of *Dyrk1a*, *Rcan1*, and *Ets2*, three genes implicated in craniofacial phenotypes (Sumarsono *et al.* 1996; Altafaj *et al.* 2001; Hammerle *et al.* 2002; Wolvetang *et al.* 2003; Arron *et al.* 2006; Hill *et al.* 2009), was analyzed. Relative expression (trisomic/euploid) by qPCR revealed an altered expression ratio corresponding to the dosage increase of *Dyrk1a* but an expression ratio close to 1 of *Rcan1* and *Ets2* in the E9.5 PA1 of mixed background embryos (Figure 4). Trisomic embryos on an inbred background also displayed increased relative *Dyrk1a* expression, slightly lower ($P = 0.13$) relative *Rcan1* expression, and significantly decreased *Ets2* expression in the PA1. Therefore, allele-specific differences appear to alter gene expression in the developing mandibular precursor.

Prenatal loss of euploid embryos due to increased lethality during development

Due to the low frequency of trisomic offspring observed during development and perinatal stages in Ts65Dn mice (Roper *et al.* 2006; Blazek *et al.* 2010), we assessed similar parameters in Ts1Rhr litters. The percentage of trisomic embryos at E9.5 on an inbred background was significantly lower than the Mendelian ratio of trisomic and euploid embryos on a mixed background (Table 2). The two Ts1Rhr crosses with different backgrounds showed no significant difference in the average number of embryos per female at E9.5 or the percentage of trisomic pups at P6 (Table 2). However, the average number of postnatal offspring per litter from an inbred mating was significantly reduced compared to litters of a mixed background. In addition, the number of euploid pups appeared to be decreasing from mid-gestation to P6 in the inbred background, but not in the mixed background. These results provide additional evidence that allelic differences in Ts1Rhr mice differentially affect offspring at perinatal stages.

Influence of parental origin of trisomy or sex on traits

The postnatal offspring in this study came from trisomic parents used in reciprocal B6.Ts1Rhr × B6 and B6 × B6.Ts1Rhr or B6129.Ts1Rhr × B6C3F1 and B6C3F1 × B6129.Ts1Rhr matings. The possible effect of parental origin of the trisomy on differences in postnatal phenotypes was investigated using the P28 weights of male and female pups on inbred and mixed backgrounds. A significant difference was observed in female inbred Ts1Rhr mice originating from different trisomic parents ($F_{3,147} = 6.84$, $P = 0.0002$). Posthoc analyses showed that euploid females weighed more than trisomic females from either a trisomic mother or father on the inbred background (Table 3). In the posthoc analyses, weight differences between male offspring from an inbred background were significant ($F_{3,152} = 3.32$, $P = 0.02$) but not as clearly divided as those between females. Euploid mice from either trisomic parent were significantly larger than trisomic mice from a trisomic father but not a trisomic

Table 2 Reproductive success and inheritance of trisomy in Ts1Rhr mice

	Inbred Ts1Rhr (% trisomy)	Mixed Ts1Rhr (% trisomy)	*P*-value (% trisomy)
Litter size E9.5	7.59 (31.8%)	8.25 (47.0%)	0.44 (0.009)
n	107 pups, 17 litters	66 pups, 8 litters	
Litter size P6	4.91 (44.0%)	6.77 (44.3%)	<0.001 (0.97)
n	452 pups, 92 litters	203 pups, 30 litters	

Table 3 Postnatal day 28 weight of inbred and mixed background offspring

	28-day females		28-day males	
	Ts	Eu	Ts	Eu
B6.Ts1Rhr × B6	11.68	13.46	13.40	14.40
n	30	34	22	38
P-value (trisomic *vs.* euploid)	0.003		0.108	
B6 × B6.Ts1Rhr	12.38	13.44	13.02	14.33
n	38	49	34	62
P-value	0.004		0.009	
129B6.Ts1Rhr × B6C3F1	14.82	13.75	14.34	14.96
n	16	16	7	15
P-value	0.030		0.320	
B6C3F1 × 129B6.Ts1Rhr	16.57	15.03	19.01	17.26
n	16	25	22	31
P-value	0.034		0.024	

mother. From these data, we found no strong parent-of-origin effect causing differences in the weight of offspring from inbred Ts1Rhr mice.

When P28 weight was examined in male offspring with a mixed background, a significant difference was observed ($F_{3,71} = 11.77$, $P < 0.0001$). Posthoc analyses revealed that both trisomic and euploid male and female mice from B6C3F1 × B6129.Ts1Rhr matings were significantly larger than trisomic and euploid mice from B6129.Ts1Rhr × B6C3F1 matings. Both female trisomic and euploid mice with a nontrisomic mother were significantly larger than euploid pups but not larger than trisomic mice from a trisomic mother. These results suggest that, on a mixed background, offspring from euploid mothers are larger at 28 days and may indicate an interaction between maternal ploidy and specific alleles from the mixed background cross.

Discussion

Developmental phenotypes affected by trisomic and disomic content

By examining the Ts1Rhr mouse model on differing genetic backgrounds, we provide evidence that interaction between allelic differences in trisomic content and genetic background causes variability in DS phenotypes, including PA1 volume, pre- and postnatal body size, and percentage of trisomic embryonic offspring. Analyses with mouse models and partial trisomies in humans have shown that certain trisomic regions correlate with both the incidence and the severity of DS phenotypes (Richtsmeier *et al.* 2002; Olson *et al.* 2004b, 2007; Korbel *et al.* 2009; Lyle *et al.* 2009; Reynolds *et al.* 2010; Yu *et al.* 2010). Studies investigating the penetrance and variability in DS phenotypes have previously singled out nontrisomic genes as important factors in DS phenotypes (Epstein 2001; Kerstann *et al.* 2004). For example, nontrisomic *CRELD1* mutations have been linked to an increased penetrance of atrioventricular septal defects in individuals with DS, and the occurrence of DS-like heart defects in the Tc1 DS mouse model were dependent upon genetic background (Maslen *et al.* 2006; Dunlevy *et al.* 2010). Certain alleles of *GATA1*, also not found on Hsa21, may predispose individuals with Ts21 to DS-related acute megakaryoblastic leukemia (Wechsler *et al.* 2002). Similarly, allelic differences in trisomic and nontrisomic genes may also account for phenotypic variability and some differences in brain volume and LTP observed in studies using Ts1Rhr mice, although methodological differences may also be responsible for some of these divergent phenotypes (Table 1) (Olson *et al.* 2007; Belichenko *et al.* 2009).

Contribution of Dyrk1a, Rcan1, and Ets2 to embryonic mandibular development

Our qPCR gene expression analysis demonstrates that copy number may not necessarily correlate with gene expression in a specific tissue at any given time point. *Rcan1* is found in two copies in Ts1Rhr embryos and seemed to be equivalently expressed in trisomic and euploid embryos on a mixed background, but expression appeared slightly reduced in the PA1 of inbred Ts1Rhr embryos. *Dyrk1a* is found in three copies in the Ts1Rhr embryos and was upregulated in Ts1Rhr as compared to euploid littermate E9.5 PA1 on both backgrounds. Although *Ets2* is also found in three copies in all Ts1Rhr embryos, in inbred Ts1Rhr embryos its expression was significantly reduced in trisomic as compared to euploid E9.5 PA1. However, no significant difference in expression was seen between trisomic and euploid embryos on a mixed background.

Interestingly, in previous studies reducing *Ets2* to two copies in Ts65Dn mice, little effect was seen on the DS-like craniofacial abnormalities (Hill *et al.* 2009). In Ts65Dn *Ets2+/−* mice, the mesoderm and not the neural crest-derived skeletal elements had shape differences that were of a greater magnitude than those found between Ts65Dn and normal mice. Our results suggest that differential expression of *Ets2* and its possible contribution to the embryonic mandibular precursor phenotype occurs because of differential allelic contributions in the Ts1Rhr embryos. Taken together, the results of our work and others demonstrate complex genetic interactions involving *Ets2* and other genes in determining craniofacial abnormalities (Sumarsono *et al.* 1996; Wolvetang *et al.* 2003; Hill *et al.* 2009). Furthermore, a susceptibility region containing trisomic genes may have a major influence on a distinct phenotype but only as it interacts with other trisomic and nontrisomic genes. This hypothesis may provide a genetic explanation to account for the incidence and variability of DS phenotypes (Aldridge *et al.* 2007; Lyle *et al.* 2009).

Relationships between developmental stage, embryo volume, and structural phenotypes

Structures from trisomic and euploid Ts65Dn embryos matched for size or developmental stage may display significant differences in their development (Blazek *et al.* 2010). In Blazek *et al.* 2010, developmental differences were controlled by using somite-matched embryos and measuring the volume of the E9.5 embryos. In the present study, no significant difference existed in the average overall

somite stage between the two backgrounds or between the two genotypes within that background. Significant differences were present, however, between the total volumes of the trisomic and euploid embryos from differing backgrounds. Our work implies that changes in overall embryonic size may affect developmental processes. For example, in mandibular development when PA1 size was compared in somite-matched Ts1Rhr embryos, only the PA1 from inbred Ts1Rhr embryos was significantly larger than euploid, although scaled PA1 volume results for mixed Ts1Rhr embryos appeared to approach significance. Later in development, mandibular precursor differences between Ts1Rhr and euploid embryos on a mixed background may become significant. Although definitive craniofacial analysis has not been performed in inbred Ts1Rhr mice, the scaled PA1 volume supports the hypothesis that the larger, dysmorphic mandible seen in adult Ts1Rhr mice is caused by differences in the mandibular precursor as typified by the PA1 (Olson *et al.* 2004a). Additionally, the loss in euploid offspring from midgestation to P6, contrary to what has been shown in Ts65Dn offspring (Roper *et al.* 2006; Blazek *et al.* 2010), may be due to the reduced embryonic size of the euploid as compared to the trisomic embryos *in utero*. Because embryos that appear similar according to traditionally defined developmental markers such as somite or Theiler staging may actually display differences in growth parameters, investigators may need to account for both developmental stage and size when examining developmental phenotypes in trisomic and euploid embryos.

Our work investigated developmental phenotypes in the Ts1Rhr mouse model with two different genetic backgrounds using identical methodologies and environmental conditions. We show that allelic differences affect PA1 phenotypes, tissue-specific differential gene expression, and developmental variability. These results suggest that the phenotypic variability in other DS mouse models may also be affected by allelic differences. These data also support the hypothesis of the complex genetics and interaction between trisomic and disomic genes in developmental phenotypes associated with DS.

Acknowledgments

This work was supported by funding from an Indiana University-Purdue University Indianapolis Honors Program Research Fellowship (S.L.D. and R.J.R.) and by National Institutes of Health grant DE021034 from the National Institute of Dental and Craniofacial Research (R.J.R.). The contents are solely the responsibility of the authors and do not necessarily represent the official views of the NIDCR.

Literature Cited

Aldridge, K., R. H. Reeves, L. E. Olson, and J. T. Richtsmeier, 2007 Differential effects of trisomy on brain shape and volume in related aneuploid mouse models. Am. J. Med. Genet. A 143: 1060–1070.

Altafaj, X., M. Dierssen, C. Baamonde, E. Martí, J. Visa *et al.*, 2001 Neurodevelopmental delay, motor abnormalities and cognitive deficits in transgenic mice overexpressing Dyrk1A (minibrain), a murine model of Down's syndrome. Hum. Mol. Genet. 10: 1915–1923.

Arron, J. R., M. M. Winslow, A. Polleri, C. P. Chang, H. Wu *et al.*, 2006 NFAT dysregulation by increased dosage of DSCR1 and DYRK1A on chromosome 21. Nature 441: 595–600.

Baek, K. H., A. Zaslavsky, R. C. Lynch, C. Britt, Y. Okada *et al.*, 2009 Down's syndrome suppression of tumour growth and the role of the calcineurin inhibitor DSCR1. Nature 459: 1126–1130.

Baxter, L. L., T. H. Moran, J. T. Richtsmeier, J. Troncoso, and R. H. Reeves, 2000 Discovery and genetic localization of Down syndrome cerebellar phenotypes using the Ts65Dn mouse. Hum. Mol. Genet. 9: 195–202.

Belichenko, N. P., P. V. Belichenko, A. M. Kleschevnikov, A. Salehi, R. H. Reeves *et al.*, 2009 The "Down syndrome critical region" is sufficient in the mouse model to confer behavioral, neurophysiological, and synaptic phenotypes characteristic of Down syndrome. J. Neurosci. 29: 5938–5948.

Blazek, J. D., C. N. Billingsley, A. Newbauer, and R. J. Roper, 2010 Embryonic and not maternal trisomy causes developmental attenuation in the Ts65Dn mouse model for Down syndrome. Dev. Dyn. 239: 1645–1653.

Christianson, A., C. P. Howson, and B. Modell, 2006 March of Dimes Global Report on Birth Defects: The Hidden Toll of Dying and Disabled Children, pp. 1–98. March of Dimes Birth Defects Foundation, White Plains, NY.

Cronk, C., A. C. Crocker, S. M. Pueschel, A. M. Shea, E. Zackai *et al.*, 1988 Growth charts for children with Down syndrome: 1 month to 18 years of age. Pediatrics 81: 102–110.

Delabar, J. M., D. Theophile, Z. Rahmani, Z. Chettouh, J. L. Blouin *et al.*, 1993 Molecular mapping of twenty-four features of Down syndrome on chromosome 21. Eur. J. Hum. Genet. 1: 114–124.

Dunlevy, L., M. Bennett, A. Slender, E. Lana-Elola, V. L. Tybulewicz *et al.*, 2010 Down's syndrome-like cardiac developmental defects in embryos of the transchromosomic Tc1 mouse. Cardiovasc. Res. 88: 287–295.

Eggermann, T., N. Schonherr, S. Spengler, S. Jager, B. Denecke *et al.*, 2010 Identification of a 21q22 duplication in a Silver-Russell syndrome patient further narrows down the Down syndrome critical region. Am. J. Med. Genet. A 152A: 356–359.

Epstein, C. J., 2001 Down syndrome (trisomy 21), pp. 1223–1256 in *The Metabolic and Molecular Bases of Inherited Disease*, edited by C. R. Scriver, A. L. Beaudet, W. S. Sly, and D. Valle. McGraw-Hill, New York.

Escorihuela, R. M., A. Fernandez-Teruel, I. F. Vallina, C. Baamonde, M. A. Lumbreras *et al.*, 1995 A behavioral assessment of Ts65Dn mice: a putative Down syndrome model. Neurosci. Lett. 199: 143–146.

Hammerle, B., E. Vera-Samper, S. Speicher, R. Arencibia, S. Martinez *et al.*, 2002 Mnb/Dyrk1A is transiently expressed and asymmetrically segregated in neural progenitor cells at the transition to neurogenic divisions. Dev. Biol. 246: 259–273.

Hammerle, B., C. Elizalde, J. Galceran, W. Becker, and F. J. Tejedor, 2003 The MNB/DYRK1A protein kinase: neurobiological functions and Down syndrome implications. J. Neural Transm. Suppl: 129–137.

Hill, C. A., T. E. Sussan, R. H. Reeves, and J. T. Richtsmeier, 2009 Complex contributions of Ets2 to craniofacial and thymus phenotypes of trisomic "Down syndrome" mice. Am. J. Med. Genet. A 149A: 2158–2165.

Kerstann, K. F., E. Feingold, S. B. Freeman, L. J. Bean, R. Pyatt *et al.*, 2004 Linkage disequilibrium mapping in trisomic populations: analytical approaches and an application to congenital

heart defects in Down syndrome. Genet. Epidemiol. 27: 240–251.

Korbel, J. O., T. Tirosh-Wagner, A. E. Urban, X. N. Chen, M. Kasowski *et al.*, 2009 The genetic architecture of Down syndrome phenotypes revealed by high-resolution analysis of human segmental trisomies. Proc. Natl. Acad. Sci. USA 106: 12031–12036.

Korenberg, J. R., H. Kawashima, S. M. Pulst, T. Ikeuchi, N. Ogasawara *et al.*, 1990 Molecular definition of a region of chromosome 21 that causes features of the Down syndrome phenotype. Am. J. Hum. Genet. 47: 236–246.

Lorenzi, H. A., and R. H. Reeves, 2006 Hippocampal hypocellularity in the Ts65Dn mouse originates early in development. Brain Res. 1104: 153–159.

Lyle, R., F. Bena, S. Gagos, C. Gehrig, G. Lopez *et al.*, 2009 Genotype-phenotype correlations in Down syndrome identified by array CGH in 30 cases of partial trisomy and partial monosomy chromosome 21. Eur. J. Hum. Genet. 17: 454–466.

Maslen, C. L., D. Babcock, S. W. Robinson, L. J. Bean, K. J. Dooley *et al.*, 2006 CRELD1 mutations contribute to the occurrence of cardiac atrioventricular septal defects in Down syndrome. Am. J. Med. Genet. A 140: 2501–2505.

Mouton, P. R., 2002 *Principles and Practices of Unbiased Stereology: An Introduction for Bioscientists*. Johns Hopkins University Press, Baltimore.

Olson, L. E., J. T. Richtsmeier, J. Leszl, and R. H. Reeves, 2004a A chromosome 21 critical region does not cause specific Down syndrome phenotypes. Science 306: 687–690.

Olson, L. E., R. J. Roper, L. L. Baxter, E. J. Carlson, C. J. Epstein *et al.*, 2004b Down syndrome mouse models Ts65Dn, Ts1Cje, and Ms1Cje/Ts65Dn exhibit variable severity of cerebellar phenotypes. Dev. Dyn. 230: 581–589.

Olson, L. E., R. J. Roper, C. L. Sengstaken, E. A. Peterson, V. Aquino *et al.*, 2007 Trisomy for the Down syndrome "critical region" is necessary but not sufficient for brain phenotypes of trisomic mice. Hum. Mol. Genet. 16: 774–782.

Pfaffl, M. W., 2001 A new mathematical model for relative quantification in real-time RT-PCR. Nucleic Acids Res. 29: e45.

Reynolds, L. E., A. R. Watson, M. Baker, T. A. Jones, G. D'Amico *et al.*, 2010 Tumour angiogenesis is reduced in the Tc1 mouse model of Down's syndrome. Nature 465: 813–817.

Richtsmeier, J. T., L. L. Baxter, and R. H. Reeves, 2000 Parallels of craniofacial maldevelopment in Down syndrome and Ts65Dn mice. Dev. Dyn. 217: 137–145.

Richtsmeier, J. T., A. Zumwalt, E. J. Carlson, C. J. Epstein, and R. H. Reeves, 2002 Craniofacial phenotypes in segmentally trisomic mouse models for Down syndrome. Am. J. Med. Genet. 107: 317–324.

Roizen, N. J., and D. Patterson, 2003 Down's syndrome. Lancet 361: 1281–1289.

Roper, R. J., H. K. St. John, J. Philip, A. Lawler, and R. H. Reeves, 2006 Perinatal loss of Ts65Dn Down syndrome mice. Genetics 172: 437–443.

Roper, R. J., J. F. VanHorn, C. C. Cain, and R. H. Reeves, 2009 A neural crest deficit in Down syndrome mice is associated with deficient mitotic response to Sonic hedgehog. Mech. Dev. 126: 212–219.

Siarey, R. J., J. Stoll, S. I. Rapoport, and Z. Galdzicki, 1997 Altered long-term potentiation in the young and old Ts65Dn mouse, a model for Down syndrome. Neuropharmacology 36: 1549–1554.

Sumarsono, S. H., T. J. Wilson, M. J. Tymms, D. J. Venter, C. M. Corrick *et al.*, 1996 Down's syndrome-like skeletal abnormalities in Ets2 transgenic mice. Nature 379: 534–537.

Sussan, T. E., A. Yang, F. Li, M. C. Ostrowski, and R. H. Reeves, 2008 Trisomy represses Apc(Min)-mediated tumours in mouse models of Down's syndrome. Nature 451: 73–75.

Van Cleve, S. N., and W. I. Cohen, 2006 Part I: clinical practice guidelines for children with Down syndrome from birth to 12 years. J. Pediatr. Health Care 20: 47–54.

Van Cleve, S. N., S. Cannon, and W. I. Cohen, 2006 Part II: Clinical Practice Guidelines for adolescents and young adults with Down Syndrome: 12 to 21 Years. J. Pediatr. Health Care 20: 198–205.

Wechsler, J., M. Greene, M. A. McDevitt, J. Anastasi, J. E. Karp *et al.*, 2002 Acquired mutations in GATA1 in the megakaryoblastic leukemia of Down syndrome. Nat. Genet. 32: 148–152.

Wolvetang, E. J., T. J. Wilson, E. Sanij, J. Busciglio, T. Hatzistavrou *et al.*, 2003 ETS2 overexpression in transgenic models and in Down syndrome predisposes to apoptosis via the p53 pathway. Hum. Mol. Genet. 12: 247–255.

Yu, T., C. Liu, P. Belichenko, S. J. Clapcote, S. Li *et al.*, 2010 Effects of individual segmental trisomies of human chromosome 21 syntenic regions on hippocampal long-term potentiation and cognitive behaviors in mice. Brain Res. 1366: 162–171.

Communicating editor: F. F. Pardo-Manuel de Villena

GENETICS

Supporting Information
http://www.genetics.org/content/suppl/2011/09/16/genetics.111.131391.DC1

Trisomic and Allelic Differences Influence Phenotypic Variability During Development of Down Syndrome Mice

Samantha L. Deitz and Randall J. Roper

DOI: 10.1534/genetics.111.131391